Spring 5-31-2004

An investigation of position and force during gait-mimicking finger motions

Matthew Stephen Noesner
New Jersey Institute of Technology

ABSTRACT

AN INVESTIGATION OF POSITION AND FORCE DURING GAIT-MIMICKING FINGER MOTIONS

by
Matthew Stephen Noesner

Spinal cord injuries are extremely debilitating, often leaving the injured person without the ability to use their legs (paraplegia) and sometimes, without the ability to use their arms and legs (tetraplegia or quadriplegia). Currently, primitive forms of feed-forward functional electrical stimulation (FES) and special orthotics are available for persons with paraplegia. However, these forms of FES do not allow the individual to actually control their movements on a real-time basis, nor do they offer the ability for the injured person to sense the ground on which they stand.

It is the goal of the researchers at the Neuromuscular Engineering Laboratory, at the New Jersey Institute of Technology, to improve the quality of life of a paraplegic patient by restoring his/her ability to control their own leg movements with gait-mimicking finger movements. Should such movements prove to effectively mimic gait, it may be possible to develop a haptic walking system to control the user's leg muscles while providing the user control of and feedback from their legs in real-time.

This research investigated the gait cycle timing, trajectory, and ground reaction forces of finger movements as they mimic normal human gait and exposed considerable similarities. This implies there can be an effective substitution of neural commands to the legs with finger movement and sensation.

AN INVESTIGATION OF POSITION AND FORCE DURING GAIT-MIMICKING FINGER MOTIONS

by
Matthew Stephen Noesner

A Thesis
Submitted to the Faculty of
New Jersey Institute of Technology
in Partial Fulfillment of the Requirements for the Degree of
Master of Science in Biomedical Engineering

Department of Biomedical Engineering

May 2004

APPROVAL PAGE

AN INVESTIGATION OF POSITION AND FORCE DURING GAIT-MIMICKING FINGER MOTIONS

Matthew Stephen Noesner

Dr. Richard A. Foulds, Thesis Advisor — Date
Associate Professor of Biomedical Engineering, NJIT

Dr. Stanley Reisman, Committee Member — Date
Professor of Biomedical Engineering, NJIT

Dr. Sergei Adamovich, Committee Member — Date
Assistant Professor of Biomedical Engineering, NJIT

BIOGRAPHICAL SKETCH

Author: Matthew Stephen Noesner

Degree: Master of Science in Biomedical Engineering

Date: May 2003

Undergraduate and Graduate Education:

- Master of Science in Biomedical Engineering
  New Jersey Institute of Technology, Newark, NJ, 2004

- Bachelor of Science in Mechanical Engineering
  New Jersey Institute of Technology, Newark, NJ, 2002

Major: Biomedical Engineering

Presentations and Publications:

Matthew S. Noesner, Corey J. Birmingham, and Richard Foulds
"Haptic Controlled Functional Electrical Stimulation of the Lower Extremities," Proceedings of the 29th Northeast Bioengineering Conference, March 2003.

Matthew S. Noesner and Corey J. Birmingham,
"Development of Joint Implant," Society of Tribologists and Lubrication Engineers Meeting, NJIT, April 2002.

To my beloved family for their
support and guidance through life.

ACKNOWLEDGMENT

I would like to thank Dr. Richard Foulds for his support and guidance throughout this research, and for his determination to acquire funding for our department. Also, thank you to Dr. Stanley Reisman for his advisement throughout my graduate career and for his service as a committee member; and Dr. Sergei Adamovich for his devotion to the Biomedical Engineering department at NJIT and as a committee member.

I would also like to thank my fellow students in the Neuromuscular Engineering Laboratory for their help and support throughout this research. A special thank you goes to Corey Birmingham, Darnell Simon, and Donald Helt III for accompanying me through to the end of this chapter in life. And I owe a great deal of gratitude to my family and friends for their never-ending patience and unwavering support.

TABLE OF CONTENTS

TABLE OF CONTENTS
(Continued)

Chapter **Page**

TABLE OF CONTENTS
(Continued)

Chapter **Page**

LIST OF TABLES

LIST OF FIGURES

LIST OF FIGURES
(Continued)

LIST OF FIGURES
(Continued)

LIST OF FIGURES
(Continued)

CHAPTER 1

INTRODUCTION

1.1 Objective

Every year, 11,000 new spinal cord injuries occur with the average age at the time of injury being only 32.6 years. Approximately 45.9% of those injured are left paraplegic, with little or no use of their lower limbs [1]. A major goal of researchers across the world has been to conquer paralysis and improve the lives of those who are afflicted with this debilitating injury.

Current methods of treating paraplegia include a standard wheelchair, various types of orthotic devices, or functional electrical stimulation (FES) [2]. The problem with these solutions is that they do not allow the injured person to regain the feeling of control over their body, or are not applicable in all situations. The simplest method to achieve movement utilizes a standard wheelchair, but it lacks the ability to restore use of paralyzed legs. Orthotic devices can only be used in the least severe cases, but they are still awkward to use. Current FES technology does not provide any feedback to the injured person and only allows for preprogrammed motions, usually only consisting of a few steps before the program must be executed again.

Researchers at the Neuromuscular Engineering Laboratory believe it is possible for a paraplegic patient to regain control over their legs through the use of their fingers in conjunction with haptic and virtual reality technology to overcome the seemingly vast anatomical difference. The objective of this research is to determine through force and position data if finger motions (Figure 1.1) can accurately mimic normal human gait

(Figure 1.2). If it is found possible, then it will encourage the use of fingers with current haptic and virtual reality technology to conduct precise functional electrical stimulation of the lower extremities, controllable by the user.

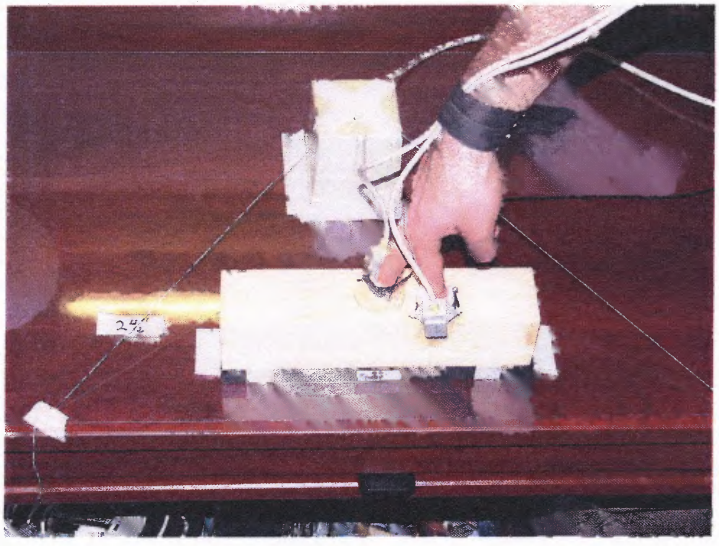

Figure 1.1 "Finger walking."

Figure 1.2 Normal human gait.

1.2 Spinal Cord and Injury

The spinal cord is a bundle of nerve fibers, making up the largest nerve in the human body [3]. The spinal cord extends approximately 18 inches from the base of the brain, down the back, and through the vertebrae. Extending from the spinal cord are 31 pairs of nerves as shown in Figure 1.3. The nerves are divided into four different categories – cervical (C), thoracic (T), lumbar (L), and sacral (S). It is the job of these nerves to communicate messages to and from the brain.

The vertebrae provide protection that is sometimes insufficient and injury to the spinal cord can result due to trauma or infection. When an individual experiences an injury of the spinal cord, nerve function above the injury remains intact, while the nerves below the injury cannot function normally. Therefore, an injury occurring lower on the spine will cause less paralysis since fewer peripheral nerves lose their connection to the brain.

When an injury occurs in the C1 to T1 region, the injured person is often considered a tetraplegic (quadriplegic), maintaining only a minimal amount of movement and/or feeling in his or her head, neck, and shoulders. If there is an injury in the T2 to S5 region, the injured person is considered a paraplegic, having lost movement and/or feeling in his or her chest, stomach, hips, legs, and/or feet. Table A.1 in Appendix A shows the remaining functionality after an injury is sustained in defined sections of the spinal cord.

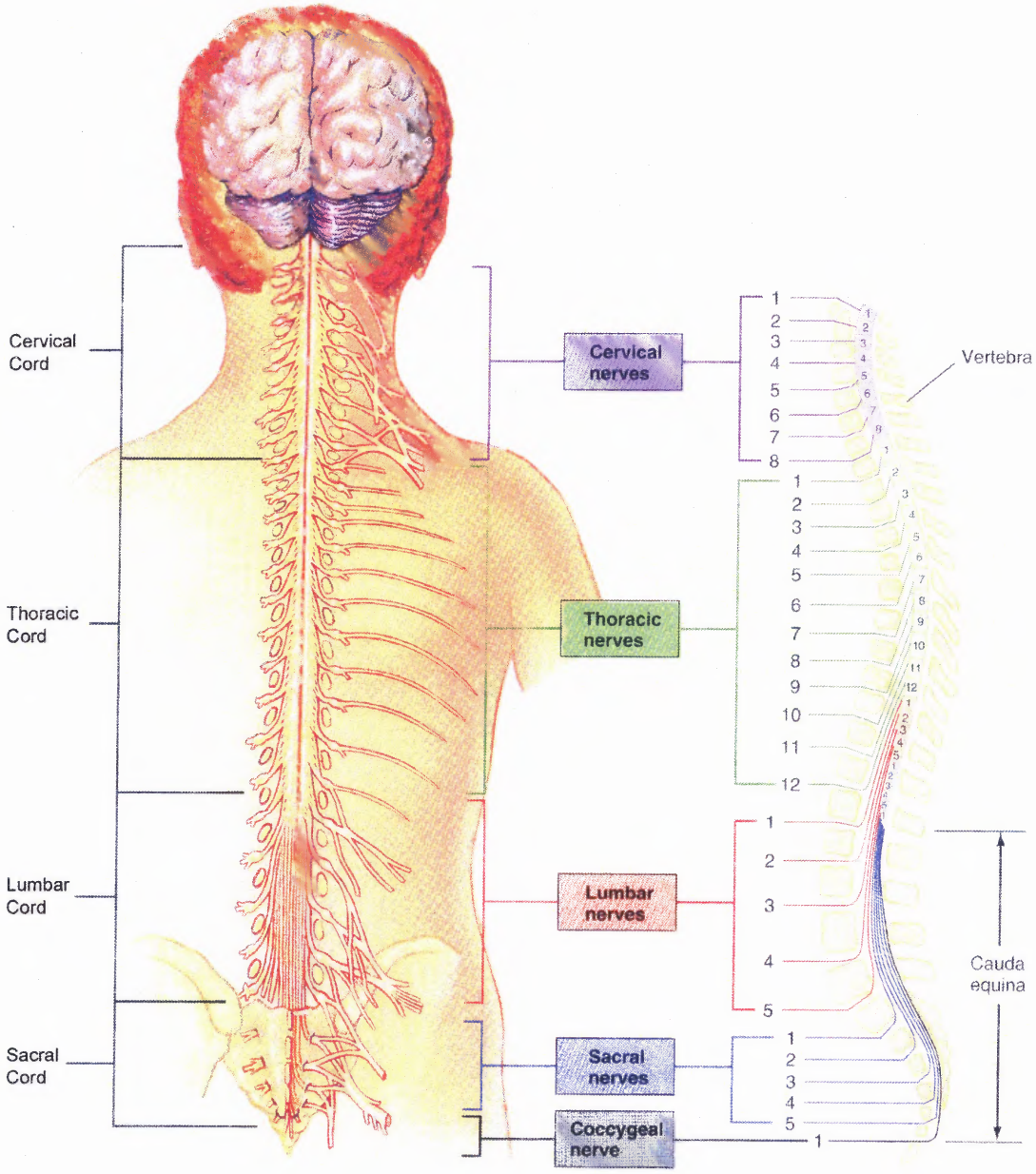

Figure 1.3 The Spinal Cord and its Divisions [4].

1.3 Current Orthotic Solutions

When an individual sustains a spinal cord injury leading to permanent paraplegia, there are few options available for restoring mobility. One option of restoring mobility is the wheelchair – either conventional or electrically powered. A wheelchair, however, is very limiting and difficult to maneuver in some situations because of its size and height. Also, a wheelchair generally does not improve an individual's psychological health.

Alternatives to a wheelchair include a variety of orthotic devices. Shown in Figure 1.4 is the knee-ankle-foot orthosis (KAFO). The KAFO is normally utilized by patients who have control over their abdominal section and hip, but lack control of their knee and ankle. In addition to providing the necessary support to the knee and ankle, the KAFO transfers the increased load during weight bearing gait to a better suited part of the skeletal system [5]. When a pair of KAFO devices is used in combination with a set of crutches, an energy *inefficient* tripod gait can be produced [6].

Figure 1.4 Knee-ankle-foot orthosis [5].

A more functional orthotic device is the reciprocating gait orthosis (RGO). Developed in the late 1960s at Louisiana State University, the RGO greatly reduces the amount of energy exerted by the disabled individual by helping to generate a more natural, reciprocating gait. The RGO creates a more efficient gait by using a mechanical

linkage to physically force one hip into flexion as the other hip moves into extension. A more recent RGO design, developed in conjunction with Fillauer Inc. is currently offered through the Center for Orthotics Design and is shown in Figure 1.5.

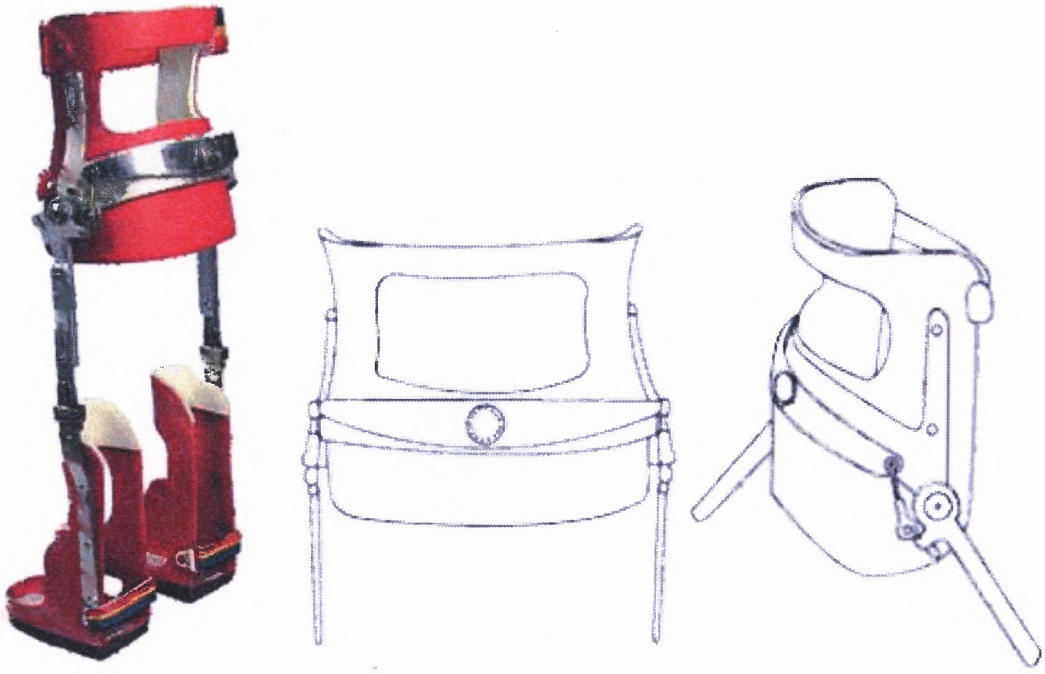

Figure 1.5 The ISOCENTRIC® RGO [7].

1.4 Functional Electrical Stimulation

Functional electrical stimulation (FES) uses externally generated electrical current pulses to activate healthy muscles that have been neurally separated from the spinal cord. The electrical currents can be applied by means of externally placed surface electrodes, internally placed fine wire electrodes, or implanted electrodes [8].

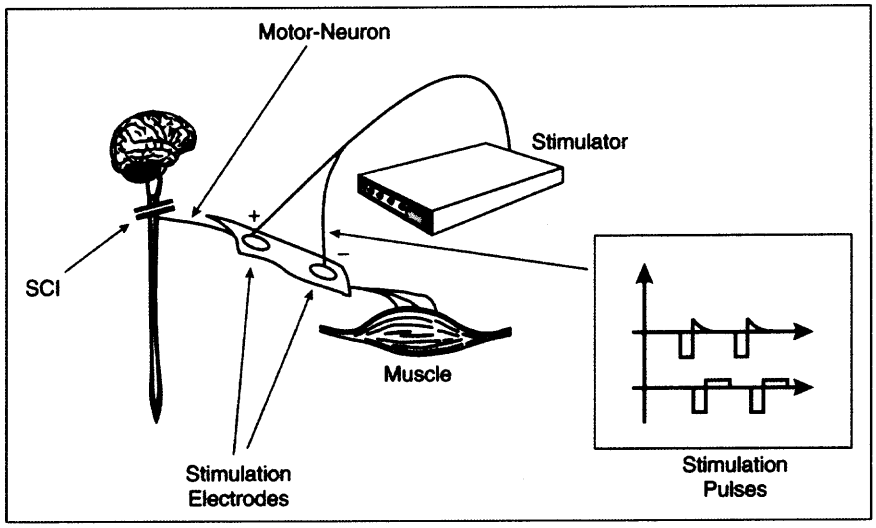

Figure 1.6 The FES system and its connection to the motor neuron [8].

When a spinal cord injury occurs, the muscles controlled by the nerves below the injury are neurally separated from the spinal cord. Even though the muscles are healthy and intact, they are no longer capable of receiving electrical impulses from the brain. In such a case, FES can be used to generate a muscle contraction by applying a current to the motor neuron between the spinal cord and the muscle, as shown in Figure 1.6. If the muscle is damaged or has atrophied, it is less capable of receiving electrical impulses regardless of where they originate. In this case, FES may not be applicable and other rehabilitation alternatives must be sought [9].

Some orthotic devices have been combined with FES to improve mobility and rehabilitation. In such cases, users are given the ability to activate leg muscles and generate a walking motion through an external switch. Examples of external switches include a push button control on a walker or crutches; a foot switch that activates the FES system when the users lifts his or her heel; or a gait phase recognition sensor system which, through various sensors, will identify each gait phase and activate muscles accordingly. With such systems, however, the user must still have a good sense of

balance and must have the ability to use a walker or crutches [8]. Even though the user will experience more mobility with the FES assisted orthotic devices, the mobility gained will be provided in a feed-forward fashion. In other words, the user will still have no sensation of the floor and no ability to make adjustments based on what they would have normally felt, in addition to being dependent on a walker or crutches.

1.5 Gait and Gait Terminology

The seemingly simple act of normal walking allows humans to transport themselves from one location to another without the use of an external device or vehicle. Human locomotion can be characterized by one's gait cycle. While every person has a unique gait, the cycle follows the same general pattern for people not afflicted with a pathological gait. For the purposes of this research, only non-pathological, or normal, gait is considered.

1.5.1 Gait Cycle

The gait cycle is defined as the amount of time between any two identical events during walking [10], or one stride. Illustrated in Figure 1.7 are the two periods of gait, stance and swing. The stance period occurs while the foot is in contact with the ground, and the swing phase occurs while the foot is traveling through the air.

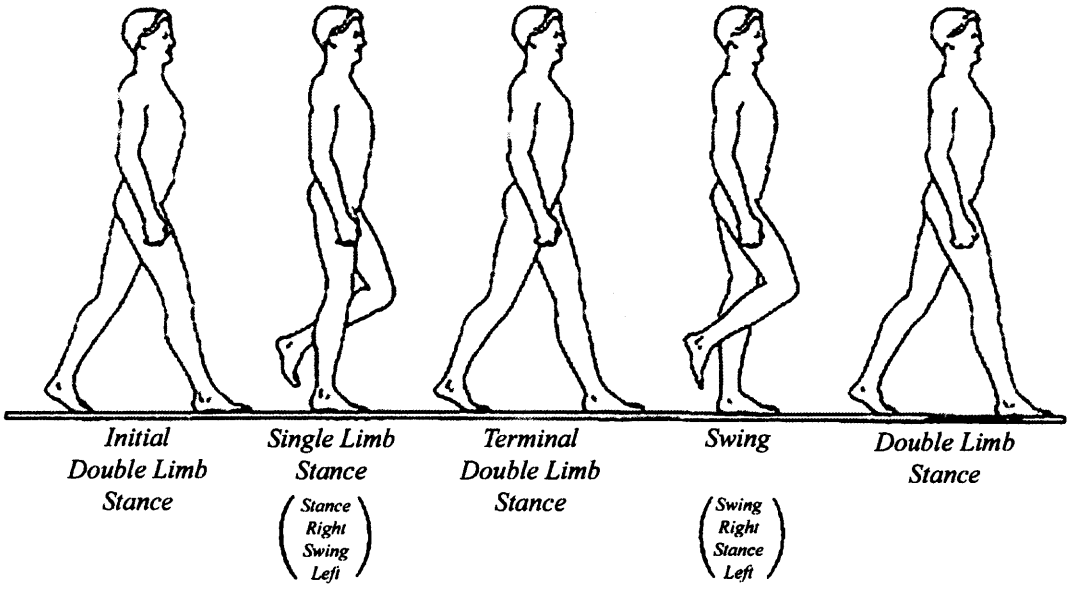

Figure 1.7 Stance and swing periods during normal walking [10].

Approximately 40% of the walking gait cycle is spent in the swing period, while the remaining 60% is spent in stance [11]. As shown in Figure 1.8, an increase in locomotion velocity results in a decrease in both the gait cycle time and the time spent in stance.

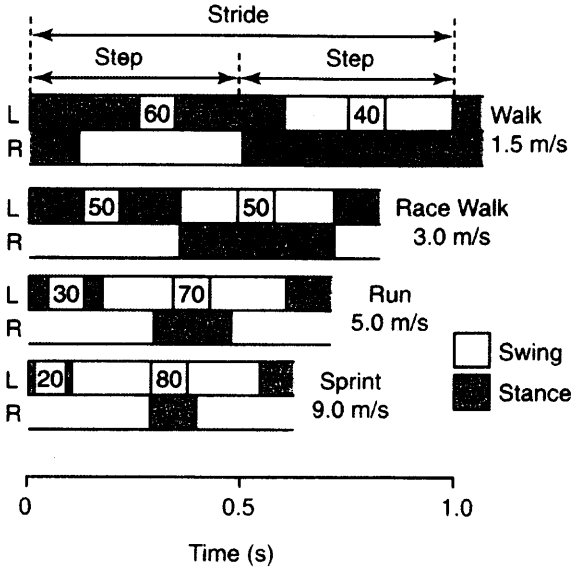

Figure 1.8 Gait cycle timing during walking and running gaits [11].

1.5.2 Swing and Stance Periods

The swing and the stance periods can be further divided, as depicted in Figure 1.9, to ease the reference of various actions during the gait cycle. The swing and stance phases are subcategorized into three different tasks – weight acceptance, single limb support, and limb advancement [11].

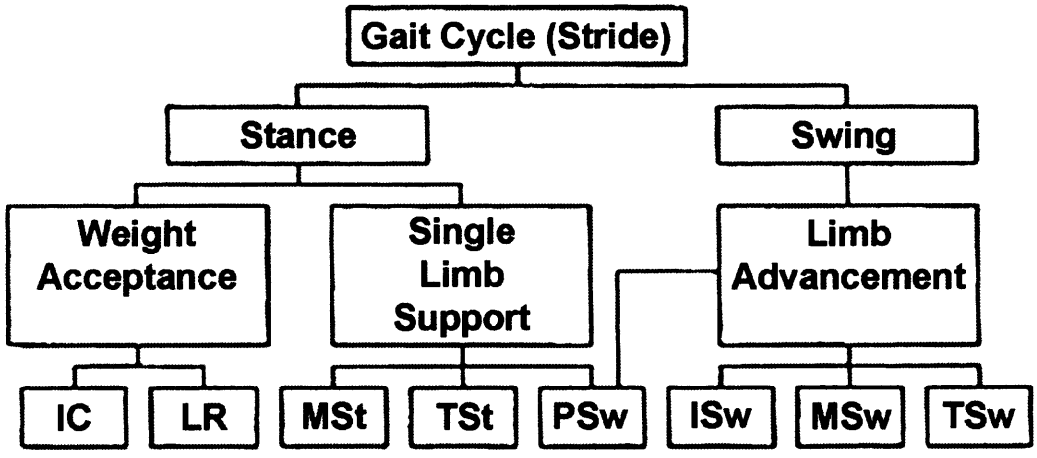

Figure 1.9 The subcatagories of the gait cycle [11].

Weight acceptance is subdivided into initial contact (IC) and loading response (LR). Initial contact marks the instant in time when the heel first comes in contact with the ground. At this point, the body prepares for the loading response. The loading response is characterized by the foot achieving complete contact with the floor and a shift of body weight to the stance limb. The end of the loading response phase is determined by the first peaking in the vertical force graph as shown in Figure 1.10, and marks the beginning of the midstance phase when the swing foot leaves the ground.

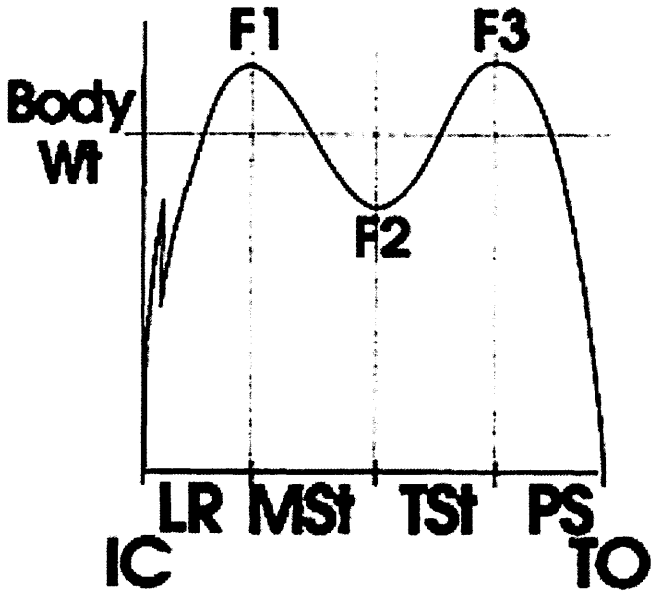

Figure 1.10 Vertical ground reaction force curve during normal walking from initial contact (IC) to toe off (TO) [11].

Single limb support is subdivided into midstance (MSt), terminal stance (TSt), and preswing (PSw). During midstance, the vertical ground reaction force vector travels along the stance foot until it reaches the forefoot. The dip in the vertical force graph represents the end of the midstance and the beginning of the terminal stance. Terminal stance can be visually noted by viewing the rise of the heel off of the ground. The vertical ground reaction force vector travels beyond the forefoot in this phase, which begins to load the leg muscles for propulsion. At the second peak of the vertical force graph, the swing foot makes its initial contact with the ground while the stance foot simultaneously begins to unload. The stance foot finishes unloading and enters its swing phase at the end of the preswing phase which is characterized by toe off.

Limb advancement is subdivided into initial swing (ISw), midswing (MSw), and terminal swing (TSw). Initial swing marks the beginning of the swing phase. It continues for the first one-third of the swing phase and ends when the knee reaches

maximum flexion. Midswing continues for the next 15%, being characterized mainly by limb advancement. Midswing ends once the tibia reaches the vertical position. Terminal swing marks the end of the swing phase as the tibia continues past the vertical position and the leg begins to brace itself for initial contact once again [11].

1.5.3 Gait Parameters

Three important terms used when discussing gait are velocity, cadence, and stride length [11]. Velocity is simply the distance traveled per unit time. Cadence, on the other hand, is the number of steps per unit time. It is essential that stride length is not confused with step length [11]. Step length is defined as the distance from a phase in the gait cycle on one foot to the corresponding phase on the other foot. Shown in Figure 1.11, stride length is defined as the distance covered by one foot to make one complete gait cycle, i.e. swing and stance.

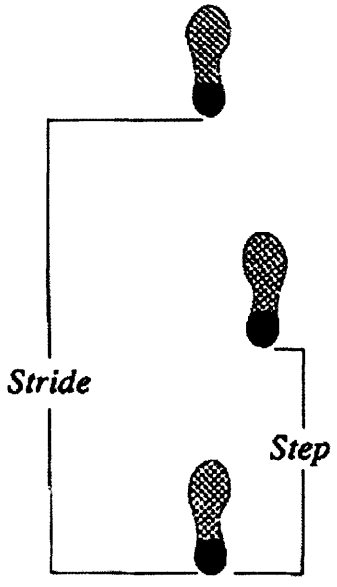

Figure 1.11 Stride length compared to step length [11].

1.6 Muscle Activation in the Leg During Walking

Walking is a very body intensive action [12]. Even though it may appear as though the legs are doing all of the work, movements of the upper body also have a great effect on the activation of muscles throughout the phases of walking. In addition, the way a person walks and precisely when their muscles activate varies from person to person based on their physical characteristics and their environment (i.e. clothing and shoes). The amount of variation is what uniquely identifies a person's gait.

1.6.1 Weight Acceptance

As previously discussed in Section 1.3, during normal walking, each leg is a half cycle out of phase with the other leg. At the beginning of the cycle, the upward angle of the foot allows the heel to strike first. As soon as the foot rolls into complete contact with the floor, the intrinsic muscles of the foot (shown in Figure 1.12) contract and change the foot into a lever, enabling it to absorb the stresses present and prepare for the next phase [12].

1.6.2 Single Limb Support

As the single limb support phase commences, the body moves forward and the ankle begins to dorsiflex. The knee moves through a small flexion wave caused by contraction of the hamstring muscles (biceps femoris, semimembranosus, and semitendinosus), and the hip extends by momentum, the gluteus maximus, and also by the hamstrings (Figure 1.14 and Figure 1.15). The gluteus medius and gluteus minimus abduct the right hip which maintains the level position of the pelvis and permits the contralateral swing phase to begin.

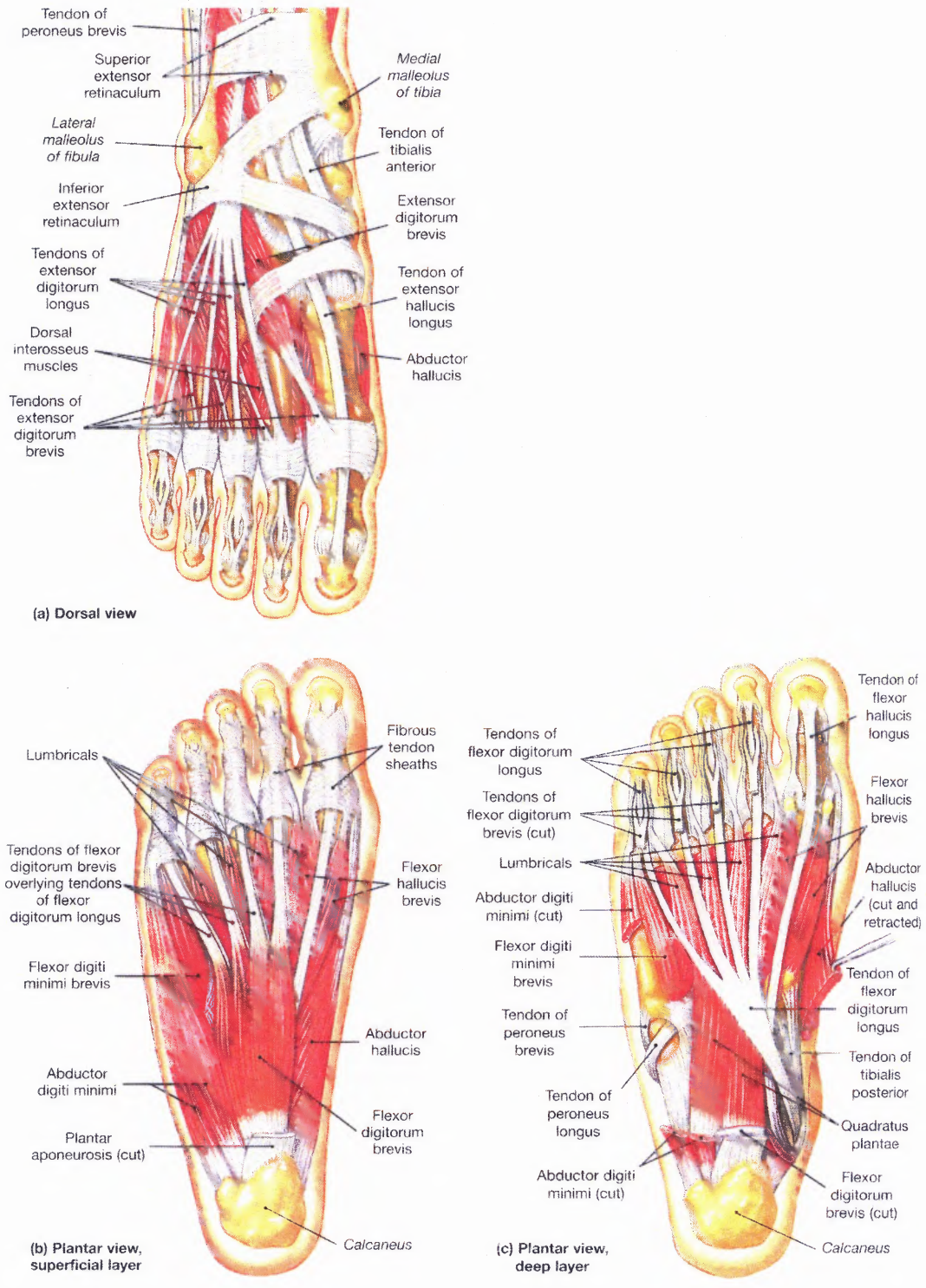

Figure 1.12 Intrinsic muscles of the foot [13].

At the end of the stance phase, the foot is preparing to propel the body and enter the swing phase by a strong plantarflexion of the ankle. This plantarflexion is brought on by means of the gastrocnemius and soleus in the calf (Figure 1.13). As the ankle is plantarflexed, the toes are being forced into extension. This extension of the toes is then being held by the toe flexors (Figure 1.12). With the quadracieps femoris holding the knee in extension, the energy released from the plantarflexed ankles then propels the body forward and begins the swing phase for that foot.

1.6.3 Limb Advancement

As the leg moves through the swing phase, there is a great deal of muscle activation. The toes are brought back into extension by the hallucis longus and the digitorum longus. The ankle is brought into dorsiflexion by the tibialis anterior and the extensor digitorum longus. The knee is brought into flexion by the hamstring muscles. The hip is brought into flexion by the psoas major, the iliacus, the rectus femoris, the sartorius, and the pectineus, and is rotated by the piriformis, the obturator internus, the obturator externus, the quadratus femoris, and the two gemelli (Figure 1.13, Figure 1.14, and Figure 1.15 below). When the leg begins the terminal swing phase, the muscle activations change yet again to prepare for initial contact once more. The dorsiflexors move the ankle and toes into a neutral position. The foot is inverted a small amount by the tibialis anterior and tibialis posterior (Figure 1.13). And lastly, the knee reaches almost full extension by contracting the quadriceps femoris (Figure 1.15).

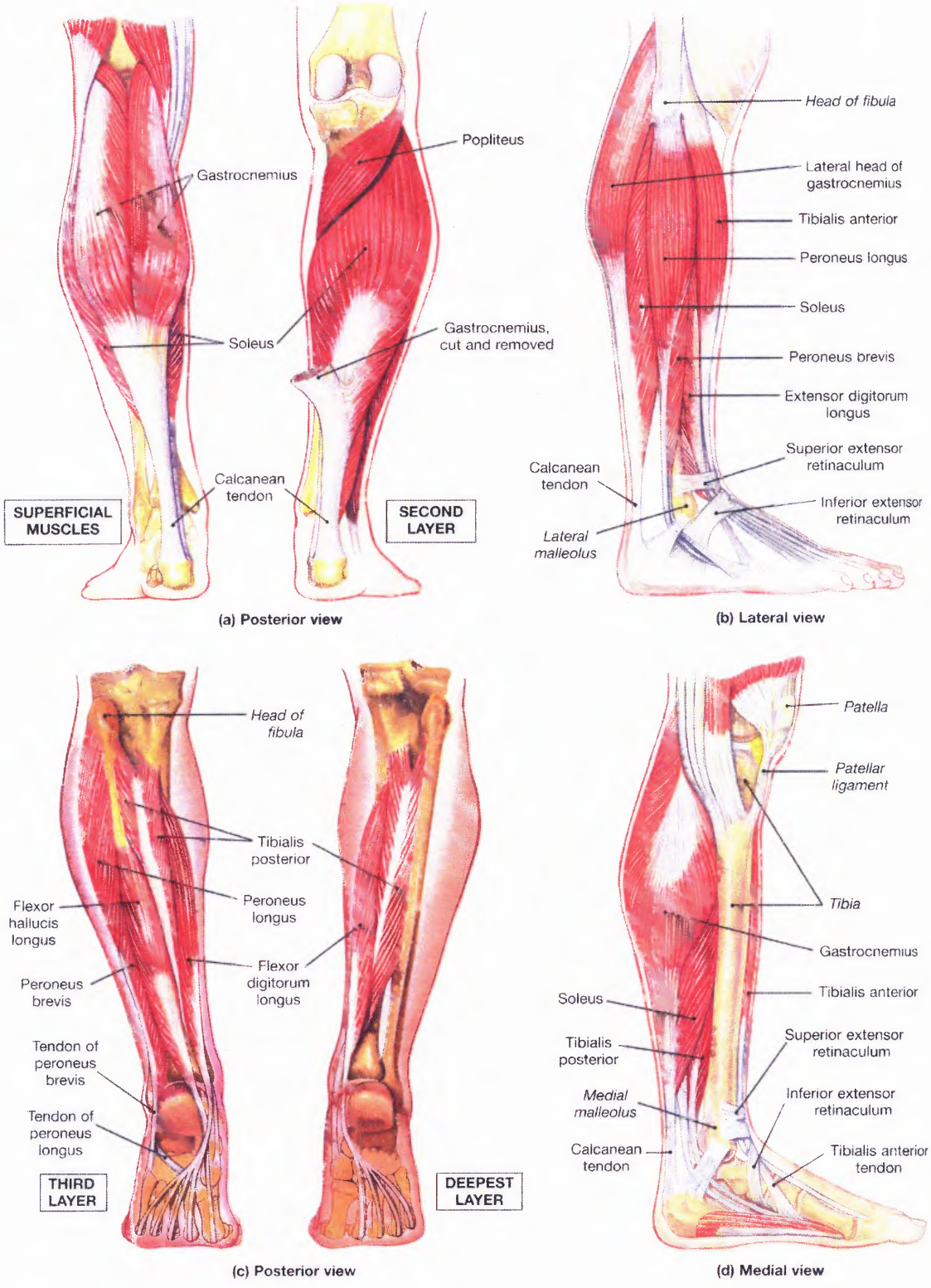

Figure 1.13 Muscles that move the foot and toes [13].

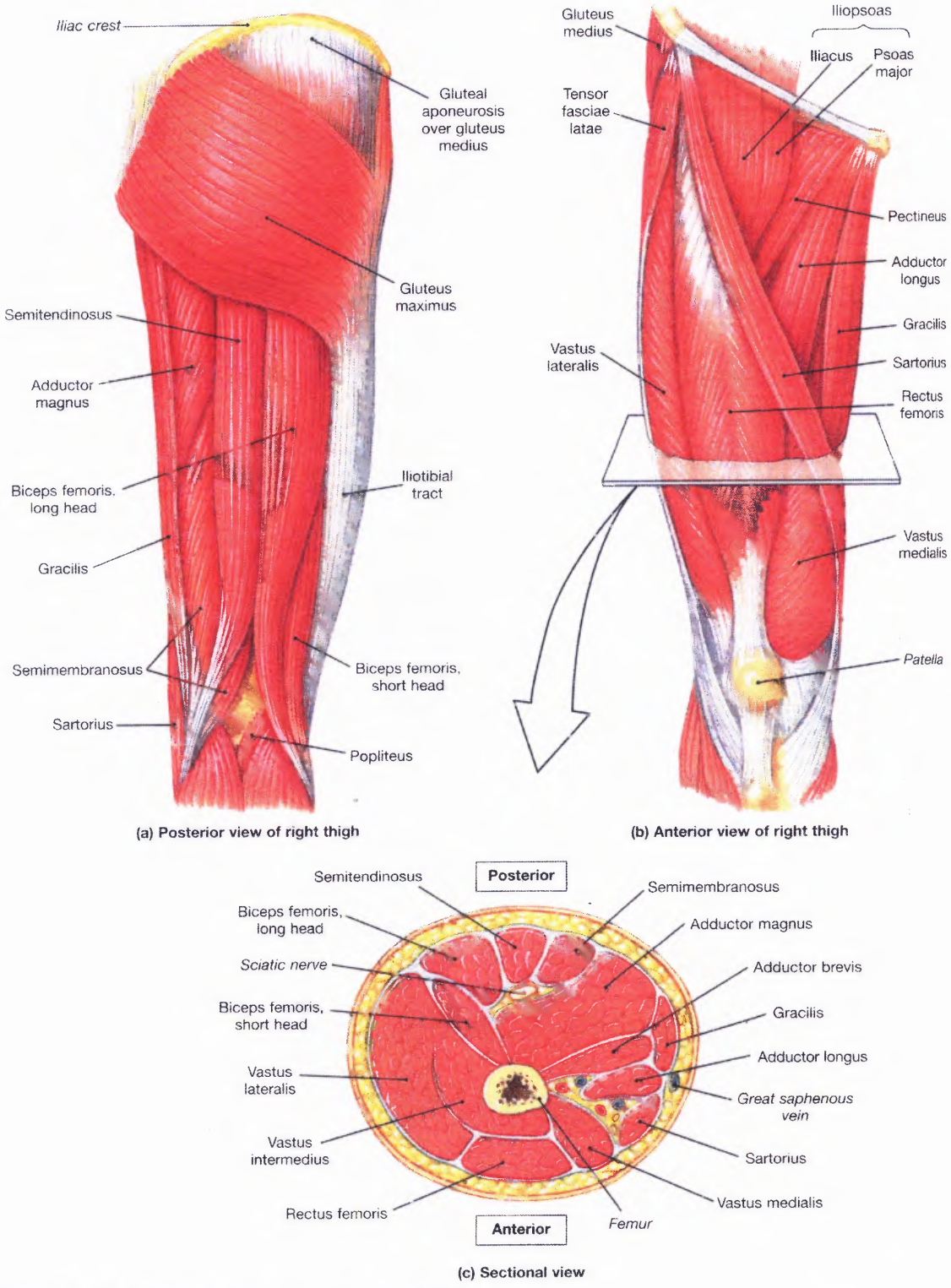

Figure 1.14 Muscles that move the leg [13].

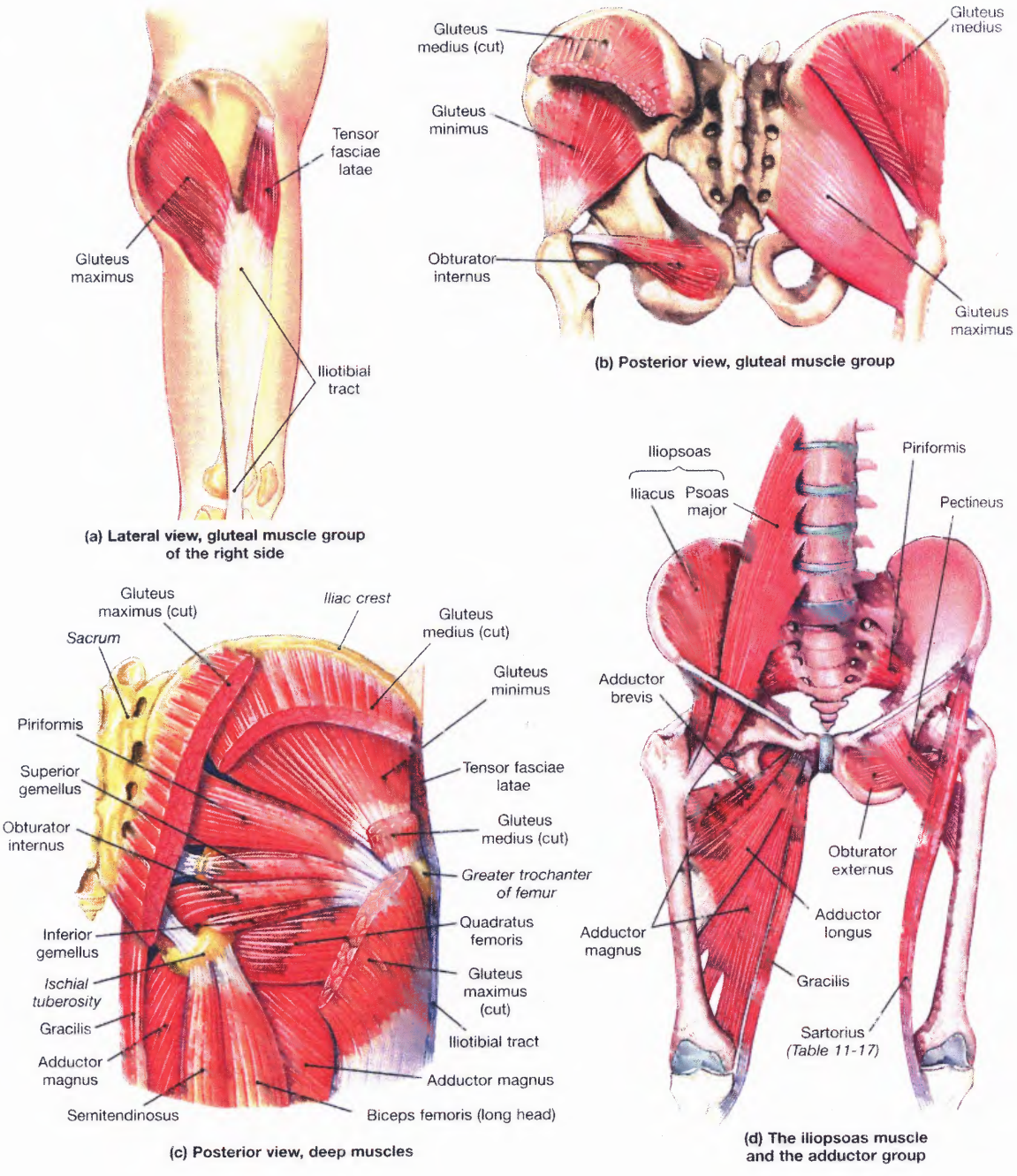

Figure 1.15 Muscles that move the thigh [13].

1.7 Muscle and Joint Anatomy of the Hand

Through evolution, the hand has been relieved of its duty to carry and propel the body and has become a tool with precise sensory discrimination that is important in everyday life [12]. This precise sensory discrimination is delivered through the fingers and thumb by means of their acute dexterity and sensitivity. The fingers allow the hands to grasp and manipulate objects, as well as provide feedback to the brain regarding local environments, such as texture and temperature. Since the scope of the research being covered deals with the index and middle fingers, only the anatomy of the fingers will be discussed in this section.

1.7.1 The Fingers

On the hand, there are five digits – four fingers and a thumb. As illustrated in Figure 1.16, the first digit is the thumb; second is the index finger; third is the middle finger; forth is the ring finger; and fifth is the little finger. Each finger contains three bones (phalanges) and three joints. The phalanges present are the proximal, middle, and distal. The joints are the metacarpophalangeal and two interphanageal joints – a proximal and a distal.

The fingers themselves are rather simple in nature. No muscles originate on the phalanges [13]. Rather, the intrinsic muscles that originate on the carpel and metacarpal bones provide the dexterity to the fingers via tendons that continue past the distal joint. A detailed view of the muscle architecture in the hand is in Figure 1.17.

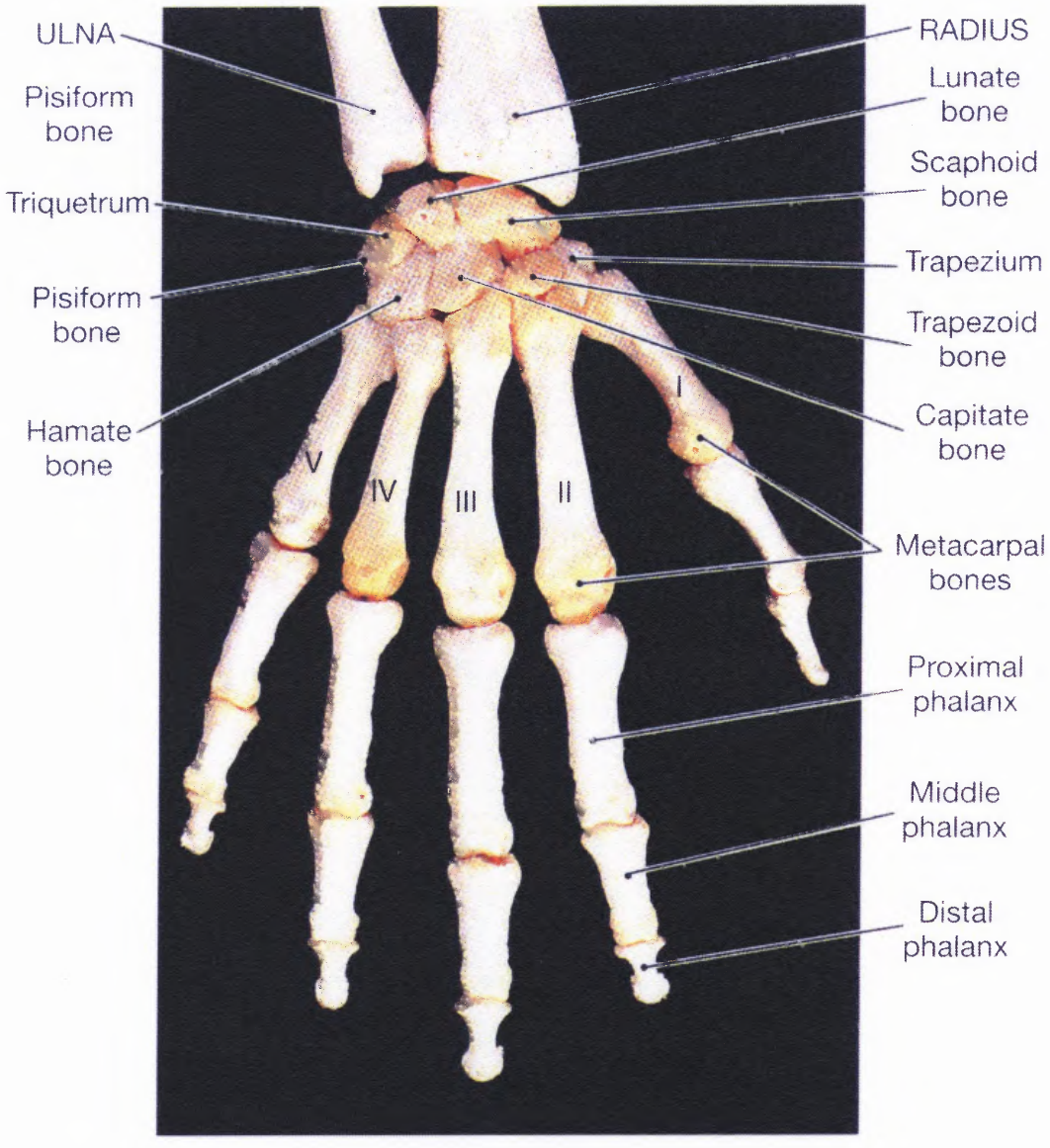

Figure 1.16 Posterior view of the right hand [13].

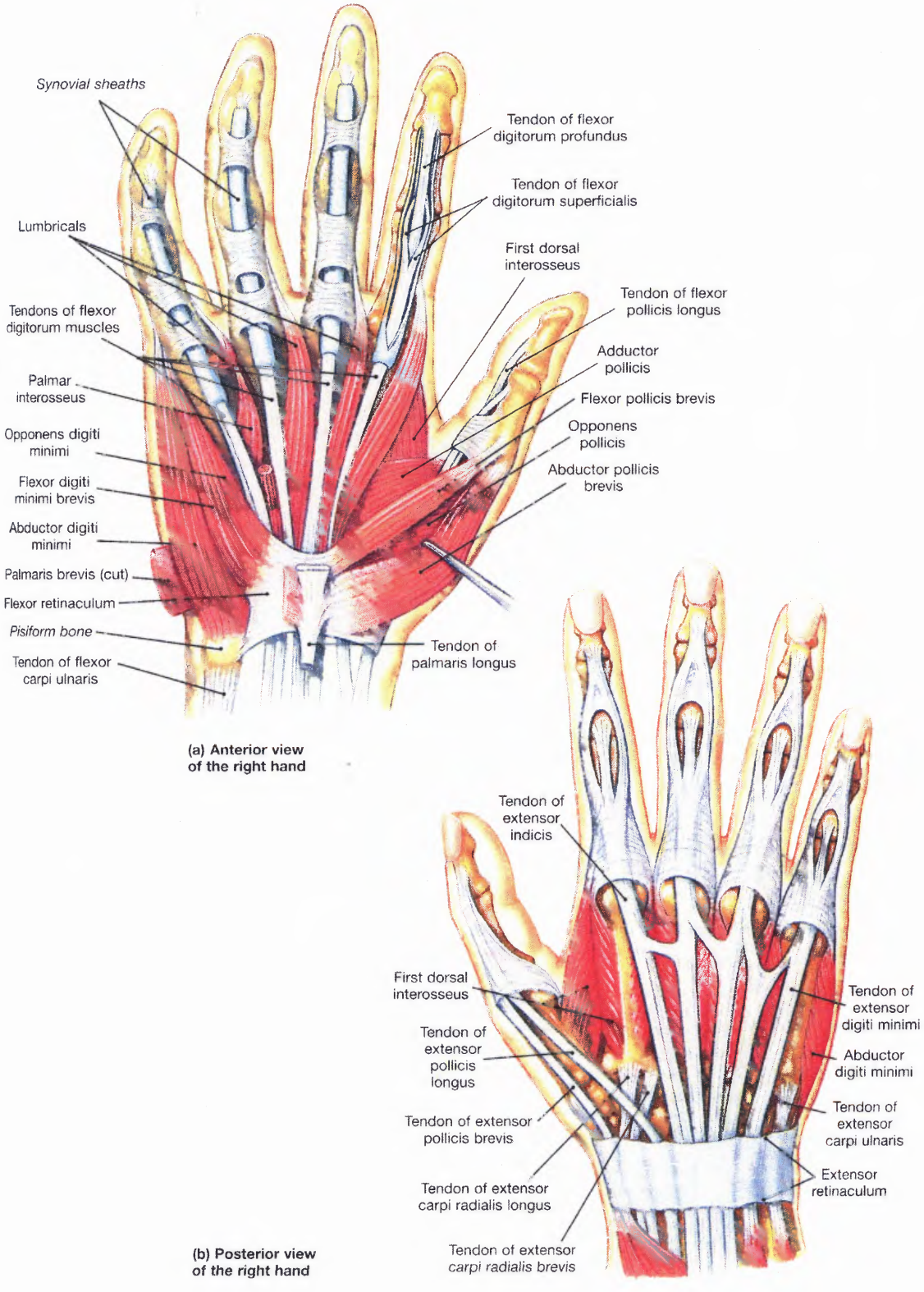

Figure 1.17 Intrinsic muscles of the hand [13].

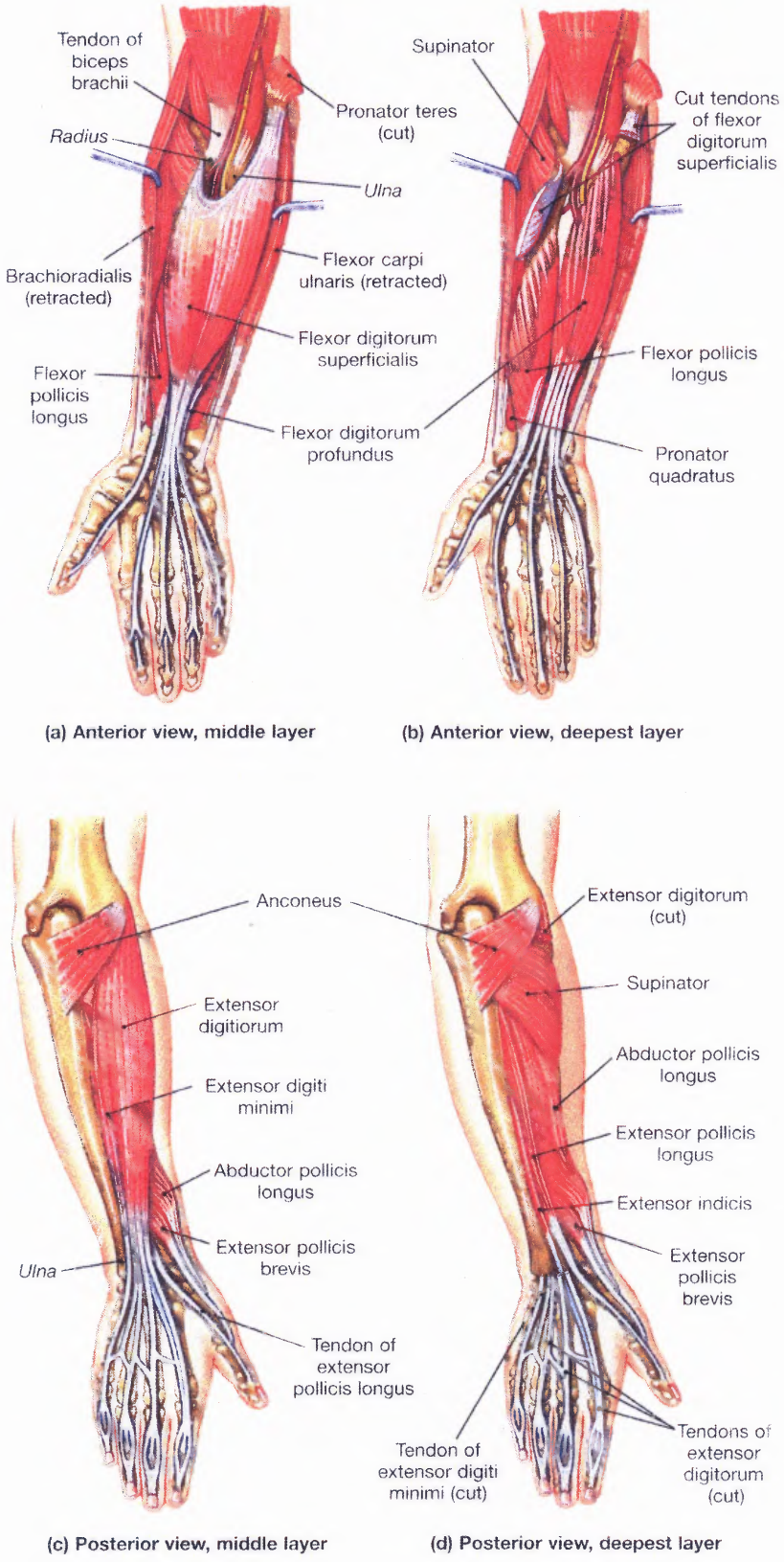

Figure 1.18 Arm muscles that move the hand and fingers [13].

1.7.2 The Metacarpophalangeal Joint

Each finger is capable of movement about the metacarpophalangeal joint in two axes. The movements are flexion and extension; and abduction and adduction as shown in Figure 1.19.

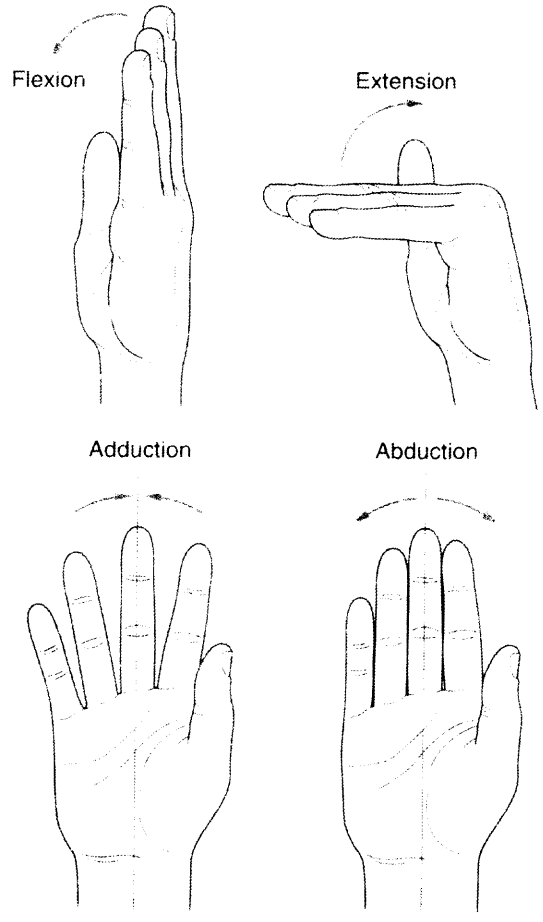

Figure 1.19 Active movements about the metacarpophalangeal joints [12].

In general, flexion at the metacarpophalangeal joint is produced by the lumbrical muscles with the help of the tendons of flexor digitorum profundus and superficialis, as well as the interossei (refer to Figure 1.17 and Figure 1.18). Flexion in the little finger is aided by the flexor and abductor digiti minimi. Extension about the metacarpophalangeal joints in all of the fingers is produced by the extensor digitorum, with the extensor indicis

aiding in the extension of the index finger, and the extensor digiti minimi aiding in the extension of the little finger. Total approximate range of active flexion and extension for the index finger is 148°, 145° for the middle finger, 149° for the ring finger, and 152° for the little finger [12].

Abduction and adduction at the metacarpophalangeal joint occurs in a direction towards or away from the middle finger. When the finger is in full extension, the range of side-to-side movement can be as much as 30°, however, in flexion, the tension in the collateral ligaments limits the side-to-side movement to a maximum of 10° [12].

Abduction at the metacarpophalangeal joint is, in general, produced by the dorsal interossei for the index, middle, and ring fingers, and by the digiti minimi for the little finger. Assistance can be provided by the first and second lumbricals for the index and middle fingers. Adduction is produced by the palmar interossei for all fingers. Assistance can be provided by the third and fourth lumbricals for the ring and little fingers, and if in flexion, from the digitorium superficialis and profundus.

1.7.3 The Interphalangeal Joints

Movement about the interphalangeal joints is limited solely to flexion and extension since they are simple hinge joints. As shown in Figure 1.20, flexion and extension occur on an oblique transverse axis for the middle, ring, and little fingers. This allows those fingers to oppose the thumb more easily. Alternatively, the index finger moves in a transverse axis in a sagittal plane [12].

Flexion is produced at the proximal interphalangeal joint by the flexor digitorum superficialis with assistance from the flexor digitorum profundus. Flexion at the distal interphalangeal joint is produced only by the flexor digitorum profundus. Extension of

the interphalangeal joints is produced by the lumbrical and interossei with assistance from the extensor digitorum in each finger and by the extensors indicis and digiti minimi of the index and little fingers.

The range of flexion at each interphalangeal joint varies with each finger. The proximal interphalangeal joint is capable of more than 90° of flexion on each finger with a maximum of 135° occurring at the little finger. The distal interphalangeal joint has a maximum of 90° of flexion on the little finger and a gradual decrease towards the index finger. Active extension of the interphalangeal joints is minimal with the distal joints having no more than 5° of motion and the proximal having no more than 2° of motion [12].

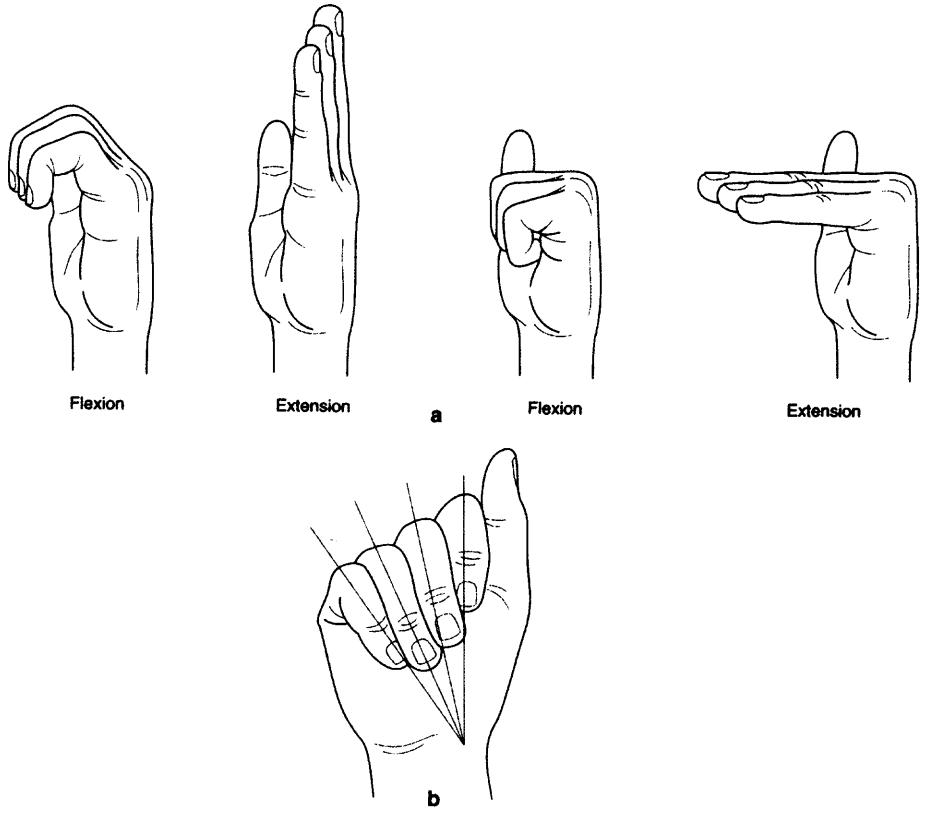

Figure 1.20 (a) Flexion and extension of the interphalangeal joints with and without flexion at the metacapophalangeal joint, (b) transverse axis of the fingers showing opposition with the thumb [12].

CHAPTER 2

INSTRUMENTATION

2.1 Gait Recording

The two main properties of gait that can be recorded digitally on a personal computer are position and ground reaction force. Position tracking can be achieved using magnetic, video, mechanical, or ultrasonic based technology. Forces can be measured using many different systems, some of which include strain gages, piezoelectric crystals, or hydraulic/pneumatic load cells.

For this research, position tracking was performed using a magnetic field based system, while ground reaction force data was collected using a silicon strain gage transducer system.

2.2 Position Tracking

2.2.1 Hardware

To record the position of the feet during normal human gait and the position of the finger tips during finger gait, the Flock of Birds by Ascension Technology Corporation was used (see Appendix B). Shown in Figure 2.1, the Flock of Birds is a magnetic tracking system capable of recording both position and orientation in six-degree-of-freedom motion. It connects to a personal computer via a RS-232 (serial port) connection. The system can simultaneously record data from up to four sensors per transmitter when connected in a master/slave configuration [14]. Each sensor has a tracking range of up to 1.2 meters from the transmitter. The static accuracy for position and orientation of each

sensor is 1.8 mm RMS and 0.5° RMS within a range of 76.2 cm from the transmitter. The static resolution for position and orientation of each sensor is 0.5 mm and 0.1° within a range of 30.5 cm [14]. Dynamic accuracy and resolutions were not provided by the manufacturer.

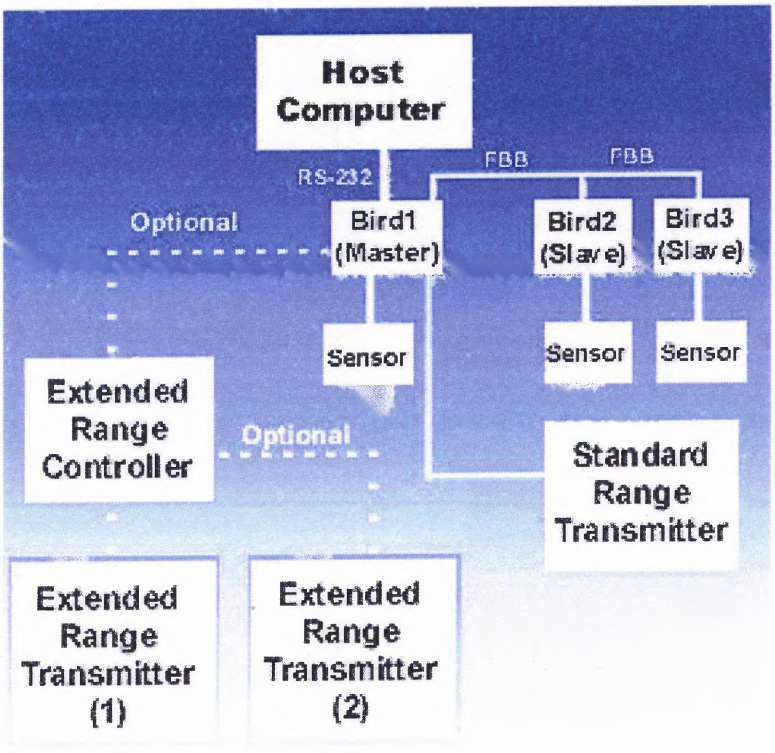

Figure 2.1 Flock of Birds schematic diagram [14].

The main components of the Flock of Birds unit are the base unit ("Bird1" in Figure 2.1), sensor, and transmitter. The transmitter contains three concentric antennae that generate a DC magnetic field which is picked up by the sensors. The sensors contain three orthogonal antennae that are sensitive to the DC magnetic field of the transmitter and the DC magnetic field of the earth.

After the Flock of Birds base unit is turned on, but prior to the transmitter initialization, a baseline reading of the earth's magnetic field is recorded internally. Once the transmitter is initialized, the base unit can then determine the position of the sensors relative to the transmitter by interpreting the magnetic signals picked up in the sensor antennae. The base unit can also determine the absolute orientation of the sensors by first determining their orientation relative to the transmitter through the magnetic field, then subtracting out the baseline reading of the earth's magnetic field taken before initialization of the transmitter. Once the base unit has received all position and orientation data for that instant in time, it filters the data for noise, amplifies it, and then converts it to a digital form usable by the personal computer connected via the RS-232 cable [15].

2.2.2 Software

After the signal is sent from the Flock of Birds base unit to the computer through the RS-232 cable, it must be converted into a form that is valuable to the end user. For this specific purpose, Robert De Marco [16] has developed an easy-to-use interface with National Instrument's LabView, called CyberFlock. A version of De Marco's software that is publicly available on National Instrument's web page was used for this research. The version used, shown in Figure 2.2, allows for two Flock of Birds units to communicate with the computer.

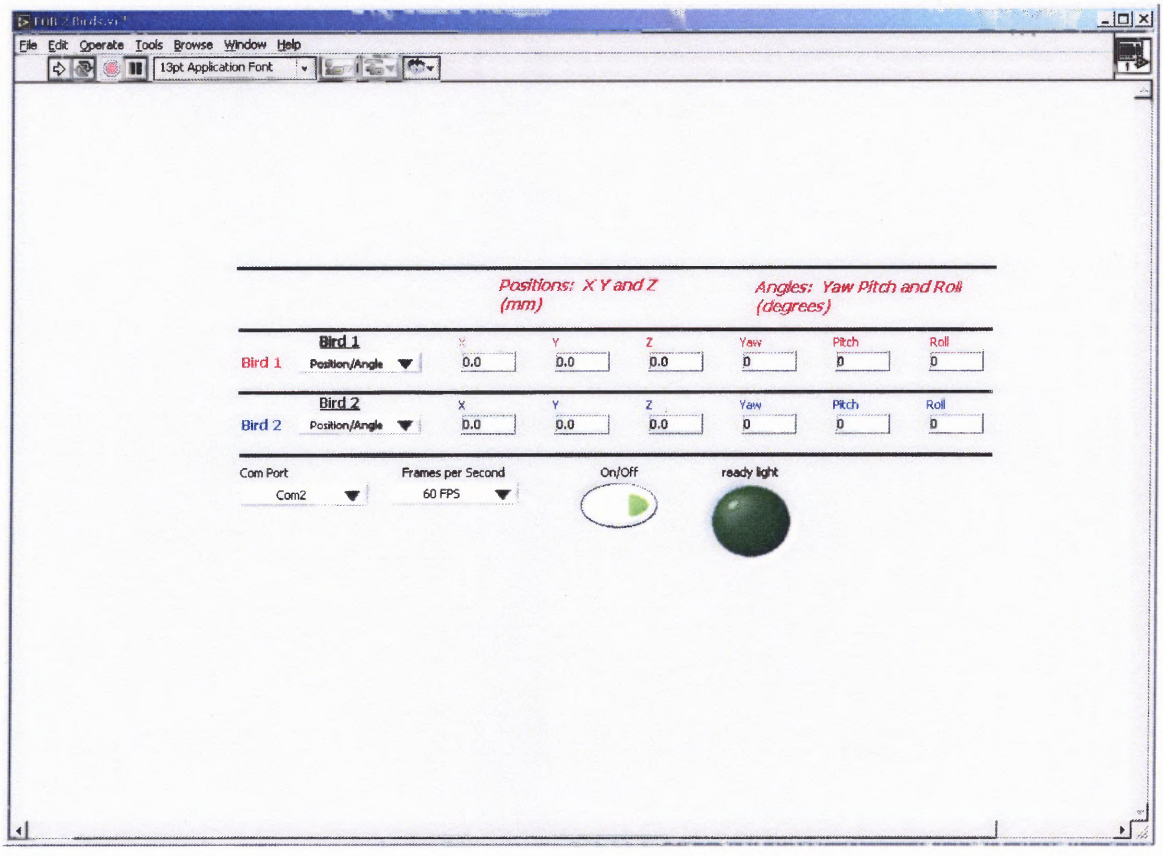

Figure 2.2 CyberFlock user interface in LabView 6.0.

CyberFlock has the ability to collect the position/angle, position/matrix, position/quaternion, or just position, angle, matrix, or quaternion data for one or two base units. The communication ports available are COM1 through COM4, and the available frame rates are 20, 30, 40, 50, and 60 FPS. Once all of the selectable options have been made, the program is started using the **Run** button. A window opens asking where to save the data file, which can be saved to a file usable by Microsoft Excel (.xls or .txt). Once opened in Excel, various forms of analysis and comparison can be performed. The data can also be exported to a generic text file readable by MatLab where the data can be filtered. The filtered data can then be exported back into the generic text file and imported into Excel for interpretation.

2.3 Force Recording

2.3.1 Hardware

To record the ground reaction force generated by the finger tips during finger gait, the Mini40 F/T (Force/Torque) transducer made by Assurance Technologies, Inc. – Industrial Automation (ATI-IA), was used (see Appendix C). The Mini40 uses a monolithic instrumented transducer made of silicon strain gages. It is capable of measuring all six components of force and torque (Fx, Fy, Fz, Tx, Ty, and Tz) with a resolution of 0.16 N (0.02 pounds) and 0.16 N-m (0.02 foot-pounds) within the calibrated operating ranges shown in Table 2.1 [17].

In general, silicon strain gages are made from the 'n' or 'p' type silicon. They have a ratio of relative change in resistance to applied strain (gage factor) equal to 100 – 150, whereas alternative strain gages have a gage factor of 2 – 4 [18]. Transducers made with silicon strain gages are used for forces ranging from 1 N to 10 kN and have an error range of ± 0.2 – 1% of the full scale output [19].

Table 2.1 Maximum Calibrated Operating Ranges of the Mini40 F/T [17]

Direction	Maximum Force	Maximum Torque
X	20 lbs	40 in-lbs
	80 N	4 N-m
Y	20 lbs	40 in-lbs
	80 N	4 N-m
Z	60 lbs	40 in-lbs
	240 N	4 N-m

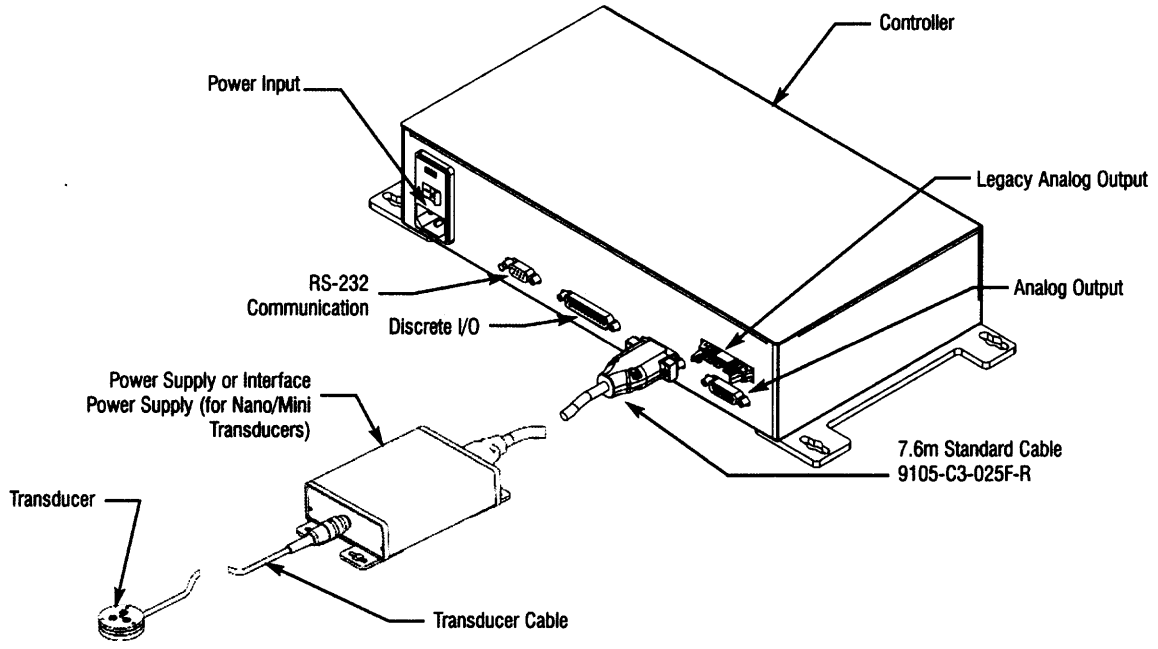

Figure 2.3 Mini40 F/T transducer system [17].

As shown in Figure 2.3, the transducer senses the forces and torques, and sends a signal back to the interface power supply (mux box) that sends a higher-level output signal back to the controller. The controller processes the signal, converts it to data usable by the host computer, and then sends the data to the interface software on the host computer where it can then be saved and analyzed [17].

2.3.2 Software

When the Mini40 F/T data reaches the computer at the RS-232 port, it is received by software provided by ATI-IA. The software interface, ATI Stand-alone F/T Demo, shown in Figure 2.4, is an easy-to-use graphical user interface (GUI) of the output from the transducer.

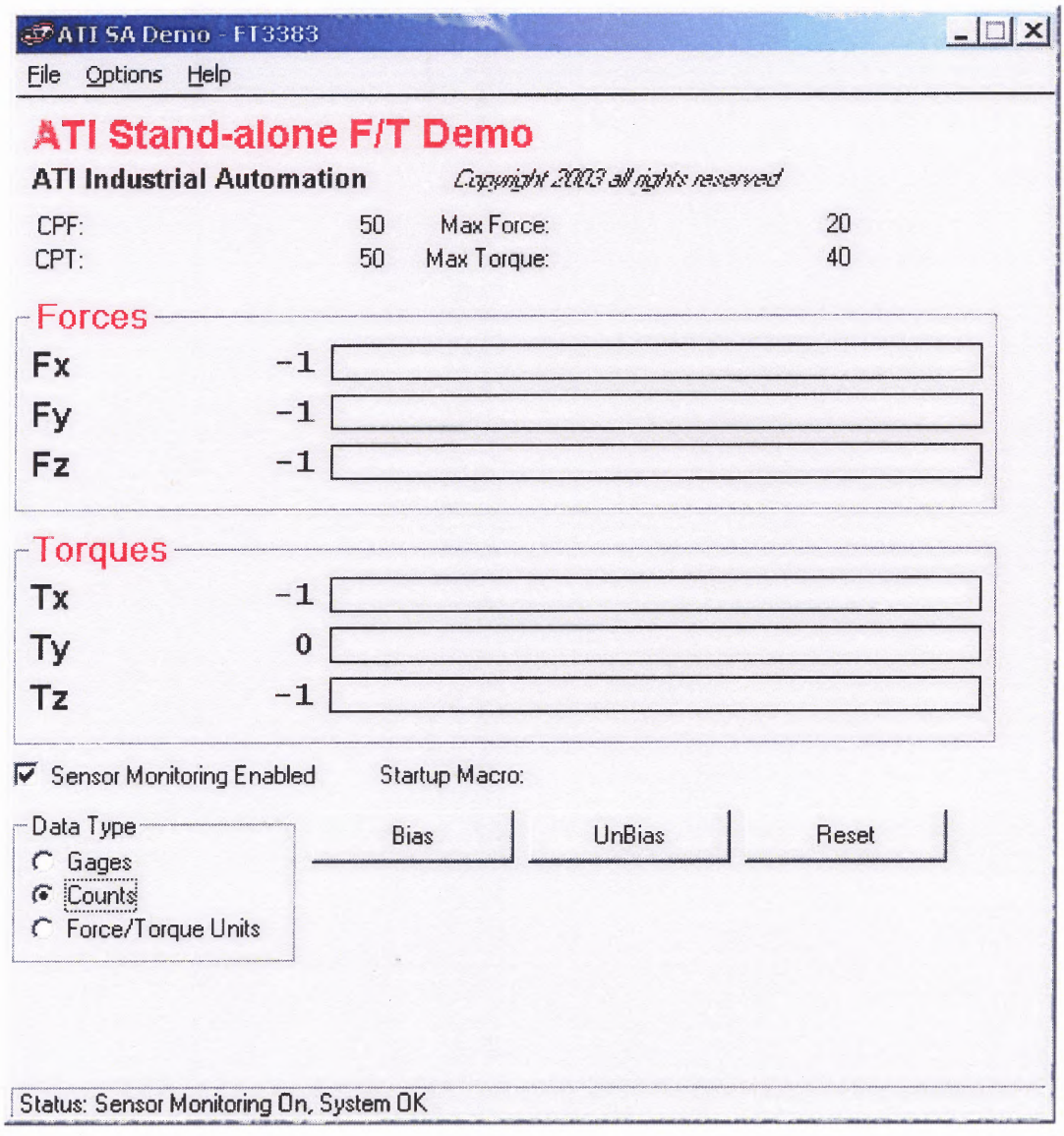

Figure 2.4 ATI Stand-alone F/T Demo GUI.

The force and torque data can be displayed in three formats – the gage data, counts, or in the force/torque units. **Gages** displays the readings taken by each of the individual gages. **Counts** simply displays the output on a scale of 1 to 1000 with 50 counts equaling one pound or one foot-pound. Finally, **Force/Torque Units** displays the actual force reading in pounds and the torque reading in foot-pounds.

When the transducer is first initialized, like any sensitive electronic load cell, it must be zeroed using the **Bias** button. If the bias needs to be removed, the **UnBias** button can be selected. Should the controller box need to be reset, it can be done so using the **Reset** button on the GUI.

Within the **Options** menu, the user can change and/or verify various operating parameters of the controller. For this research, the pertinent screens under the **Options** menu are the **Calibration** screen and the **Reading Data** menu. Shown in Figure 2.5, the **Calibration** screen is where the user can verify the calibration of the controller box and the capabilities of the transducer. Shown in Figure 2.6, the **Reading Data** menu is where the user can specify various options used for data recording.

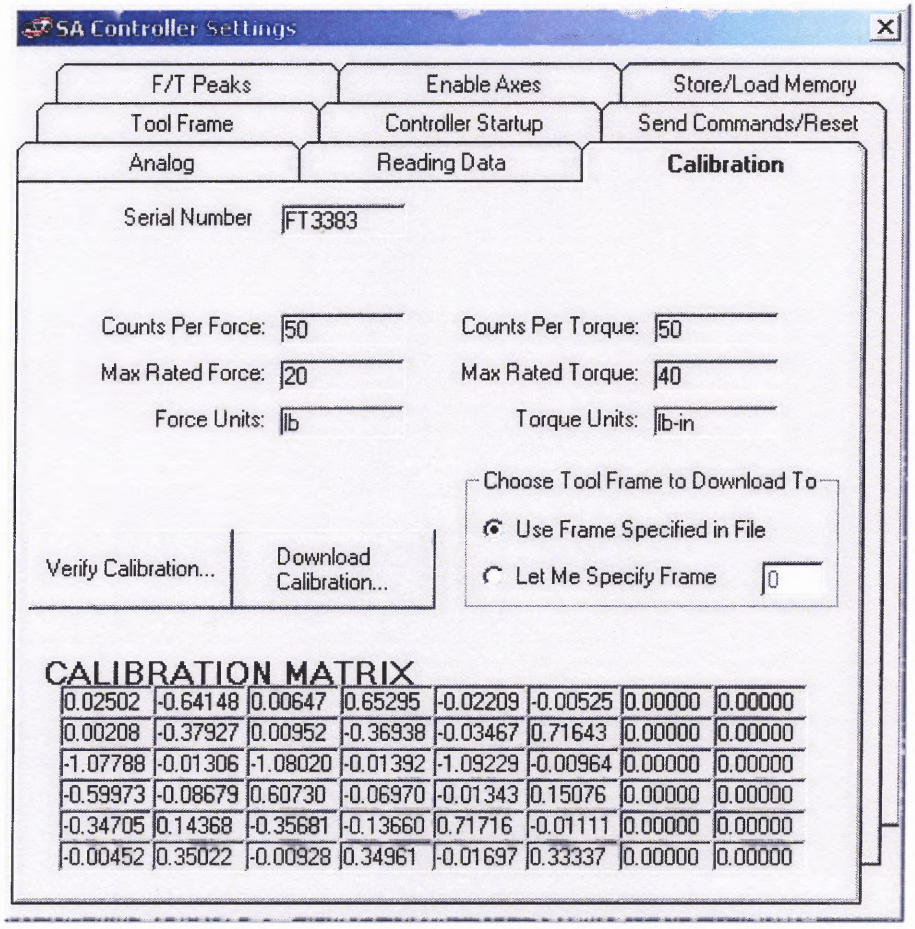

Figure 2.5 Force plate controller calibration screen.

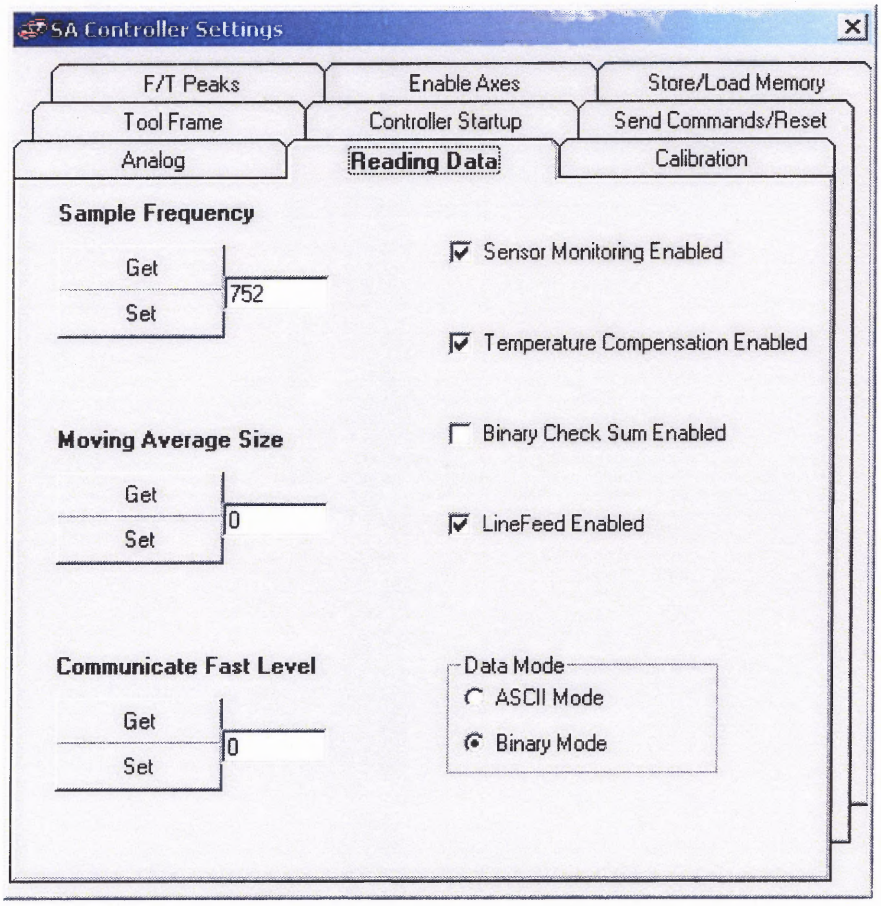

Figure 2.6 Force plate data reading options menu.

Also within the **Options** menu, the user can choose to collect the data and store it in a file for later use. Shown in Figure 2.7 is the **Collect Data** screen where the user has the option to collect data for a specific number of data records, a specific amount of time, or until a stop button is pressed. In addition, there are options to begin collecting data when a specific reading on the transducer is encountered, to gather data in gage units or in resolved counts, and to place a time/date stamp on each data point. The output of the file can be stored in a format usable by Microsoft Excel (.xls or .txt) where it can be analyzed later or exported to MatLab for filtering and processing.

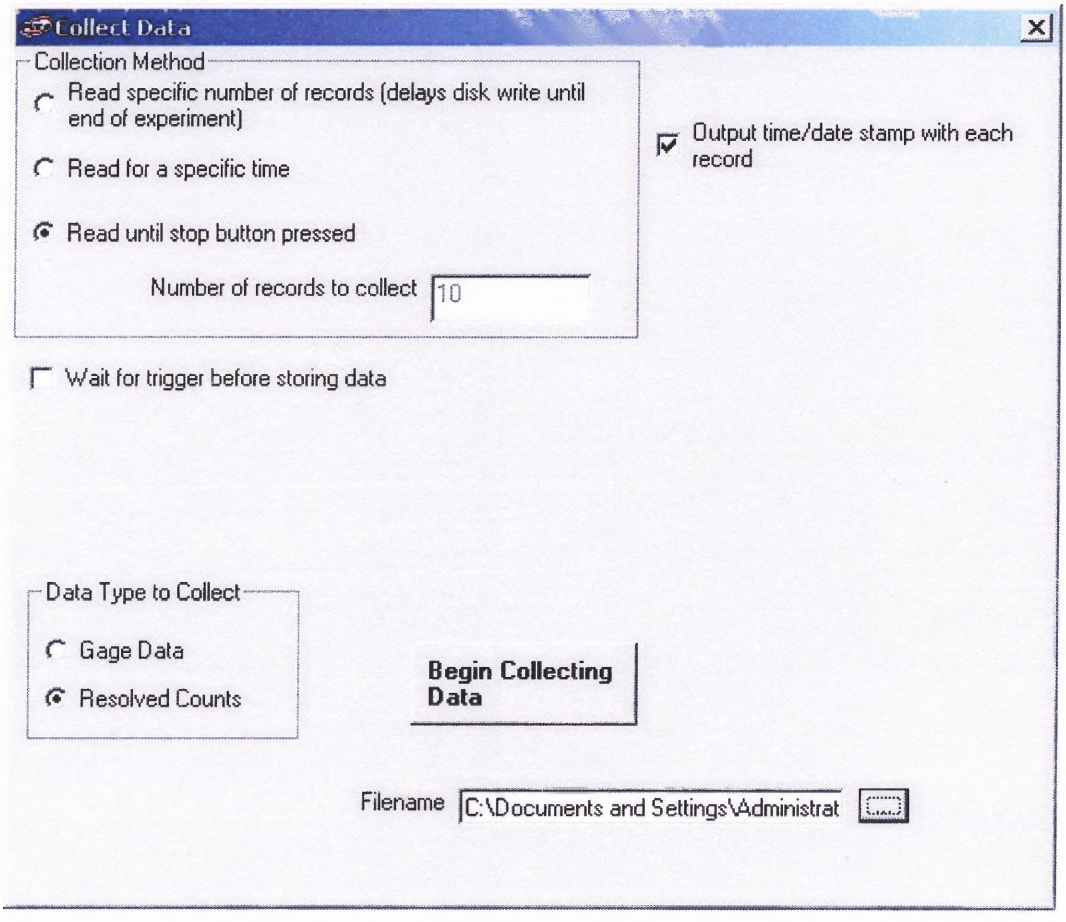

Figure 2.7 Force plate data collection screen.

CHAPTER 3

METHODOLOGY

3.1 Initial Experimentation

The Flock of Birds transmitter and the Mini40 transducer were placed in the configuration shown below in Figure 3.1. During initial experimentation, three issues arose with the hardware configuration that needed to be addressed in order to ensure accurate data.

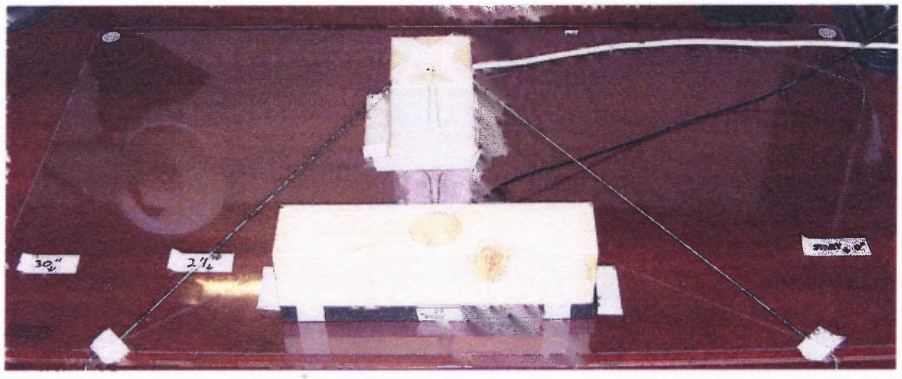

Figure 3.1 Equipment configuration.

3.1.1 Flock of Birds Transmitter Diagonals

While trying to record finger motion data with only the Flock of Birds present in the configuration, it was discovered that there was a significant error in the data produced along the diagonals extending from the transmitter. The diagonals are represented by the white strings mounted on the transmitter in Figure 3.1. When a Flock of Birds sensor passed a diagonal during data collection, a momentary inconsistency was observed in the data plots. Figure 3.2 shows what happens when a sensor is moved horizontally along the table surface from the starting point to 76.2 cm (30 inches) away.

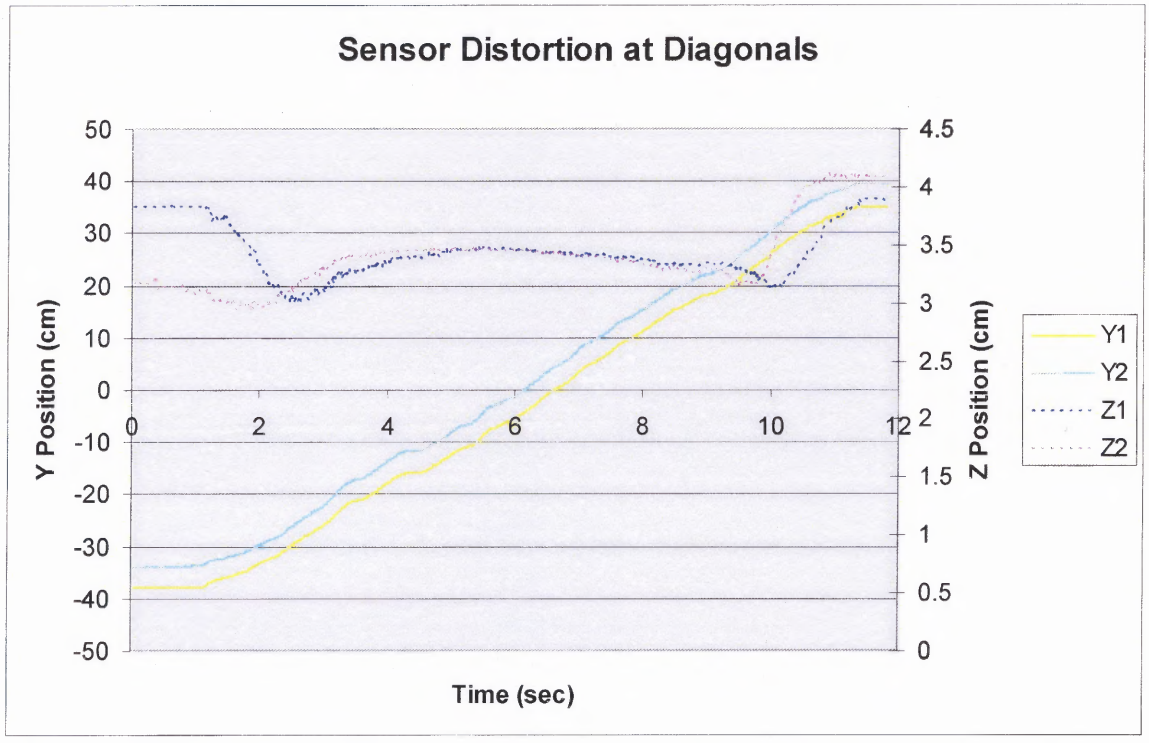

Figure 3.2 Flock of Birds sensor distortion observed at the diagonals of the transmitter.

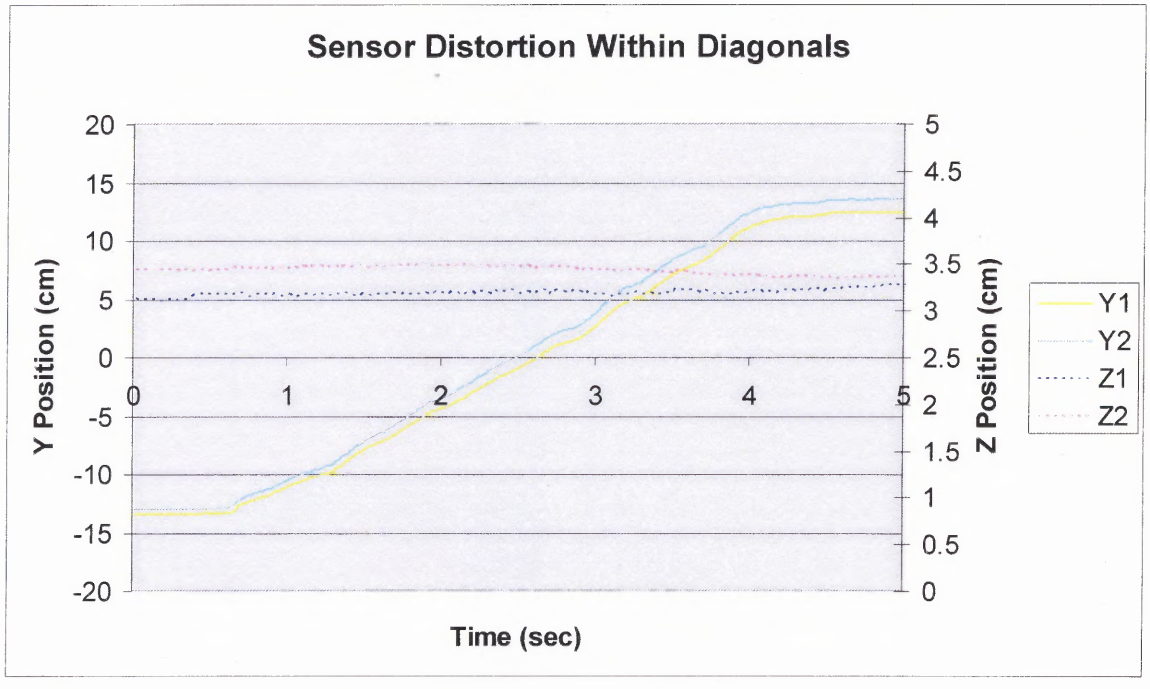

Figure 3.3 Flock of Birds sensor distortion observed within the diagonals of the transmitter.

In Figure 3.2, the Y and Z position of sensor one and sensor two are plotted against time. The Z position was held constant by sliding the sensors across the table. Observed is a maximum difference in the Z position of 0.894 cm (0.352 inches) for sensor one and 1.194 cm (0.470 inches) for sensor 2. The change in Y direction was approximately 73.66 cm (29 inches) for both sensors.

Shown in Figure 3.3, the same test was performed while keeping the sensors well within the diagonal lines yielded a maximum difference in Z location of 0.190 cm (0.075 inches) for sensor one and 0.168 cm (0.066 inches) for sensor 2. The change in Y direction was approximately 26.67 cm (10.5 inches) for both sensors. In an effort to minimize the Z distortion during data collection, all data was gathered between the diagonals illustrated by the white lines in Figure 3.1.

3.1.2 Force Plate Distortion of the Flock of Birds Magnetic Field

The second configuration issue that needed to be addressed was the proximity of the Flock of Birds sensor to the force plate transducer during simultaneous data recording. Because the force plate transducer contains ferrous material, it produced a large distortion in the magnetic field generated by the Flock of Birds transmitter. Shown in Figure 3.4, this distortion caused the Flock of Birds sensor to misreport their position in space.

To perform this test, Flock of Birds sensor one was moved along the surface of the force plate runway, maintaining a constant Z-position in space. When the sensor came within close proximity of the force plate, the distortion in the Z-direction was clearly in excess of 15 cm at the maximum.

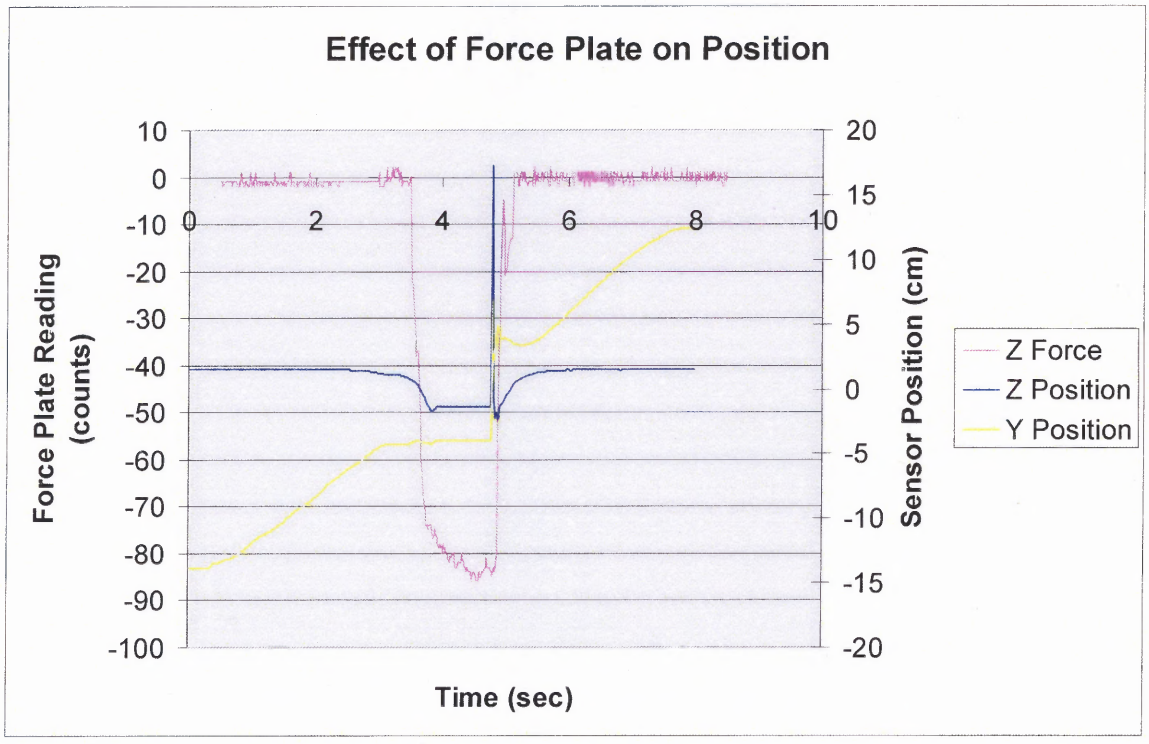

Figure 3.4 Effect of force plate proximity on Flock of Birds sensor.

To overcome this, a wooden isolator was fabricated. The isolator is shown in Figure 3.1 and more clearly in Figure 3.5. It consists of a 6.4 cm (2.5 inch) thick block of wood containing a free-floating plug over the force plate transducer. Use of the isolator may inhibit readings of force in directions other than the Z-direction; however, without the isolator no position readings would be acceptable.

Shown in Figure 3.6, the wooden isolator was able to reduce the error in Z-position reading to the same level seen without the force plate in use. The maximum recorded Z-position error was 0.102 cm (0.040 inches) over the length of the force plate runway.

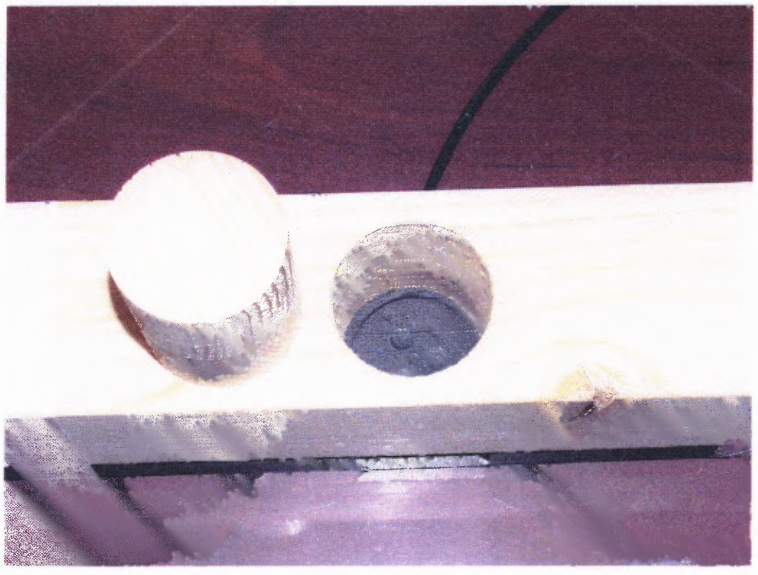

Figure 3.5 Wooden isolator mounted on force plate runway with plug removed.

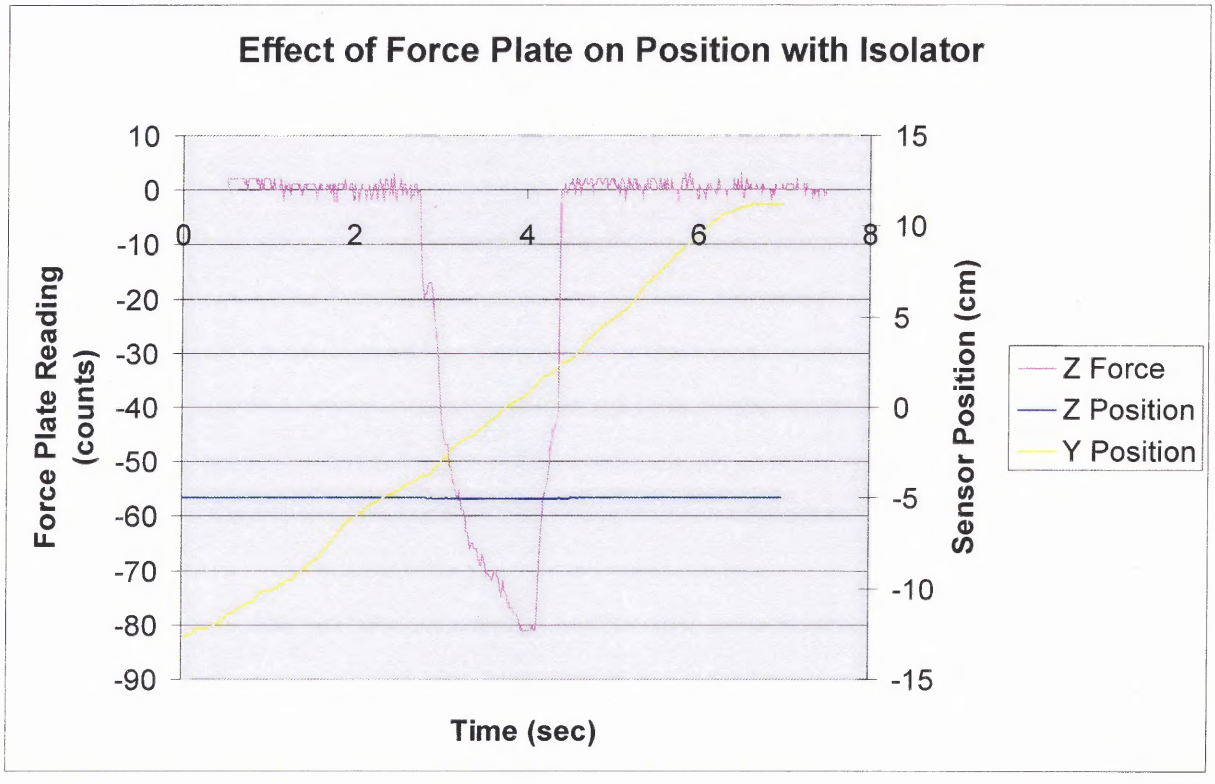

Figure 3.6 Effect of force plate proximity on Flock of Birds sensor with isolator present.

3.1.3 Force and Position Data Synchronization

The final source of inconsistency arose during the synchronization of the force and position data. Because the force and position data were recorded using two independent devices and software packages, the time at which the incoming data are time-stamped varies, and the rate at which data are sampled varies. In order to determine the phase shift, a test was performed where one Flock of Birds sensor was slowly raised and lowered on to the wooden force platform extension. When the Flock of Birds sensor began its rest period on the wooden extension, the force plate would obtain readings until the sensor began to move again. Figure 3.7 shows that there is a phase lag in the Z-position data.

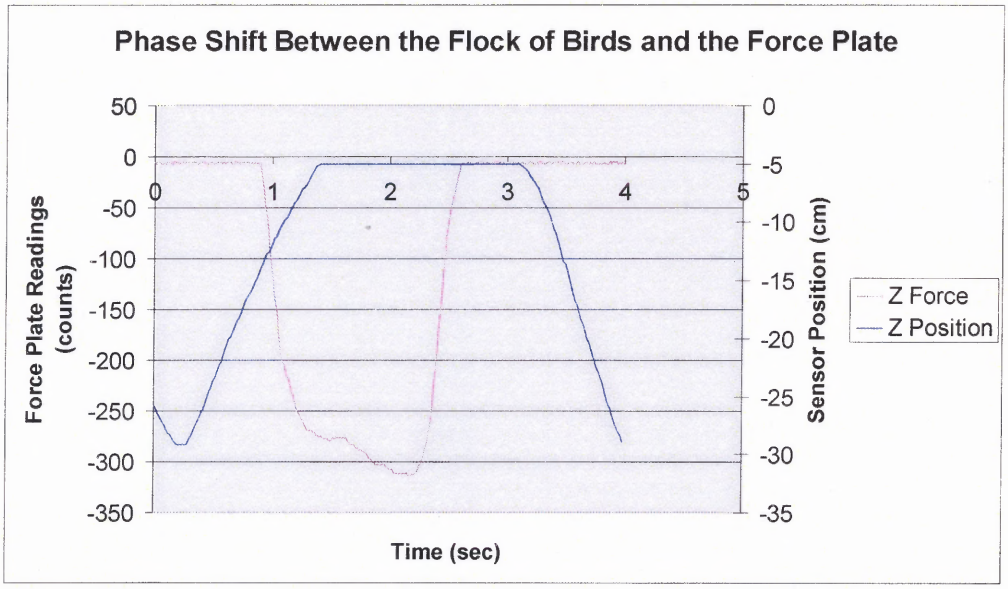

Figure 3.7 Phase shift between the Flock of Birds and ATI-IA force plate.

By adding time to the force plate time-stamp, it was found that the two data sets were out of phase by 0.49 seconds. Shown in Figure 3.8 is how the data looks with the phase shift correction factor of 0.49 seconds.

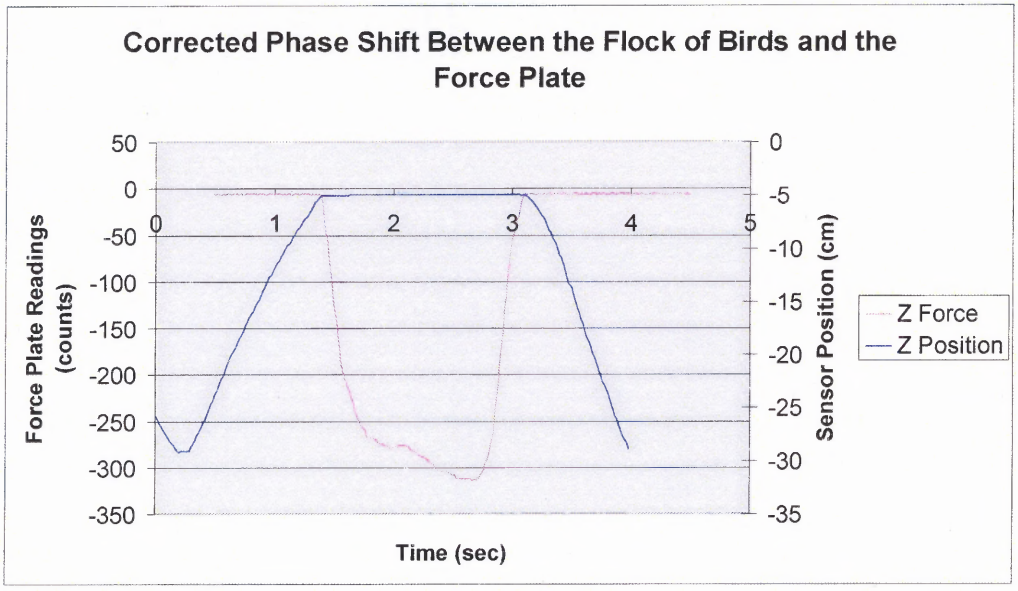

Figure 3.8 Corrected phase shift between the Flock of Birds and ATI-IA force plate.

It was also observed that the force plate data was sampled at a higher frequency than the sensor position data. In order to compensate for this, the sampling frequency had to be calculated and a relative time stamp given to each data point. Any data points which were not part of a full second on the time stamp were removed. The total number of data points were counted and then divided by the number of total seconds to find the actual sampling rate. Theoretically, the sampling rate for the Flock of Birds was set to 60 Hz and the ATI-IA F/T Mini40 was unknown. However, it was found that the Flock of Birds sampled data at approximately 58 Hz, while the ATI-IA F/T Mini40 sampled data at approximately 73 Hz. Knowing the exact sampling frequency for each set of data, a relative time stamp can then be given to each data point to ensure that the force point matches the simultaneous position point.

3.2 Data Collection

Data collected for this research consists of finger tip position and finger tip ground reaction force during "finger walking", and leg position during normal human gait. In addition, published human gait position and ground reaction force data [20] was utilized for comparison. Shown in Figure 3.9 are the two Flock of Birds base units used for this research. They were set up in a master/slave configuration using one standard range transmitter. Since the Extended Range Controller and the Extended Range Transmitter were unavailable, all data was gathered within the 1.2 m accuracy range. Above the Flock of Birds base units in Figure 3.9 is the ATI-IA controller box with the smaller mux box on top. The sensors were arranged as shown in Figure 3.1.

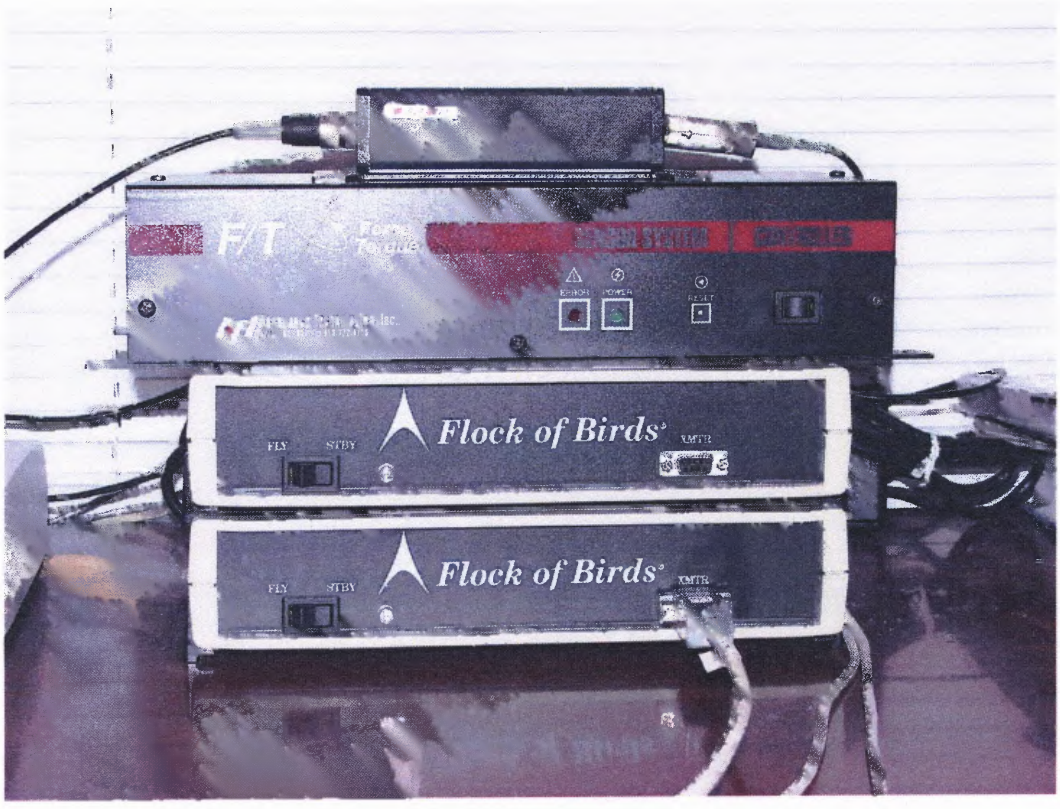

Figure 3.9 Controller box configuration.

3.2.1 Finger Tip Position

Finger tip position during "finger walking" was acquired using the Flock of Birds sensors in the configuration shown in Figure 3.10.

Figure 3.10 The hand ready for data collection.

The two fingers used were the index and the middle fingers of the right hand. Since there is a noticeable difference in length of the two fingers, foam finger extensions shown in Figure 3.11 were constructed and attached to the fingers. To ensure that both finger tip surfaces were identical, a foam extension of negligible thickness was attached to the middle finger.

Figure 3.11 Fingers showing foam extension attachments.

In order to mount the Flock of Bird sensors to the finger tips, it was necessary to affix a strap to the bottom of the sensor. Shown in Figure 3.12 are the sensors with the rubber mounting straps. The straps are simply stretched around the finger and buckled using a non-ferrous pin. To reiterate, ferrous material cannot be used within close proximity of the Flock of Birds sensor as it distorts the magnetic field around the sensor.

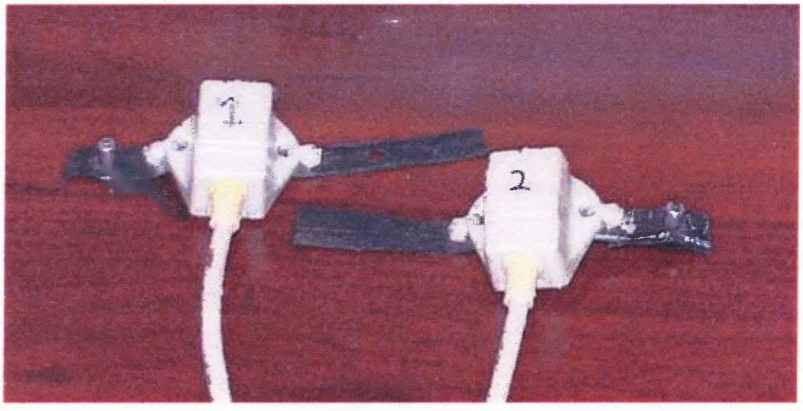

Figure 3.12 Flock of Birds sensors with rubber mounting straps.

Since the Flock of Birds sensors are attached to the base unit by a data cable, it was important to secure that data cable so as not to inhibit the motion of the fingers during data collection. To restrain the cables at the wrist, another rubber strap was used. Shown in Figure 3.13, the rubber wrist strap utilized the same buckling system as the sensor mounting straps.

Figure 3.13 Rubber wrist strap to restrain sensor data cables.

3.2.2 Finger Tip Ground Reaction Force

The ATI-IA Mini40 F/T transducer, shown in Figure 3.14, was used to acquire the ground reaction force data for the "finger walking".

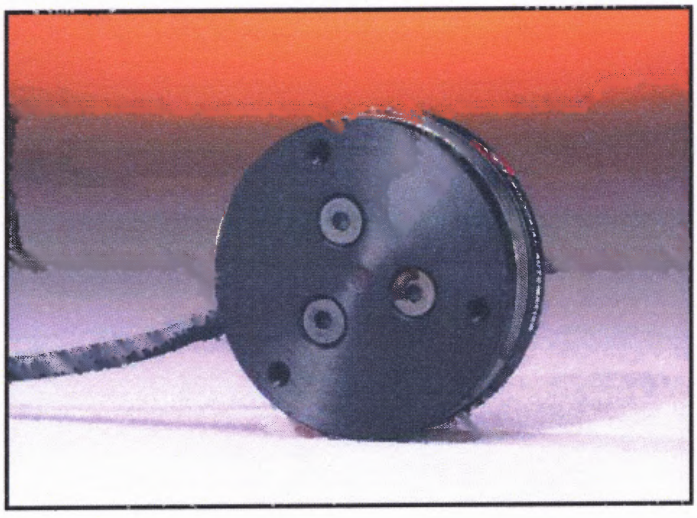

Figure 3.14 Mini40 force plate.

As shown in Figure 3.14, the Mini40 force plate was mounted inside a block of wood measuring 1.9 cm x 6.4 cm x 28 cm (0.75 in. x 2.5 in. x 11 in.), and flush with the surface. This provided a sturdy platform to hold the force plate and a walking runway that was flush with the surface of the force plate. In an effort to prevent the strong color contrast between the wood and the force plate from drawing the attention of the user and subconsciously causing them to artificially aim for the plate, it was covered and the entire runway was painted black. So as not to forget the direction of the axes during data collection, the axes were marked on the side of the runway. It should be noted that the X-axis pointed in the direction of travel, dissimilar to the Flock of Birds transmitter where the X-axis pointed against the direction of travel.

Figure 3.15 Force plate runway.

As mentioned earlier in Section 3.1.1, if the force plate runway is to be used in conjunction with the Flock of Birds sensors, it is mandatory that the force plate isolator be attached. One must remember that the ATI-IA software must be zeroed using the **Bias** button to remove the mass of the isolator attachment from the measurements. Shown below in Figure 3.16 is the isolator attachment ready for data collection.

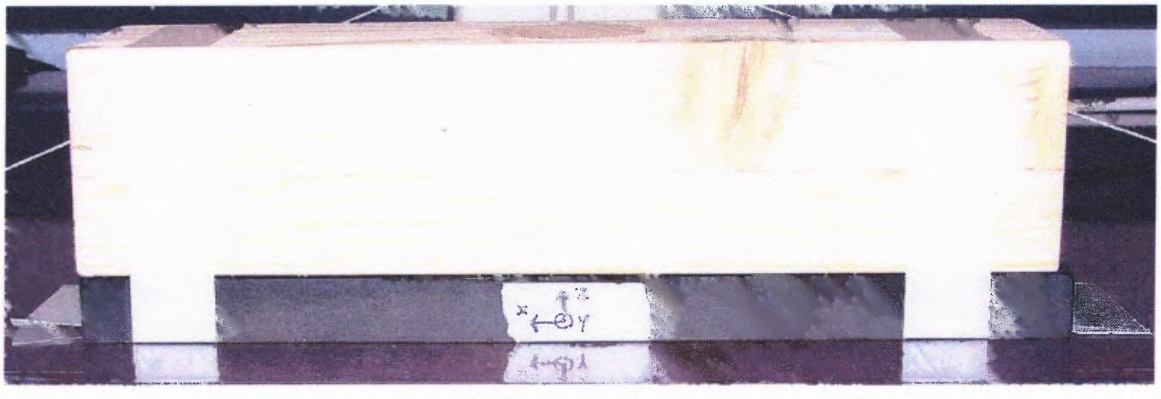

Figure 3.16 Force plate runway with isolator attached.

3.2.3 Foot Position

In order to record foot position data, it was necessary to move the Flock of Birds transmitter to a different location. The transmitter was set up in an area of the floor free from ferrous metal objects and computer equipment (i.e. – table legs, chair legs, and monitors). The sensors could then be mounted using adhesive tape to any point on the

leg for which the position is desired. Figure 3.17 shows the Flock of Birds set up for regular human ambulation. Note that the direction of travel is from right to left so as to be consistent with the "finger walking".

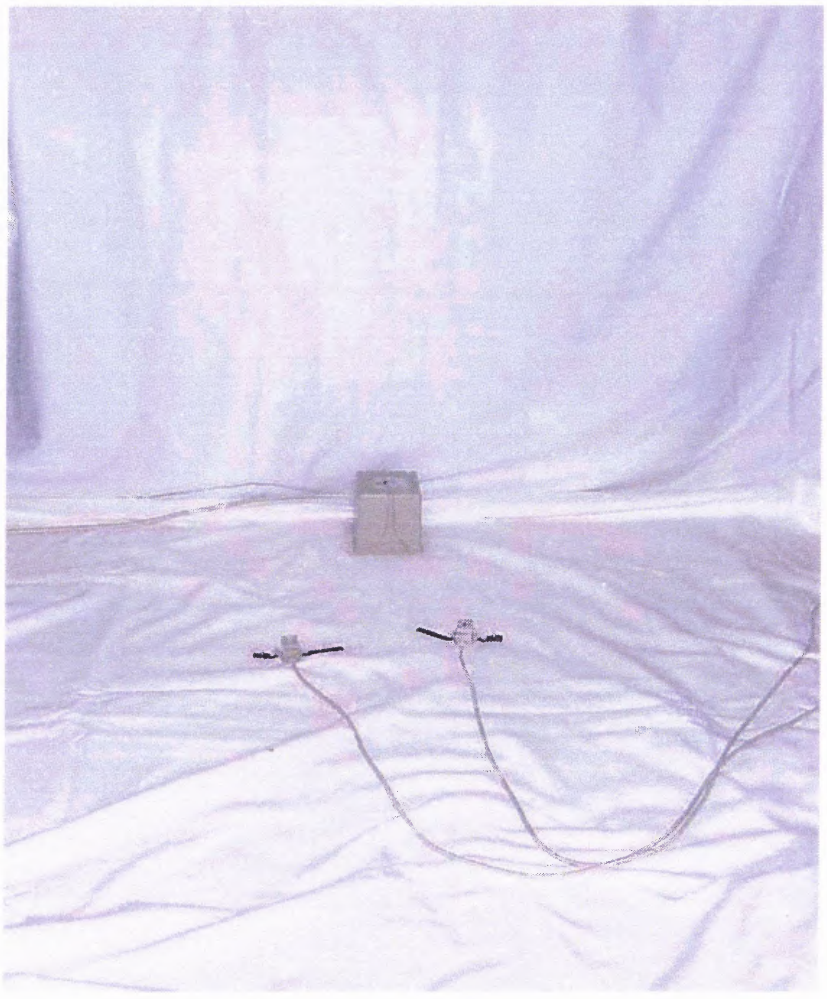

Figure 3.17 Flock of Birds set up for human ambulation.

3.3 Data Preparation

After the data was recorded, it was necessary that the data be filtered before analysis to minimize the amount of noise in the signal. The best filter to use when analyzing human movement data is a low-pass Butterworth filter, specifically of the second-order [20].

Because technology has advanced since the publication of the literature [20], it is now easier to use higher order filters to produce even cleaner data. For the purpose of this research, a fourth-order low-pass Butterworth filter was utilized in MatLab 6.1. The frequency of human movement data is generally on the lower side of the frequency range and noise is on the higher side. Thus, a low-pass filter is used to eliminate the high frequency noise and leave the true signal. All position data was filtered completely while force data was only filtered over the areas of significant data since the Butterworth filter causes significant amounts of overshoot on impulse type data [20].

Prior to data filtering, it was necessary to determine the cutoff frequency, f_c. All frequencies below the cutoff frequency will be allowed to pass unattentuated and all frequencies above the cutoff frequency will be severely attenuated. In order to calculate which cutoff frequency would be best to use, it is recommended that the residual be calculated according to [20]:

$$R(fc) = \sqrt{\frac{1}{N}\sum_{i=1}^{N}(X_i - \hat{X}_i)^2} \tag{3.1}$$

where: X_i = raw data at the ith sample

$\hat{X}_i$ = filtered data at the ith sample

N = number of data points

When the residual curve was calculated and plotted, it appears as shown in Figure 3.18. If the signal was 100% noise, then the residual plot would follow along line *ae*, where intercept *a* would represent the RMS value of the noise and the abscissa intercept would be the Nyquist frequency (one half the sampling frequency). In reality, the signal is made up of true signal plus noise. The line *de* represents the estimate of the noise residual and anything above *d* represents signal distortion due to a low cutoff frequency.

A cutoff frequency that is chosen too low will result in excessive true signal distortion while a cutoff frequency chosen too high will result in excessive noise passed through the filter. A reasonable balance is chosen where a horizontal line traveling through point *a* intersects the residual curve (point *b*) [20].

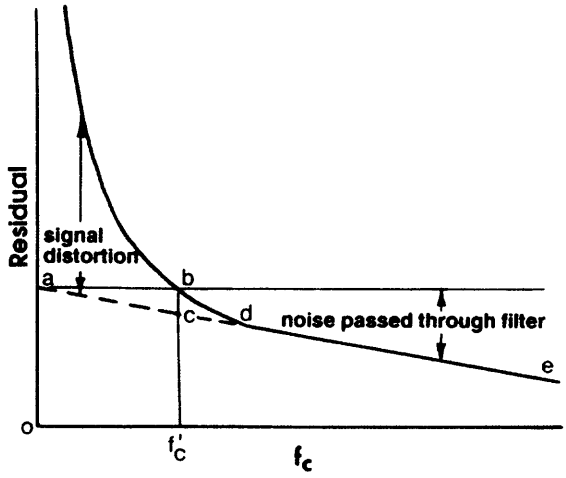

Figure 3.18 Plot of residual according to Equation 3.1 [20].

To ease the calculation of the residual curve, MatLab 6.1 was employed. The function ***residual.m***, shown in Figure D.1 in Appendix D, was created to easily calculate the residual curve given the maximum cutoff frequency desired, sampling frequency, number of samples gathered, and the file where the data is stored. In order for the data to be imported into MatLab, the file must first be stripped of all headers and data columns other than the one being prepared. Upon execution of the function, the residual graph is generated. Then by visual estimation, the lines *ad*, *ab*, and bf_c can be overlaid using the MatLab **Figure Toolbar**.

Once a cutoff frequency has been selected, the original data set can be filtered in MatLab using the fourth-order Butterworth filter calculated with the chosen f_c. It is important to note that when performing the filtering in MatLab that the ***filtfilt()*** command

is used and not ***filter()***. If ***filter()*** is used, then a phase lag distortion occurs at the cutoff frequency. In addition, the use of ***filter()*** will cause all of the data trends to originate at the origin, when in fact, most do not. In order to remove the phase lag and the trend origination relocation, the data is passed through the filter a second time. MatLab is programmed to perform this operation automatically when the ***fitlfilt()*** command is utilized. After the data is filtered in MatLab, it can be exported to a text file using the ***save*** command, and the text file can then be imported into Microsoft Excel for easier interpretation and storage.

CHAPTER 4

RESULTS

4.1 A Comparison of Position Timing and Force

4.1.1 Leg and Finger Position

Position data collected for the normal human gait cycle and the "finger walking" gait cycle produced similar timing trends for two persons, Subject 1 and Subject 2. As shown below in Figure 4.1, the "finger walking" gait of the middle finger had a timing of approximately 48% swing and 52% stance for Subject 1. For Subject 2, Figure 4.2 shows approximately 47% swing and 53% stance for the same finger.

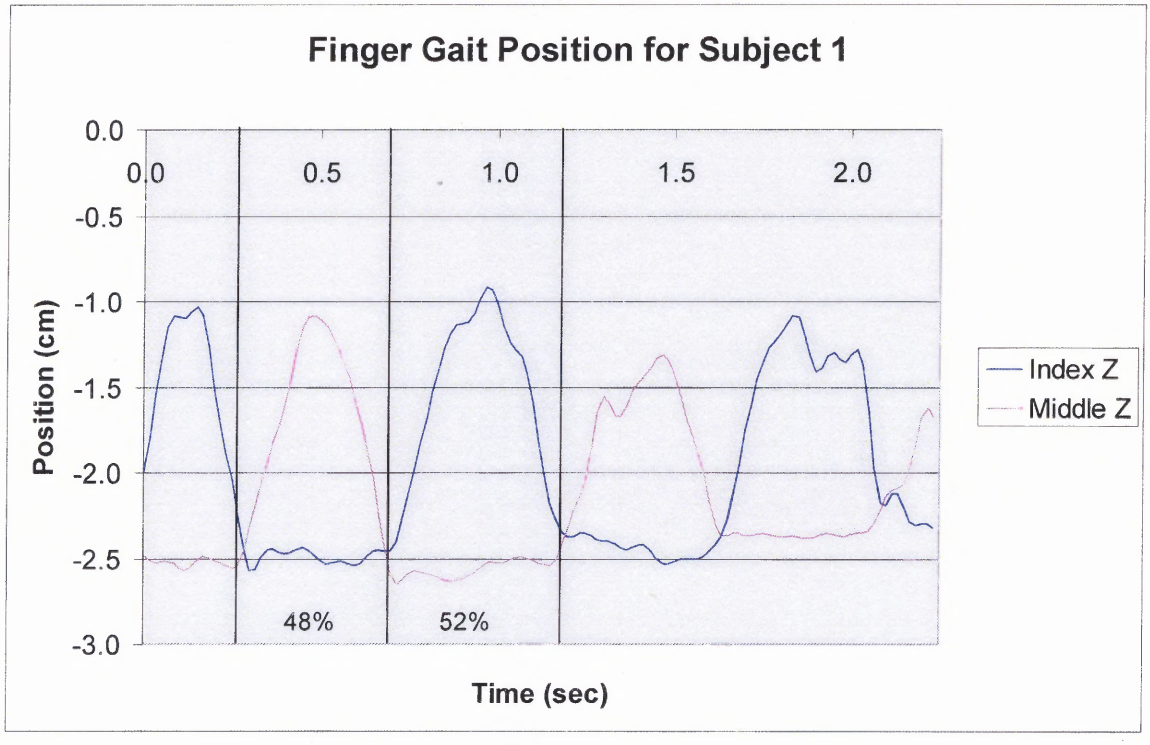

Figure 4.1 "Finger walking" position data for middle and index fingers of Subject 1.

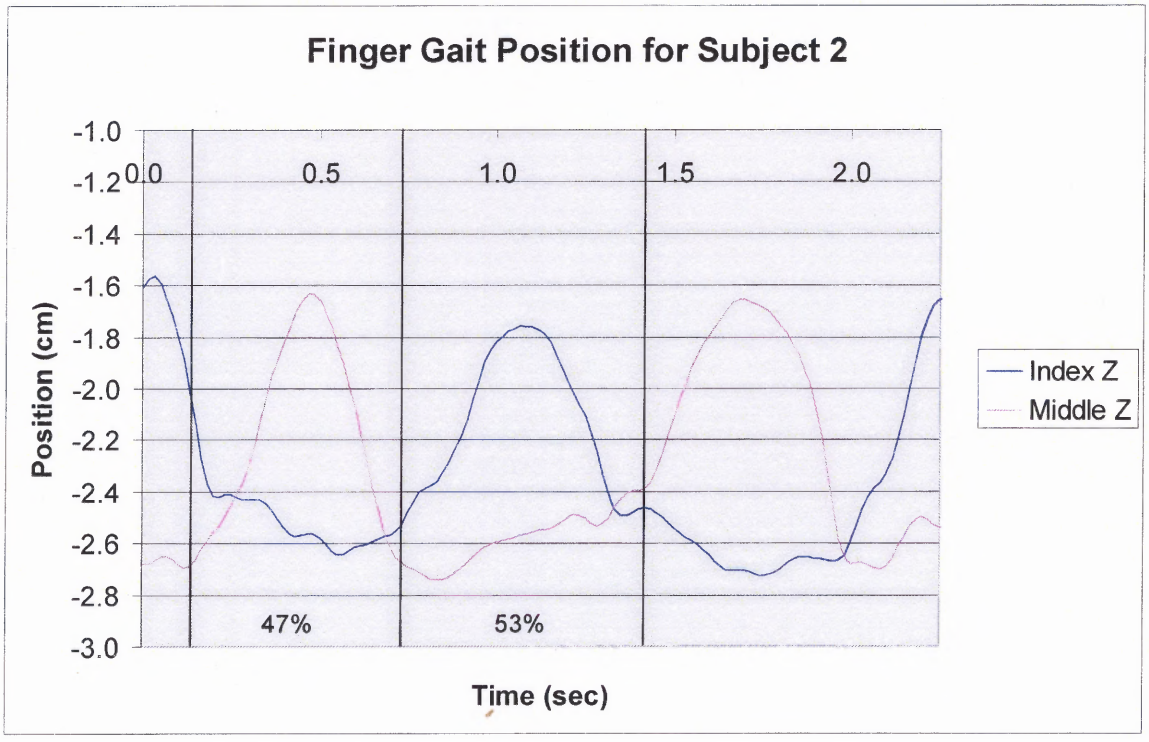

Figure 4.2 "Finger walking" position data for middle and index fingers of Subject 2.

In Figure 1.8, a self-selected walking speed of approximately 1.5 m/s should yield timing of 40% swing and 60% stance [11]. For a faster walk of 3.0 m/s, the timing should be 50% each. At a first glance, this would indicate that "finger walking" would seem to mimic a fast paced walk. This is because contact of any area of the foot is considered part of the stance phase. Analyzing the stance and swing phases for individual parts of the foot yielded different results. As seen in Figure 4.3, the right ankle of Subject 1 experienced a timing of 46% swing and 54% stance – almost identical to that of the fingers for Subject 1. A similar trend of 45% stance and 55% swing is shown in Figure 4.4 for Subject 2. To support this, presented in Figure 4.5 is data [20], showing that virtually the same timing was present in the ankle of the test subject.

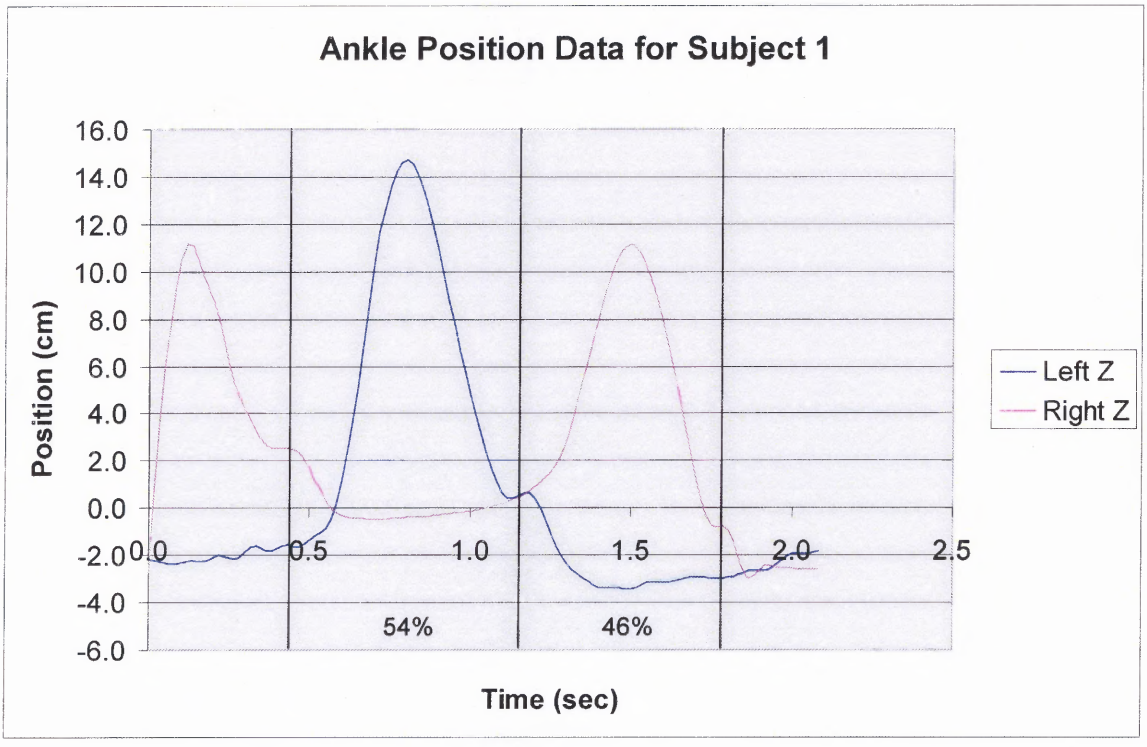

Figure 4.3 Left and right ankle position data of Subject 1.

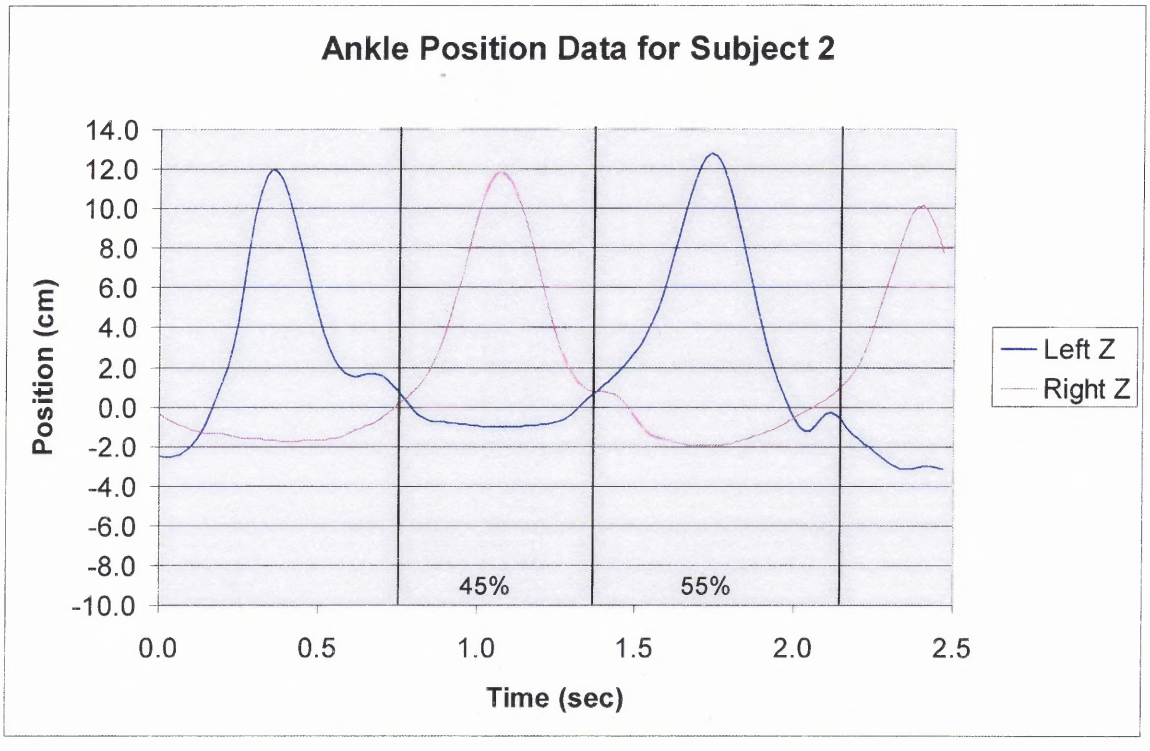

Figure 4.4 Left and right ankle position data of Subject 2.

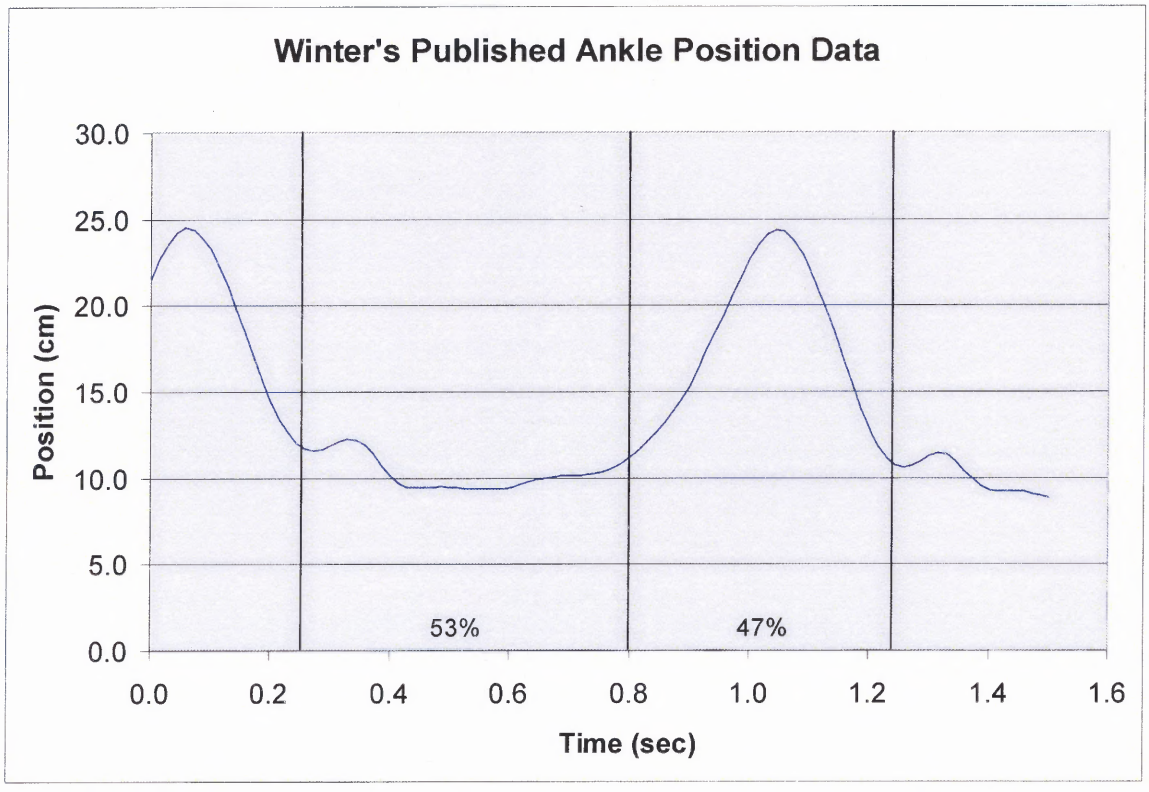

Figure 4.5 Published ankle position data [20].

In addition to an identical swing and stance timing, a closer examination of the position data revealed that there was a parallel in the time it takes to complete one full stride. Figure 4.6 shows the finger gait timing for a more leisurely self-selected pace. Presented in Figure 4.6 is a stride time of approximately 1.4 seconds while maintaining the same 48% swing and 52% stance ratio of the middle finger seen in Figure 4.1. Meanwhile the ankle data for Subject 1, shown in Figure 4.3, revealed a stride time of approximately 1.4 seconds. Figure 4.2 and Figure 4.4 exhibit a similar stride time trend for Subject 2 with 1.3 seconds for "finger walking" stride time and 1.4 seconds for the ankle stride time. The published data in Figure 4.5 does not show this same trend, likely because every individual has his/her own self-selected comfortable / natural walking paces.

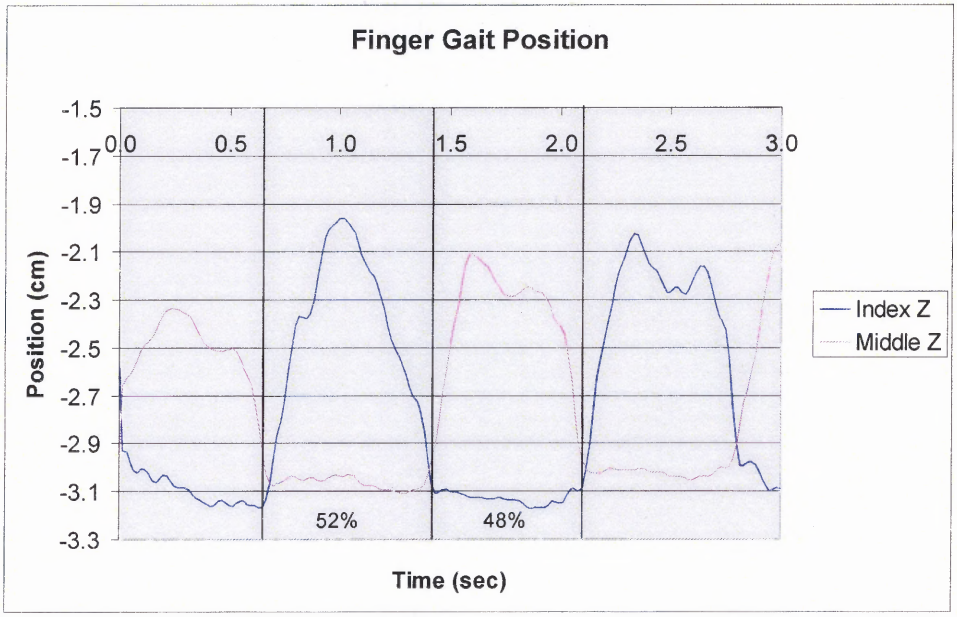

Figure 4.6 Finger gait position data showing a stride time of approximately 1.4 seconds.

4.1.2 Leg and Finger Ground Reaction Forces

Comparison of both absolute and normalized ground reaction forces (GRF) during "finger walking" and normal human walking confirms that there was a similarity between the forces acting on the finger tips and those acting on the feet during walking. Figure 4.7 shows a simultaneous absolute vertical direction force and position plot, where there is clearly a similarity in the increase in GRF between the loading response and midstance phases. The increase in GRF between the terminal stance and preswing phases and the decrease in GRF between midstance and terminal stance normally seen during human walking was not as prevalent during "finger walking" mainly because of the anatomical differences between the fingers and the legs.

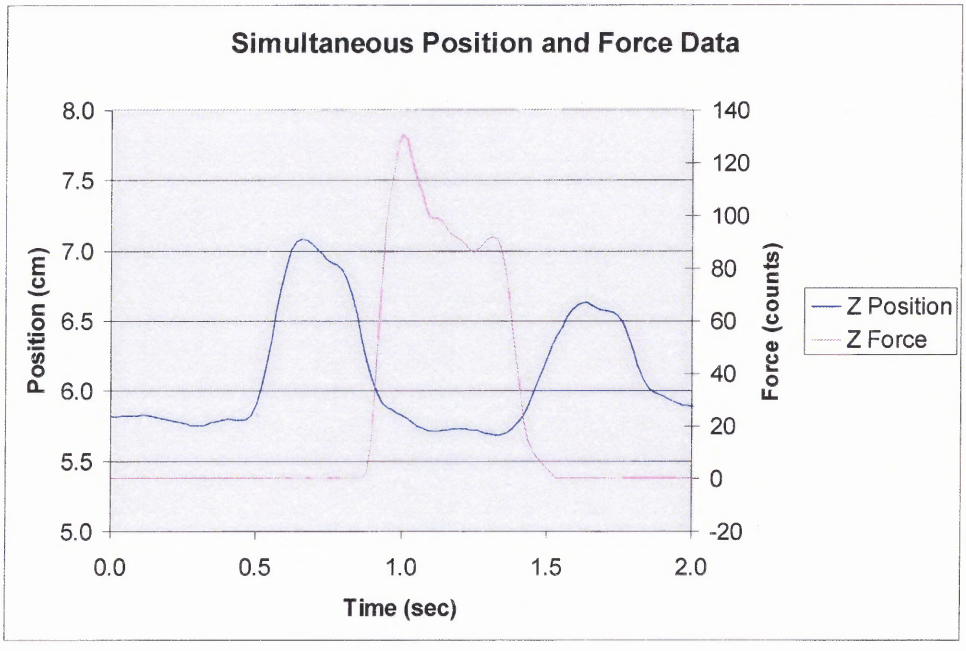

Figure 4.7 "Finger walking" force and position data for the middle finger.

Figure 4.8 through Figure 4.11 show sets of 10 normalized data curves for "finger walking" GRF in the vertical and horizontal directions for Subjects 1 and 2. The heavy red line represents the average curve. The error bars on the average curve represent one standard deviation at that point. Figure 4.12 shows a set of published normal human walking GRF in the horizontal and vertical directions that have been normalized for comparison to the "finger walking" data.

The average normalized GRF in the vertical direction also displays the increase of force during initial contact and the absence of a second force peak. The average normalized GRF in the forward horizontal direction during "finger walking" more closely resembles that of normal human walking. Present in both the normalized "finger walking" GRF data for Subjects 1 and 2 and the normalized human GRF data, is the rearward force of initial contact and forward force of preswing.

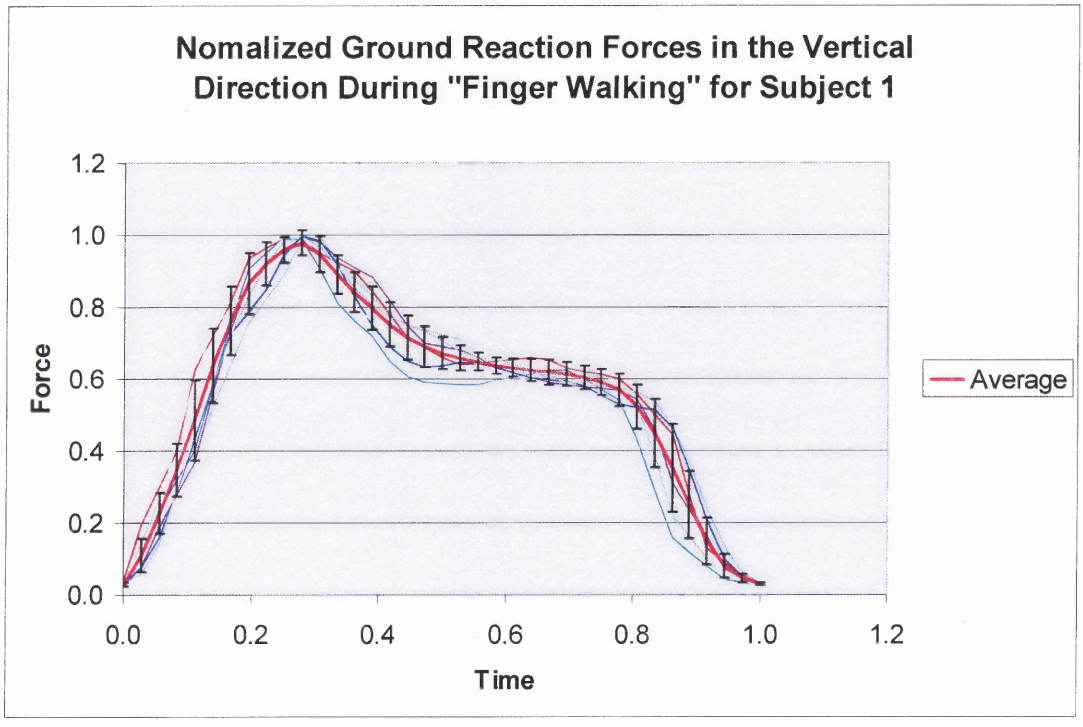

Figure 4.8 Normalized vertical "finger walking" force data of the middle finger for Subject 1 showing one standard deviation bars.

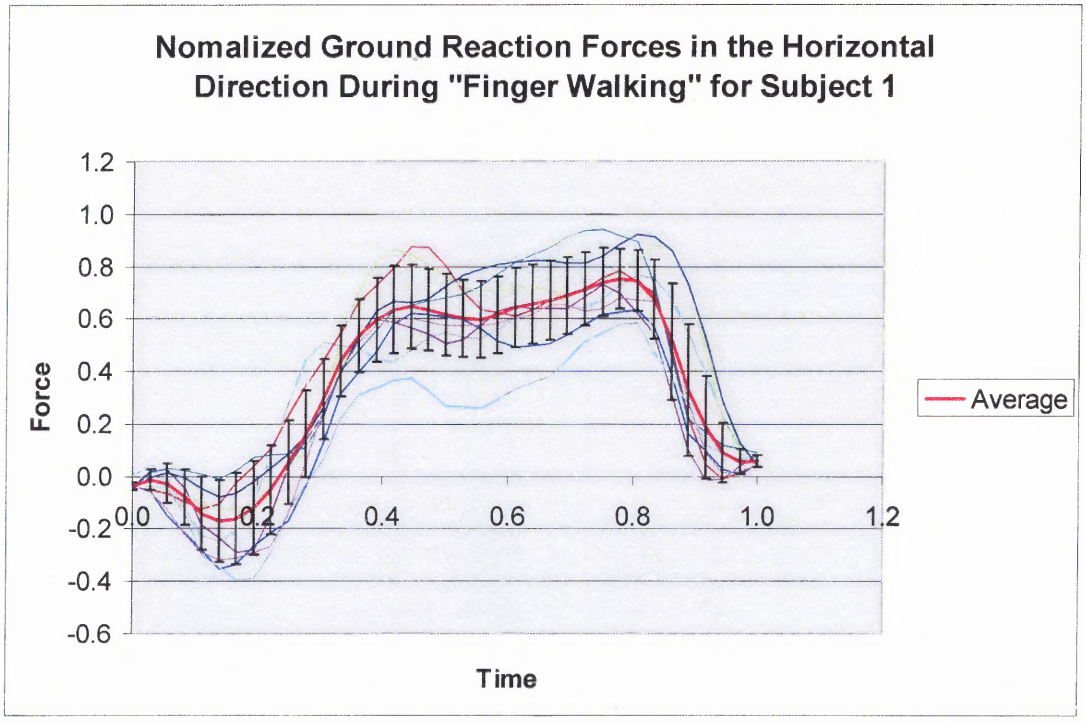

Figure 4.9 Normalized horizontal "finger walking" force data of the middle finger for Subject 1 showing one standard deviation bars.

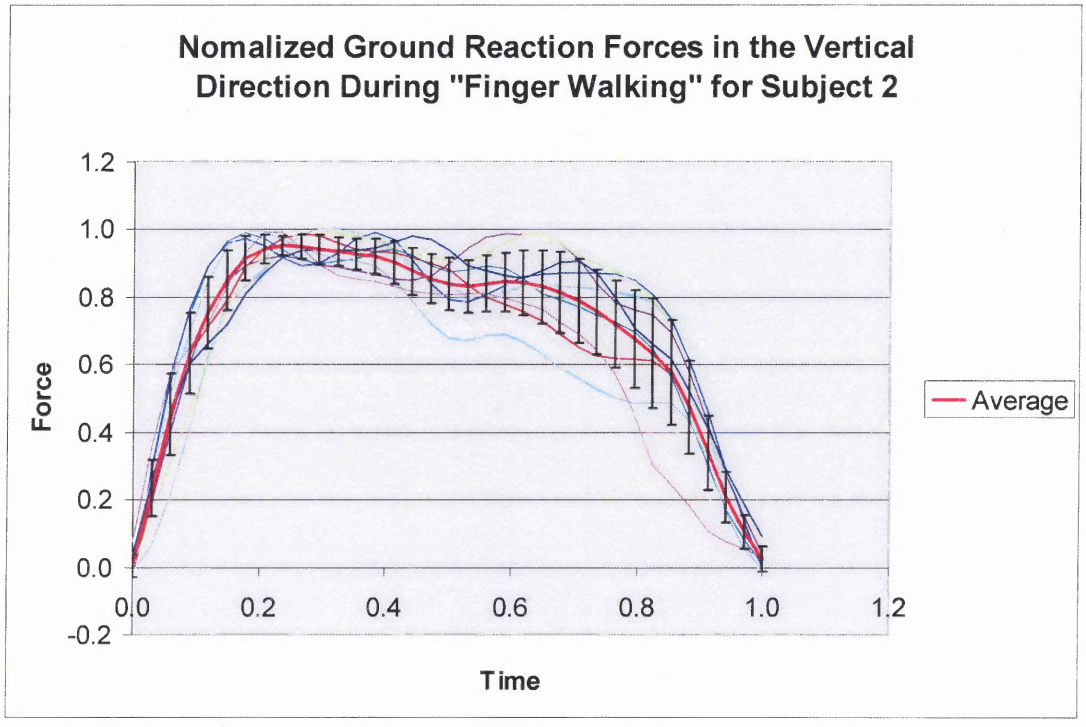

Figure 4.10 Normalized vertical "finger walking" force data of the middle finger for Subject 2 showing one standard deviation bars.

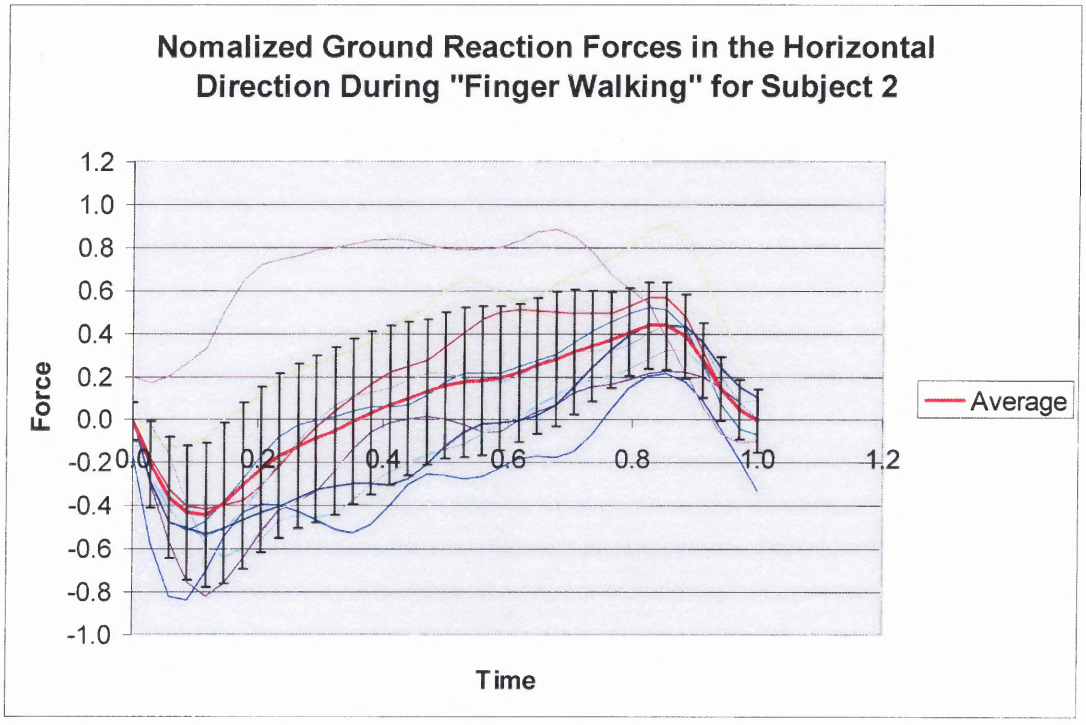

Figure 4.11 Normalized horizontal "finger walking" force data of the middle finger for Subject 2 showing one standard deviation bars.

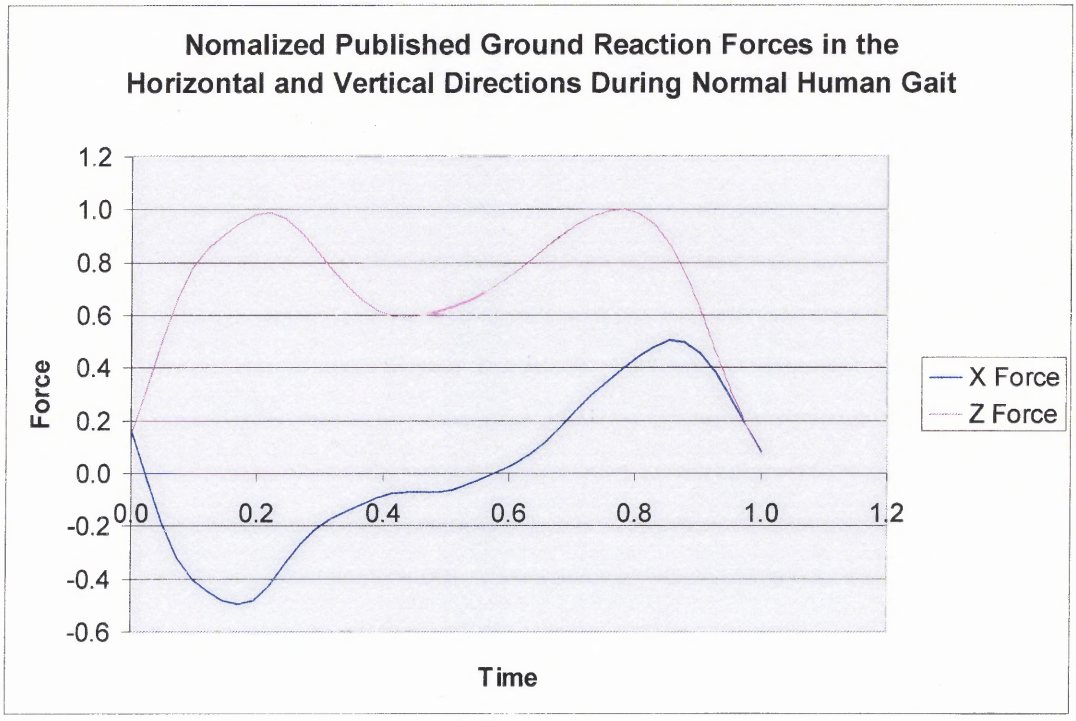

Figure 4.12 Normalized ground reaction force data for normal human walking [20].

CHAPTER 5

CONCLUSION

The goal of this research was to determine if the timing, trajectory, and ground reaction forces associated with gait-mimicking finger motions are comparable to those of normal human walking. This research successfully determined that "finger walking" motions do in fact closely mimic the trajectory and gait cycle timing of the ankle during normal human walking and the ground reaction forces of the foot.

Although "finger walking" position and gait cycle timing does not directly match that of the foot itself, this difference can be accounted for by using software that determines the correct position in space of other points on the foot and leg given the location of the ankle. As long as one point on the lower leg is known and accurately controllable, software can deliver the functional electrical stimulation charge to the correct muscles at the appropriate time to produce a functional gait pattern. Software such as JACK by EDS is capable of these kinematic calculations and is currently used for computer simulation. The same kinematic calculation algorithm could easily be applied to a central control unit for a haptic functional electrical stimulation device.

Given the similarities between the gait cycle timing, trajectory, and ground reaction forces, it appears possible for finger tip motor control and sensory capabilities to be a comfortable and effective substitute for those of the legs when used in conjunction with kinematic simulation software. Future research will develop this needed kinematic software control unit, in addition to the haptic interface used for the force feedback to the finger tips.

APPENDIX A

PARALYSIS FUNCTIONAL GOALS

The following table presents the functional abilities that a person with a spinal cord injury can expect to have remaining after extensive rehabilitation efforts.

Table A.1 Typical Abilities and Functionality after Spinal Cord Injury [2]

Level	Abilities	Functional Goals
C1-C3	C3-limited movement of head and neck	**Breathing:** Depends on a ventilator for breathing. **Communication:** Talking is sometimes difficult, very limited or impossible. If ability to talk is limited, communication can be accomplished independently with a mouth stick and assistive technologies like a computer for speech or typing. Effective verbal communication allows the individual with SCI to direct caregivers in the person's daily activities, like bathing, dressing, personal hygiene, transferring as well as bladder and bowel management. **Daily tasks:** Assistive technology allows for independence in tasks such as turning pages, using a telephone and operating lights and appliances. **Mobility:** Can operate an electric wheelchair by using a head control, mouth stick, or chin control. A power tilt wheelchair also for independent pressure relief.
C3-C4	Usually has head and neck control. Individuals at C4 level may shrug their shoulders	**Breathing:** May initially require a ventilator for breathing, usually adjust to breathing full-time without ventilatory assistance. **Communication:** Normal. **Daily tasks:** With specialized equipment, some may have limited independence in feeding and independently operate an adjustable bed with an adapted controller.
C5	Typically has head and neck control, can shrug shoulder and has shoulder control. Can bend his/her elbows and turn palm	**Daily tasks:** Independence with eating, drinking, face washing, brushing of teeth, face shaving and hair care after assistance in setting up specialized equipment. **Health care:** Can manage their own health care by doing self-assist coughs and pressure reliefs by leaning forward or side -to-side. **Mobility:** May have strength to push a manual wheelchair for short distances over smooth surfaces. A power wheelchair with hand controls is typically used for daily activities. Driving may be possible after being evaluated by a qualified professional to determine special equipment needs
C6	Has movement in head, neck, shoulders, arms and wrists. Can shrug shoulders, bend elbows,turn palms up and down and extend wrists.	**Daily tasks:** With help of some specialized equipment, can perform with greater ease and independence, daily tasks of feeding, bathing, grooming, personal hygiene and dressing. May independently perform light housekeeping duties. **Health care:** Can independently do pressure reliefs, skin checks and turn in bed. **Mobility:** Some individuals can independently do transfers but often require a sliding board. Can use a manual wheelchair for daily activities but may use power wheelchair for greater ease of independence.
C7	Has similar movement as an individual with C6, with added ability to straighten his/her elbows.	**Daily tasks:** Able to perform household duties. Need fewer adaptive aids in independent living. **Health care:** Able to do wheelchair pushups for pressure reliefs. **Mobility:** Daily use of manual wheelchair. Can transfer with greater ease.
C8-T1	Has added strength and precision of fingers that result in limited or natural hand function.	**Daily tasks:** Can live independently without assistive devices in feeding, bathing, grooming, oral and facial hygiene, dressing, bladder management and bowel management. **Mobility:** Uses manual wheelchair. Can transfer independently.
T2-T6	Has normal motor function in head, neck, shoulders, arms, hands and fingers. Has increased use of rib and chest muscles, or trunk control	**Daily tasks:** Should be totally independent with all activities. **Mobility:** A few individuals are capable of limited walking with extensive bracing. This requires extremely high energy and puts stress on the upper body, offering no functional advantage. Can lead to damage of upper joints.
T 7-T12	Has added motor function from increased abdominal control.	**Daily tasks:** Able to perform unsupported seated activities. **Mobility:** Same as above. **Health care:** Has improved cough effectiveness.
L1-L5	Has additional return of motor movement in hips and knees.	**Mobility:** Walking can be a viable function, with the help of specialized leg and ankle braces. Lower levels walk with greater ease with the help of assistive devices.
S1-S5	Depending on level of injury, there are various degrees of return of voluntary bladder, bowel and sexual functions.	**Mobility:** Increased ability to walk with fewer or no supportive devices.

APPENDIX B

ASCENSION FLOCK OF BIRDS SPECIFICATION SHEETS

The following specification sheets were provided by Ascension Technology Corporation. They provide various capabilities and constraints of the Flock of Birds system.

Flock of Birds

Real-time Motion Tracking

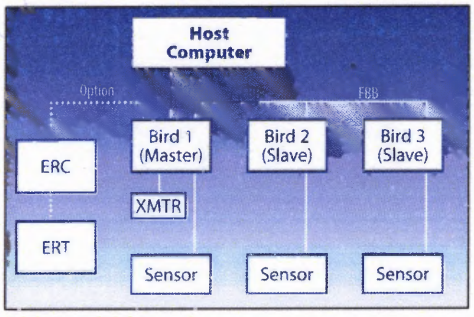

Flock of Birds Block Diagram
(Sample 3-sensor Flock configuration)

The Flock can be configured to track from one to four sensors simultaneously with one or more RS-232 interfaces to a host computer. Long range coverage is easily added by "clicking in" our Extended Range Transmitter (ERT/ERC). For high speed operations, add more RS-232 ports and use our fast Bird bus (FBB).

Specifications

TECHNICAL	
Tracking Range:	±4' (1.2m) ±10' (3.05m) optional in any direction
Angular Range:	±180° Azimuth & Roll, ± 90° Elevation
Static Accuracy*:	Position: 0.07" (1.8mm) RMS Orientation: 0.5° RMS
Static Resolution:	Position: 0.02' (0.5mm) @ 12" (30.5cm) Orientation: 0.1° @ 12" (30.5cm)
Update Rate:	Up to 144 measurements/second
Ouputs:	X, Y, Z positional coordinates and orientation angles, or rotation matrix
Interface:	RS-232 with selectable baud rates to 115,200
Format:	Binary
Modes:	Point or Stream
PHYSICAL	
Transmitter:	
Standard: Option:	3.75" (9.6cm) cube with 10' (3.05m) cable; or Extended Range Transmitter: 12" (30.5cm) cube with 20' (6.1m) cable
Sensor:	1.0" x 1.0" x 0.8" (25.4mm x 25.4mm x 20.3mm) cube (or optional 3-button mouse) with 10' (3.05m) or 35' (10.7m) cable
Enclosure:	9.5" x 11.5" x 2.6" (24cm x 29cm x 6.6cm)
Power:	User provided or optional external plug-in: US/European version
Operating Temperature:	10°C to 40°C (50°F to 104°F)
Operating Humidity:	10% to 90% non-condensing

* Accuracy verified over range from 20.3cm to 76.2cm at constant orientation.

Applications

- Head/hand/body tracking
  - Virtual design, analysis, interaction
  - Flight & vehicle simulation
  - Real-time visualization
  - Entertainment
  - Telerobotics/Telepresence
- Instrument tracking
- Biomechanical tracking for research and rehabilitation
- 3D graphics control and manipulation

Benefits

- Unrestricted tracking without line-of-site restrictions
- Consistently fast measurements even with multiple sensors
- Fast dynamic performance without degradation
- Proven long-range operation
- Real-time interaction with virtual images
- Cost-effective performance
- Free interface software and technical support

Notes on Accuracy

Accuracy is defined as the root mean squared (RMS) deviation of a true measurement of the magnetic center of a single sensor with respect to the magnetic center of a single transmitter measured over the translation range. Accuracy varies from one location to another over this translation range and will be degraded if there are interfering electromagnetic noise sources or metal in the operating environment.

Regulatory Certifications

- FCC Part 15, Class A
- CE: EN 50081-1, Class A
  EN 50082-1, Class 2
  EN 61010-1

CERTIFIED ISO 9001

Ascension Technology Corporation

Call: 800-321-6596
Outside N. America: 802-893-6657
Visit our web site at: www.ascension-tech.com
e mail: ascension@ascension-tech.com Fax: 802-893-6659
PO Box 527, Burlington, VT 05402 USA

APPENDIX C

ATI-IA MINI40 FORCE PLATE SPECIFICATION SHEETS

The following specification sheets were provided by Assurance Technologies Inc. – Industrial Automation. They provide various capabilities and physical dimensions of the Mini40 force plate system.

Mini40

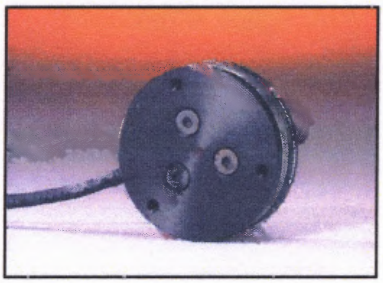

The Mini40 F/T transducer
The transducer is made of hardened stainless steel with integral interface plates made from high-strength aircraft aluminum.

"ATI's force transducers have given us high accuracy and easy to use tools that integrate perfectly with our research needs."
Dr. Douglas Weeks, Dept. of Physical Therapy, Regis University, Denver, CO

BENEFITS AND FEATURES

One of the Smallest 6-axis Sensors in the World
The Mini40 has a compact, low-profile design.

Extremely High Strength
- EDM wire-cut from high yield-strength stainless steel.
- Maximum allowable overload values are 4.3 to 18 times rated capacities.

High Signal-to-Noise Ratio
Silicon strain gauges provide a signal 75 times stronger than conventional foil gauges. This signal is amplified, resulting in near-zero noise distortion.

TYPICAL APPLICATIONS

- **Telerobotics**
- **Robotic hand research**
- **Robotic Surgery**
- **Finger-force Research**

English-Calibrated Sensing Ranges	US-5-10		US-10-20		US-20-40	
Fx, Fy (±lb)	5		10		20	
Fz (±lb)	15		30		60	
Tx, Ty (±in-lb)	10		20		40	
Tz (±in-lb)	10		20		40	
Resolution						
F/T System Type †	**CON**	**DAQ**	**CON**	**DAQ**	**CON**	**DAQ**
Fx, Fy (lb)	1/200	1/3200	1/100	1/1600	1/50	1/800
Fz (lb)	1/100	1/1600	1/50	1/800	1/25	1/400
Tx, Ty (in-lb)	1/200	1/3200	1/100	1/1600	1/50	1/800
Tz (in-lb)	1/200	1/3200	1/100	1/1600	1/50	1/800

Metric-Calibrated Sensing Ranges	SI-20-1		SI-40-2		SI-80-4	
Fx, Fy (±N)	20		40		80	
Fz (±N)	60		120		240	
Tx, Ty (±N-m)	1		2		4	
Tz (±N-m)	1		2		4	
Resolution						
F/T System Type †	**CON**	**DAQ**	**CON**	**DAQ**	**CON**	**DAQ**
Fx, Fy (N)	1/50	1/800	1/25	1/400	2/25	1/200
Fz (N)	1/25	1/400	2/25	1/200	4/25	1/100
Tx, Ty (N-m)	1/2000	1/32000	1/1000	1/16000	1/500	1/8000
Tz (N-m)	1/2000	1/32000	1/1000	1/16000	1/500	1/8000

Contact ATI for complex loading information. Resolutions are typical. †CON = Controller F/T System, DAQ = 16-bit DAQ F/T System

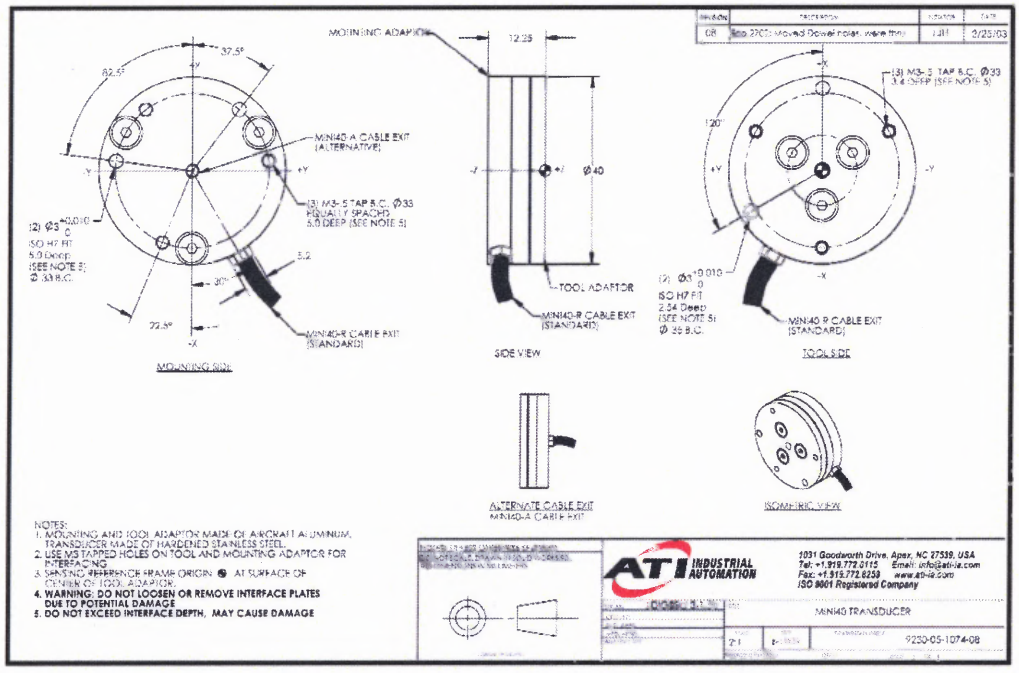

Single-Axis Overload	English	Metric
Fxy	±200 lb	±870 N
Fz	±610 lb	±2700 N
Txy	±190 in-lb	±22 N-m
Tz	±190 in-lb	±21 N-m
Stiffness (Calculated)	**English**	**Metric**
X-axis & Y-axis force (Kx, Ky)	65×10^3 lb/in	11×10^6 N/m
Z-axis force (Kz)	130×10^3 lb/in	23×10^6 N/m
X-axis & Y-axis torque (Ktx, Kty)	29×10^3 in-lb/rad	3.3×10^3 N-m/rad
Z-axis torque (Ktz)	38×10^3 in-lb/rad	4.3×10^3 N-m/rad
Resonant Frequency (Measured)		
Fx, Fy, Tz	3200 Hz	
Fz, Tx, Ty	4900 Hz	
Physical Specifications	**English**	**Metric**
Weight	0.11 lb	50 g
Diameter	1.57 in	40 mm
Height	0.482 in	12.2 mm

APPENDIX D

MATLAB PROGRAM FOR DETERMINING CUTOFF FREQUENCY

Figure D.1 is a screen capture of the MatLab code used to calculate the residual plots necessary to determine the cutoff frequency for filtering motion data.

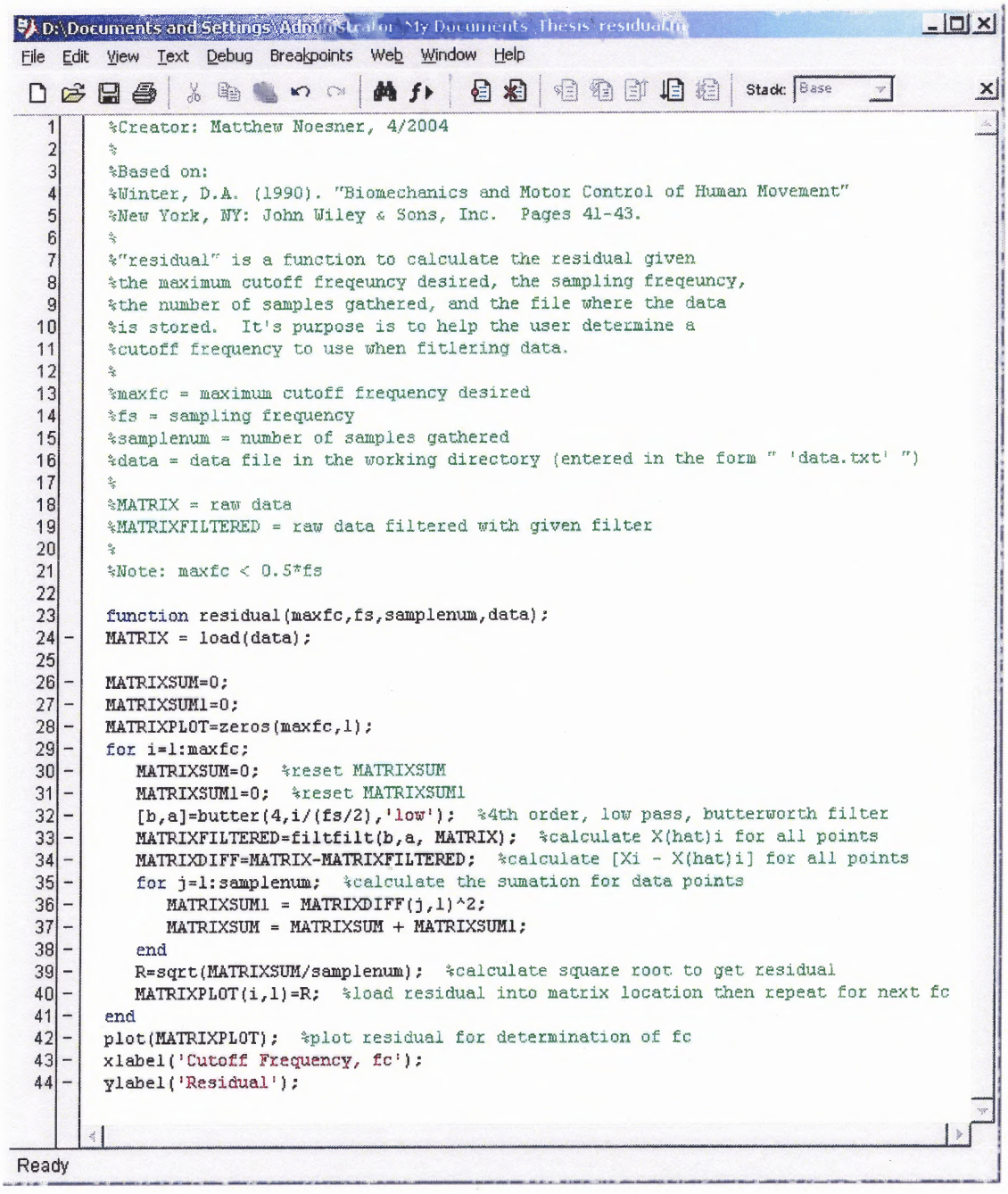

Figure D.1 MatLab residual code to find cutoff frequency.

APPENDIX E

FILTERED DATA AND RESIDUAL ANALYSIS FOR FINGER POSITION OF SUBJECT 1

The finger position data shown in Table E.1 was collected at 60 Hz on COM2 using the LabView program CyberFlock. The data was filtered using the cutoff frequencies found in the residual plots shown in Figures E.1 and E.2.

Table E.1 Filtered Index and Middle Finger Position Data for Subject 1

	Index Finger (Corrected Direction)	Middle Finger (Corrected Direction)
Time Sec.	Flock 1 (z) cm	Flock 2 (z) cm
0.000	-2.0062	-2.4781
0.017	-1.7868	-2.5095
0.033	-1.5486	-2.5251
0.050	-1.3162	-2.5226
0.067	-1.1493	-2.5176
0.083	-1.0845	-2.5288
0.100	-1.0913	-2.5554
0.117	-1.0968	-2.5710
0.133	-1.0617	-2.5528
0.150	-1.0286	-2.5130
0.167	-1.0861	-2.4877
0.183	-1.2729	-2.4929
0.200	-1.5258	-2.5120
0.217	-1.7430	-2.5277
0.233	-1.8957	-2.5442
0.250	-2.0459	-2.5604
0.267	-2.2459	-2.5434
0.283	-2.4525	-2.4590
0.300	-2.5709	-2.3224
0.317	-2.5660	-2.1836
0.333	-2.4977	-2.0628
0.350	-2.4481	-1.9442
0.367	-2.4454	-1.8258
0.383	-2.4646	-1.7185
0.400	-2.4742	-1.6033
0.417	-2.4655	-1.4497
0.433	-2.4481	-1.2776
0.450	-2.4379	-1.1480
0.467	-2.4476	-1.0917
0.483	-2.4781	-1.0869
0.500	-2.5134	-1.1063
0.517	-2.5324	-1.1472
0.533	-2.5298	-1.2098
0.550	-2.5204	-1.2832
0.567	-2.5221	-1.3650
0.583	-2.5351	-1.4683
0.600	-2.5413	-1.5952
0.617	-2.5255	-1.7303
0.633	-2.4913	-1.8708

Table E.1 Filtered Index and Middle Finger Position Data for Subject 1 (Continued)

	Index Finger Position (Corrected Direction)	Middle Finger Position (Corrected Direction)
Time	Flock 1(z)	Flock 2(z)
Sec.	cm	cm
0.650	-2.4588	-2.0378
0.667	-2.4475	-2.2420
0.683	-2.4567	-2.4499
0.700	-2.4545	-2.5984
0.717	-2.3975	-2.6495
0.733	-2.2733	-2.6267
0.750	-2.1161	-2.5887
0.767	-1.9655	-2.5728
0.783	-1.8252	-2.5765
0.800	-1.6798	-2.5857
0.817	-1.5294	-2.5966
0.833	-1.3895	-2.6114
0.850	-1.2717	-2.6264
0.867	-1.1846	-2.6337
0.883	-1.1393	-2.6290
0.900	-1.1301	-2.6172
0.917	-1.1209	-2.6033
0.933	-1.0719	-2.5844
0.950	-0.9865	-2.5572
0.967	-0.9198	-2.5314
0.983	-0.9297	-2.5213
1.000	-1.0218	-2.5250
1.017	-1.1444	-2.5247
1.033	-1.2375	-2.5103
1.050	-1.2843	-2.4924
1.067	-1.3236	-2.4880
1.083	-1.4166	-2.4994
1.100	-1.5930	-2.5151
1.117	-1.8205	-2.5268
1.133	-2.0315	-2.5365
1.150	-2.1828	-2.5400
1.167	-2.2794	-2.5121
1.183	-2.3419	-2.4308
1.200	-2.3734	-2.3174
1.217	-2.3716	-2.2213
1.233	-2.3548	-2.1486
1.250	-2.3519	-2.0386
1.267	-2.3697	-1.8501

Table E.1 Filtered Index and Middle Finger Position Data for Subject 1 (Continued)

	Index Finger Position (Corrected Direction)	Middle Finger Position (Corrected Direction)
Time Sec.	Flock 1(z) cm	Flock 2(z) cm
1.283	-2.3890	-1.6495
1.300	-2.3952	-1.5557
1.317	-2.3981	-1.5960
1.333	-2.4135	-1.6711
1.350	-2.4369	-1.6750
1.367	-2.4472	-1.6027
1.383	-2.4355	-1.5208
1.400	-2.4186	-1.4702
1.417	-2.4217	-1.4346
1.433	-2.4522	-1.3868
1.450	-2.4942	-1.3338
1.467	-2.5242	-1.3099
1.483	-2.5308	-1.3427
1.500	-2.5199	-1.4323
1.517	-2.5057	-1.5547
1.533	-2.5003	-1.6785
1.550	-2.5042	-1.7868
1.567	-2.5052	-1.8904
1.583	-2.4899	-2.0176
1.600	-2.4595	-2.1712
1.617	-2.4225	-2.3045
1.633	-2.3704	-2.3664
1.650	-2.2778	-2.3633
1.667	-2.1319	-2.3476
1.683	-1.9508	-2.3521
1.700	-1.7663	-2.3666
1.717	-1.5995	-2.3701
1.733	-1.4591	-2.3611
1.750	-1.3506	-2.3527
1.767	-1.2772	-2.3551
1.783	-1.2304	-2.3658
1.800	-1.1879	-2.3740
1.817	-1.1331	-2.3730
1.833	-1.0839	-2.3691
1.850	-1.0925	-2.3727
1.867	-1.1912	-2.3823
1.883	-1.3318	-2.3853
1.900	-1.4126	-2.3757

Table E.1 Filtered Index and Middle Finger Position Data for Subject 1 (Continued)

	Index Finger Position (Corrected Direction)	Middle Finger Position (Corrected Direction)
Time Sec.	Flock 1(z) cm	Flock 2(z) cm
1.917	-1.3869	-2.3611
1.933	-1.3175	-2.3538
1.950	-1.2979	-2.3586
1.967	-1.3368	-2.3685
1.983	-1.3579	-2.3707
2.000	-1.3159	-2.3611
2.017	-1.2796	-2.3502
2.033	-1.3766	-2.3476
2.050	-1.6482	-2.3396
2.067	-1.9747	-2.2988
2.083	-2.1750	-2.2208
2.100	-2.1881	-2.1412
2.117	-2.1240	-2.0990
2.133	-2.1228	-2.0898
2.150	-2.2036	-2.0647
2.167	-2.2843	-1.9750
2.183	-2.3078	-1.8228
2.200	-2.2967	-1.6786
2.217	-2.2976	-1.6275
2.233	-2.3205	-1.6742

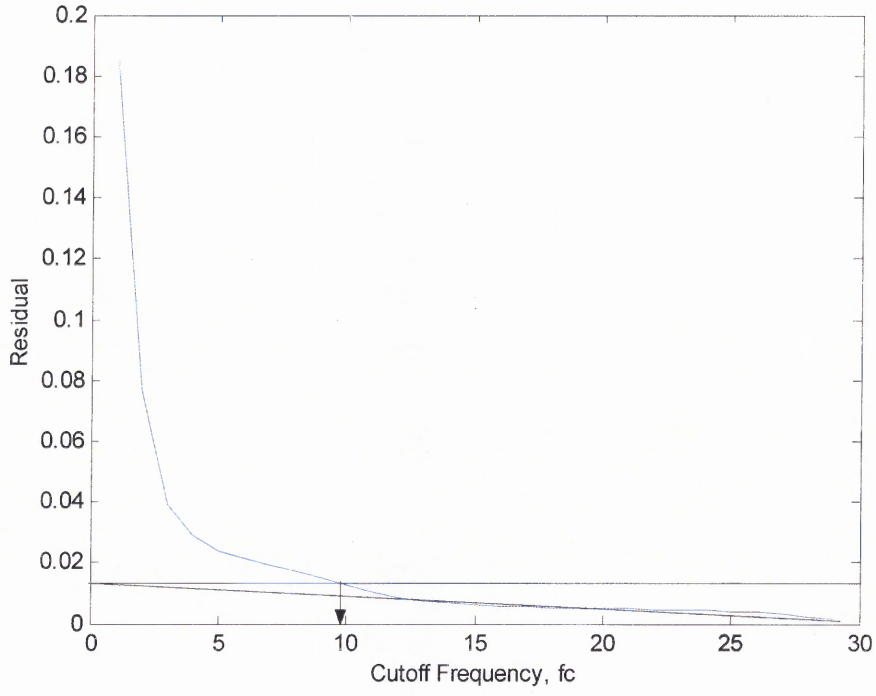

Figure E.1 Index finger Z-position data residual plot for Table E.1.

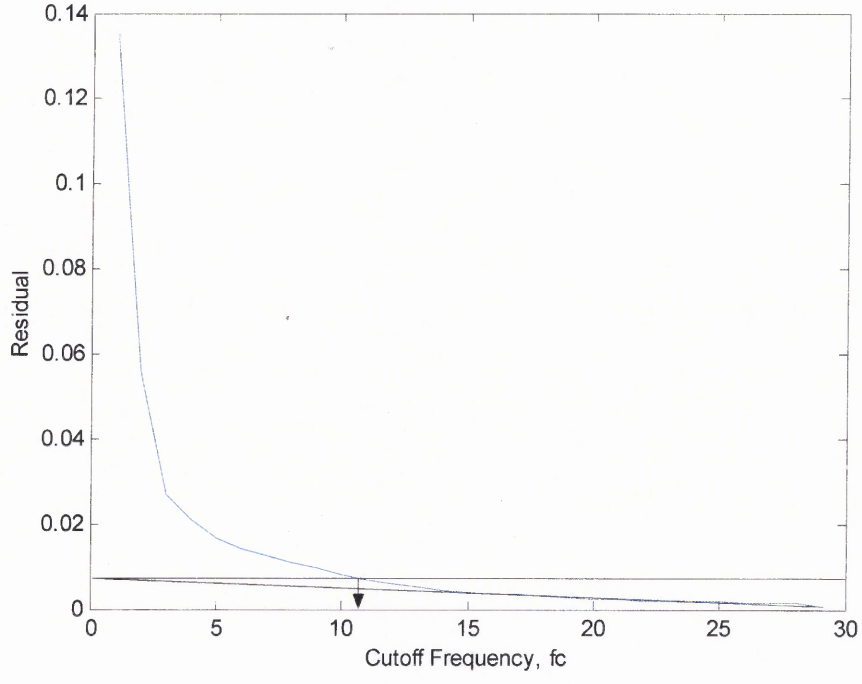

Figure E.2 Middle finger Z-position data residual plot for Table E.1.

APPENDIX F

FILTERED DATA AND RESIDUAL ANALYSIS FOR FINGER POSITION OF SUBJECT 2

The finger position data shown in Table F.1 was collected at 60 Hz on COM2 using the LabView program CyberFlock. The data was filtered using the cutoff frequencies found in the residual plots shown in Figures F.1 and F.2.

Table F.1 Filtered Index and Middle Finger Position Data for Subject 2

	Index Finger (Corrected Direction)	Middle Finger (Corrected Direction)
Time Sec.	Flock 1 (z) cm	Flock 2 (z) cm
0.000	-1.6073	-2.6789
0.017	-1.5724	-2.6781
0.033	-1.5650	-2.6701
0.050	-1.5953	-2.6573
0.067	-1.6536	-2.6513
0.083	-1.7227	-2.6609
0.100	-1.7969	-2.6817
0.117	-1.8867	-2.6971
0.133	-2.0042	-2.6914
0.150	-2.1430	-2.6628
0.167	-2.2754	-2.6237
0.183	-2.3700	-2.5881
0.200	-2.4138	-2.5593
0.217	-2.4189	-2.5306
0.233	-2.4112	-2.4952
0.250	-2.4103	-2.4541
0.267	-2.4195	-2.4112
0.283	-2.4300	-2.3645
0.300	-2.4340	-2.3045
0.317	-2.4324	-2.2239
0.333	-2.4340	-2.1275
0.350	-2.4473	-2.0313
0.367	-2.4739	-1.9501
0.383	-2.5079	-1.8853
0.400	-2.5396	-1.8271
0.417	-2.5617	-1.7671
0.433	-2.5713	-1.7076
0.450	-2.5705	-1.6598
0.467	-2.5655	-1.6344
0.483	-2.5650	-1.6351
0.500	-2.5769	-1.6596
0.517	-2.6011	-1.7036
0.533	-2.6279	-1.7627
0.550	-2.6437	-1.8326
0.567	-2.6426	-1.9094
0.583	-2.6301	-1.9921
0.600	-2.6167	-2.0822
0.617	-2.6081	-2.1803
0.633	-2.6024	-2.2833

Table F.1 Filtered Index and Middle Finger Position Data for Subject 2 (Continued)

	Index Finger Position (Corrected Direction)	Middle Finger Position (Corrected Direction)
Time	Flock 1(z)	Flock 2(z)
Sec.	cm	cm
0.650	-2.5947	-2.3848
0.667	-2.5844	-2.4778
0.683	-2.5748	-2.5566
0.700	-2.5670	-2.6167
0.717	-2.5548	-2.6558
0.733	-2.5281	-2.6769
0.750	-2.4845	-2.6882
0.767	-2.4360	-2.6986
0.783	-2.4003	-2.7125
0.800	-2.3840	-2.7276
0.817	-2.3760	-2.7389
0.833	-2.3589	-2.7427
0.850	-2.3256	-2.7388
0.867	-2.2824	-2.7291
0.883	-2.2365	-2.7155
0.900	-2.1856	-2.6980
0.917	-2.1214	-2.6765
0.933	-2.0429	-2.6527
0.950	-1.9623	-2.6305
0.967	-1.8953	-2.6132
0.983	-1.8492	-2.6018
1.000	-1.8192	-2.5941
1.017	-1.7967	-2.5880
1.033	-1.7777	-2.5821
1.050	-1.7643	-2.5765
1.067	-1.7586	-2.5704
1.083	-1.7591	-2.5633
1.100	-1.7629	-2.5561
1.117	-1.7709	-2.5507
1.133	-1.7883	-2.5475
1.150	-1.8197	-2.5437
1.167	-1.8649	-2.5348
1.183	-1.9178	-2.5193
1.200	-1.9711	-2.5015
1.217	-2.0196	-2.4897
1.233	-2.0633	-2.4907
1.250	-2.1091	-2.5040
1.267	-2.1673	-2.5217

Table F.1 Filtered Index and Middle Finger Position Data for Subject 2 (Continued)

	Index Finger Position (Corrected Direction)	Middle Finger Position (Corrected Direction)
Time Sec.	Flock 1(z) cm	Flock 2(z) cm
1.283	-2.2435	-2.5319
1.300	-2.3307	-2.5252
1.317	-2.4106	-2.5002
1.333	-2.4660	-2.4644
1.350	-2.4909	-2.4300
1.367	-2.4916	-2.4070
1.383	-2.4804	-2.3979
1.400	-2.4686	-2.3960
1.417	-2.4635	-2.3889
1.433	-2.4676	-2.3647
1.450	-2.4802	-2.3185
1.467	-2.4986	-2.2542
1.483	-2.5198	-2.1817
1.500	-2.5410	-2.1101
1.517	-2.5600	-2.0434
1.533	-2.5762	-1.9805
1.550	-2.5904	-1.9211
1.567	-2.6051	-1.8681
1.583	-2.6234	-1.8250
1.600	-2.6463	-1.7910
1.617	-2.6710	-1.7601
1.633	-2.6915	-1.7270
1.650	-2.7032	-1.6935
1.667	-2.7061	-1.6675
1.683	-2.7053	-1.6556
1.700	-2.7067	-1.6571
1.717	-2.7120	-1.6657
1.733	-2.7189	-1.6758
1.750	-2.7234	-1.6869
1.767	-2.7225	-1.7026
1.783	-2.7148	-1.7252
1.800	-2.7002	-1.7540
1.817	-2.6813	-1.7872
1.833	-2.6639	-1.8248
1.850	-2.6539	-1.8692
1.867	-2.6527	-1.9229
1.883	-2.6562	-1.9892
1.900	-2.6595	-2.0747

Table F.1 Filtered Index and Middle Finger Position Data for Subject 2 (Continued)

	Index Finger Position (Corrected Direction)	Middle Finger Position (Corrected Direction)
Time Sec.	Flock 1(z) cm	Flock 2(z) cm
1.917	-2.6615	-2.1875
1.933	-2.6645	-2.3260
1.950	-2.6683	-2.4707
1.967	-2.6654	-2.5897
1.983	-2.6434	-2.6595
2.000	-2.5958	-2.6809
2.017	-2.5300	-2.6769
2.033	-2.4645	-2.6737
2.050	-2.4160	-2.6828
2.067	-2.3865	-2.6973
2.083	-2.3632	-2.7027
2.100	-2.3296	-2.6895
2.117	-2.2757	-2.6584
2.133	-2.1994	-2.6165
2.150	-2.1040	-2.5718
2.167	-1.9970	-2.5325
2.183	-1.8903	-2.5066
2.200	-1.7974	-2.4997
2.217	-1.7274	-2.5097
2.233	-1.6815	-2.5265
2.250	-1.6569	-2.5375
2.267	-1.6524	-2.5353
2.283	-1.6700	-2.5207
2.300	-1.7088	-2.4984
2.317	-1.7591	-2.4734
2.333	-1.8052	-2.4501
2.350	-1.8365	-2.4341
2.367	-1.8568	-2.4302
2.383	-1.8812	-2.4393
2.400	-1.9234	-2.4566
2.417	-1.9849	-2.4738
2.433	-2.0556	-2.4849
2.450	-2.1224	-2.4885
2.467	-2.1783	-2.4868
2.483	-2.2244	-2.4827
2.500	-2.2657	-2.4781

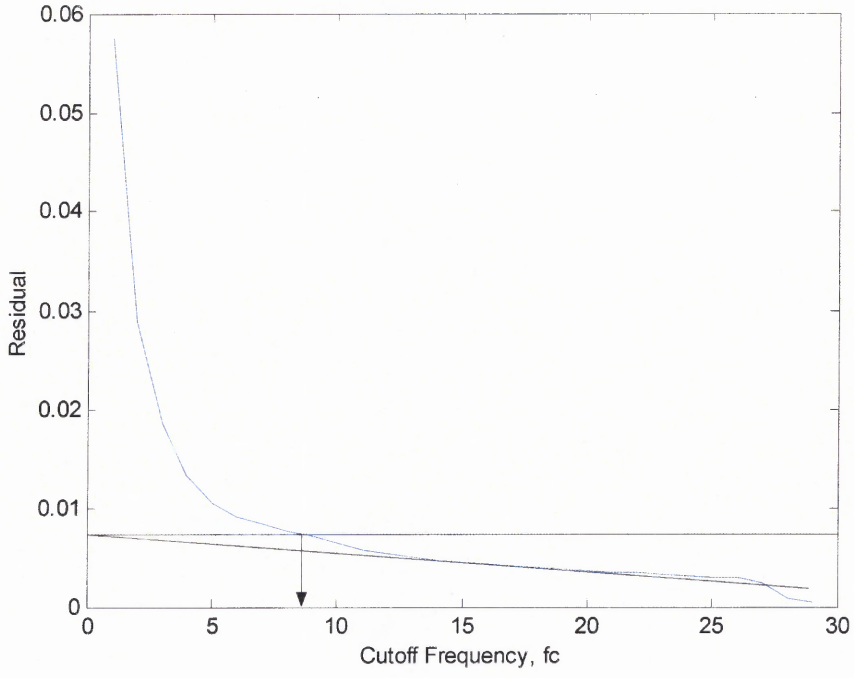

Figure F.1 Index finger Z-position data residual plot for Table F.1.

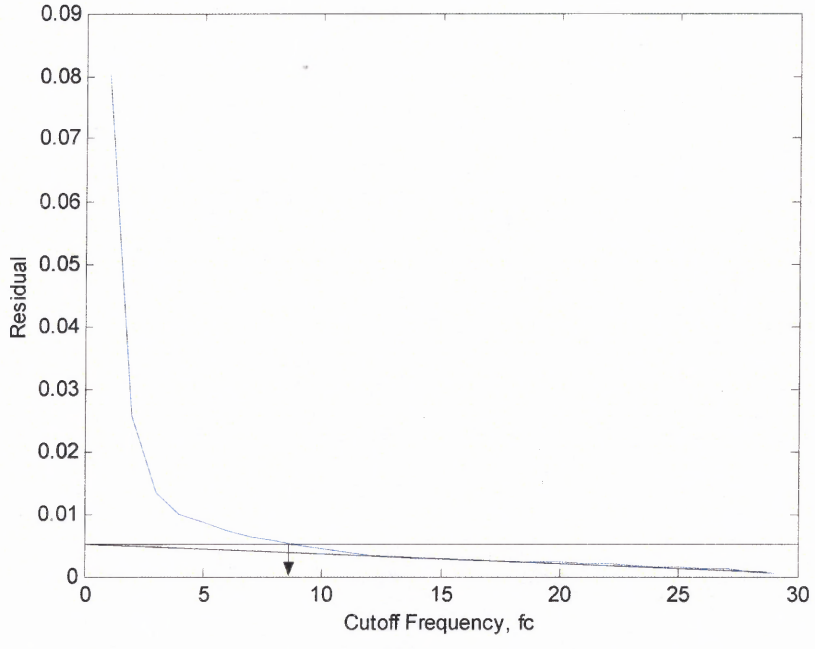

Figure F.2 Middle finger Z-position data residual plot for Table F.1.

APPENDIX G

FILTERED DATA AND RESIDUAL ANALYSIS FOR ANKLE POSITION OF SUBJECT 1

The ankle position data shown in Table G.1 was collected at 60 Hz on COM2 using the LabView program CyberFlock. Flock 1 was attached to the left ankle and Flock 2 was connected to the right ankle. The data was filtered using the cutoff frequencies found in the residual plots shown in Figures G.1 and G.2.

Table G.1 Filtered Ankle Position Data for Subject 1

	Ankle Position Data (Corrected Direction)	
Time Sec.	Flock 1 (z) cm	Flock 2 (z) cm
0.000	-2.2198	-2.7723
0.017	-2.2264	0.7901
0.033	-2.2635	3.7535
0.050	-2.3231	5.9704
0.067	-2.3643	7.7167
0.083	-2.3536	9.2541
0.100	-2.2994	10.4977
0.117	-2.2462	11.1453
0.133	-2.2325	11.0717
0.150	-2.2516	10.5138
0.167	-2.2541	9.8598
0.183	-2.1943	9.3062
0.200	-2.0859	8.7543
0.217	-2.0057	8.0165
0.233	-2.0250	7.0710
0.250	-2.1233	6.0932
0.267	-2.1828	5.2729
0.283	-2.0929	4.6523
0.300	-1.8702	4.1444
0.317	-1.6604	3.6652
0.333	-1.6040	3.2156
0.350	-1.6997	2.8533
0.367	-1.8114	2.6235
0.383	-1.8090	2.5232
0.400	-1.6943	2.5124
0.417	-1.5823	2.5380
0.433	-1.5697	2.5474
0.450	-1.6338	2.4924
0.467	-1.6605	2.3354
0.483	-1.5646	2.0582
0.500	-1.3734	1.6689
0.517	-1.1879	1.2033
0.533	-1.0551	0.7222
0.550	-0.8845	0.2966
0.567	-0.5047	-0.0203
0.583	0.1924	-0.2168
0.600	1.1737	-0.3206
0.617	2.3342	-0.3734
0.633	3.6240	-0.4063

Table G.1 Filtered Ankle Position Data for Subject 1 (Continued)

	Ankle Position Data (Corrected Direction)	
Time Sec.	Flock 1 (z) cm	Flock 2 (z) cm
0.650	5.0827	-0.4327
0.667	6.7447	-0.4545
0.683	8.5272	-0.4699
0.700	10.2322	-0.4771
0.717	11.6705	-0.4745
0.733	12.7771	-0.4620
0.750	13.6041	-0.4425
0.767	14.2152	-0.4217
0.783	14.6066	-0.4055
0.800	14.7271	-0.3971
0.817	14.5514	-0.3947
0.833	14.1183	-0.3929
0.850	13.5028	-0.3853
0.867	12.7613	-0.3682
0.883	11.9063	-0.3426
0.900	10.9334	-0.3129
0.917	9.8664	-0.2837
0.933	8.7663	-0.2571
0.950	7.6927	-0.2320
0.967	6.6674	-0.2059
0.983	5.6841	-0.1763
1.000	4.7441	-0.1416
1.017	3.8651	-0.1012
1.033	3.0577	-0.0548
1.050	2.3149	-0.0017
1.067	1.6367	0.0587
1.083	1.0575	0.1260
1.100	0.6389	0.1996
1.117	0.4294	0.2797
1.133	0.4215	0.3696
1.150	0.5356	0.4734
1.167	0.6444	0.5944
1.183	0.6258	0.7344
1.200	0.4128	0.8962
1.217	0.0125	1.0827
1.233	-0.5102	1.2951
1.250	-1.0673	1.5379
1.267	-1.5813	1.8357
1.283	-2.0065	2.2414

Table G.1 Filtered Ankle Position Data for Subject 1 (Continued)

	Ankle Position Data (Corrected Direction)	
Time Sec.	Flock 1 (z) cm	Flock 2 (z) cm
1.300	-2.3344	2.8126
1.317	-2.5838	3.5671
1.333	-2.7836	4.4618
1.350	-2.9577	5.4214
1.367	-3.1169	6.3855
1.383	-3.2554	7.3250
1.400	-3.3556	8.2214
1.417	-3.4030	9.0468
1.433	-3.4050	9.7669
1.450	-3.3928	10.3550
1.467	-3.3969	10.7928
1.483	-3.4174	11.0619
1.500	-3.4209	11.1395
1.517	-3.3732	11.0041
1.533	-3.2788	10.6484
1.550	-3.1846	10.0935
1.567	-3.1405	9.3887
1.583	-3.1548	8.5869
1.600	-3.1871	7.7114
1.617	-3.1848	6.7551
1.633	-3.1290	5.7150
1.650	-3.0450	4.6184
1.667	-2.9739	3.5081
1.683	-2.9387	2.4137
1.700	-2.9347	1.3603
1.717	-2.9455	0.4106
1.733	-2.9591	-0.3210
1.750	-2.9714	-0.7265
1.767	-2.9802	-0.8141
1.783	-2.9805	-0.7751
1.800	-2.9644	-0.9040
1.817	-2.9230	-1.3811
1.833	-2.8527	-2.1000
1.850	-2.7639	-2.7335
1.867	-2.6833	-3.0054
1.883	-2.6392	-2.9046
1.900	-2.6351	-2.6459
1.917	-2.6357	-2.4568
1.933	-2.5840	-2.4180

Table G.1 Filtered Ankle Position Data for Subject 1 (Continued)

	Ankle Position Data (Corrected Direction)	
Time Sec.	Flock 1 (z) cm	Flock 2 (z) cm
1.950	-2.4460	-2.4731
1.967	-2.2464	-2.5349
1.983	-2.0582	-2.5638
2.000	-1.9477	-2.5699
2.017	-1.9241	-2.5749
2.033	-1.9405	-2.5854
2.050	-1.9409	-2.5943
2.067	-1.9004	-2.5936
2.083	-1.8305	-2.5827

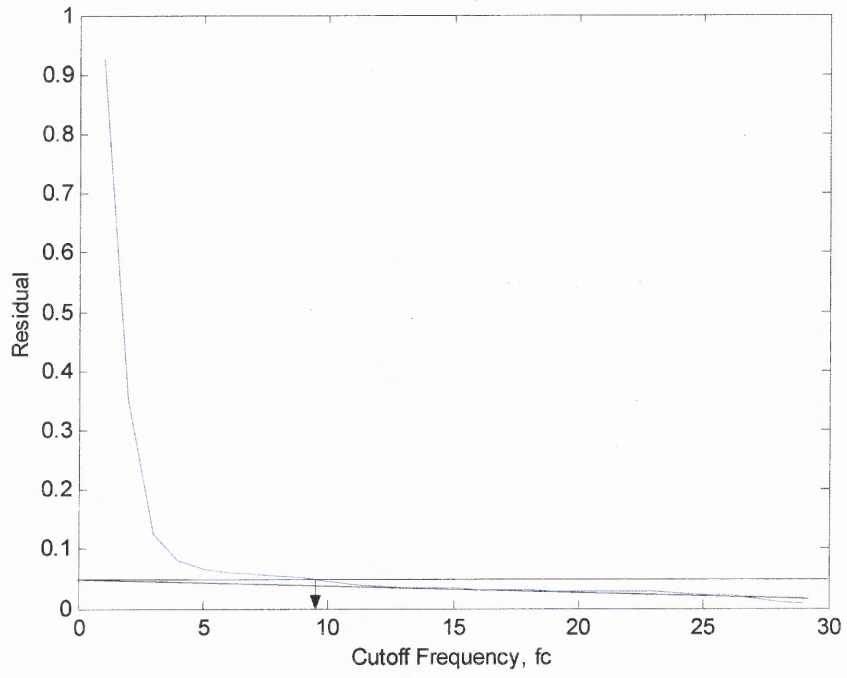

Figure G.1 Left ankle Z-position data residual plot for Table G.1.

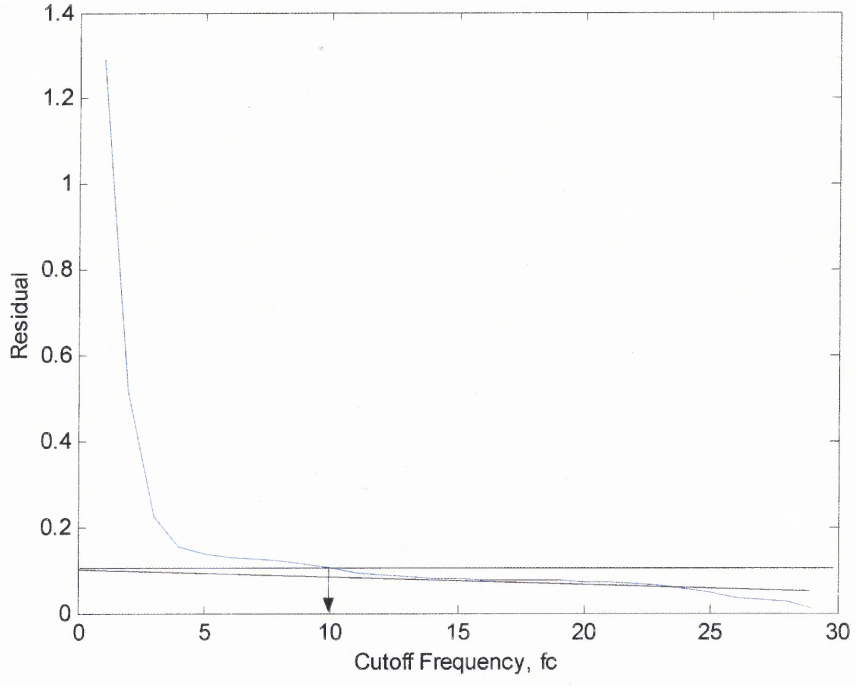

Figure G.2 Right ankle Z-position data residual plot for Table G.1.

APPENDIX H

FILTERED DATA AND RESIDUAL ANALYSIS FOR ANKLE POSITION OF SUBJECT 2

The ankle position data shown in Table H.1 was collected at 60 Hz on COM2 using the LabView program CyberFlock. Flock 1 was attached to the left ankle and Flock 2 was connected to the right ankle. The data was filtered using the cutoff frequencies found in the residual plots shown in Figures H.1 and H.2.

Table H.1 Filtered Ankle Position Data for Subject 2

	Ankle Position Data (Corrected Direction)	
Time Sec.	Flock 1 (z) cm	Flock 2 (z) cm
0.000	-2.4899	-0.3895
0.017	-2.5305	-0.5639
0.033	-2.5439	-0.7216
0.050	-2.5033	-0.8531
0.067	-2.3966	-0.9606
0.083	-2.2260	-1.0556
0.100	-1.9942	-1.1486
0.117	-1.6857	-1.2377
0.133	-1.2697	-1.3075
0.150	-0.7323	-1.3431
0.167	-0.1059	-1.3472
0.183	0.5476	-1.3439
0.200	1.2071	-1.3623
0.217	1.9531	-1.4154
0.233	2.9452	-1.4910
0.250	4.3054	-1.5627
0.267	5.9998	-1.6100
0.283	7.8230	-1.6308
0.300	9.4977	-1.6378
0.317	10.8035	-1.6461
0.333	11.6368	-1.6627
0.350	11.9900	-1.6853
0.367	11.9054	-1.7082
0.383	11.4527	-1.7269
0.400	10.7236	-1.7390
0.417	9.8167	-1.7424
0.433	8.8093	-1.7354
0.450	7.7458	-1.7195
0.467	6.6539	-1.7002
0.483	5.5731	-1.6856
0.500	4.5602	-1.6789
0.517	3.6706	-1.6739
0.533	2.9374	-1.6556
0.550	2.3672	-1.6081
0.567	1.9522	-1.5257
0.583	1.6809	-1.4164
0.600	1.5396	-1.2979
0.617	1.5059	-1.1860
0.633	1.5446	-1.0849

Table H.1 Filtered Ankle Position Data for Subject 2 (Continued)

	Ankle Position Data (Corrected Direction)	
Time Sec.	Flock 1 (z) cm	Flock 2 (z) cm
0.650	1.6099	-0.9861
0.667	1.6537	-0.8746
0.683	1.6373	-0.7362
0.700	1.5400	-0.5633
0.717	1.3610	-0.3576
0.733	1.1146	-0.1299
0.750	0.8213	0.1025
0.767	0.5012	0.3247
0.783	0.1751	0.5361
0.800	-0.1330	0.7558
0.817	-0.3958	1.0171
0.833	-0.5903	1.3518
0.850	-0.7084	1.7778
0.867	-0.7625	2.2994
0.883	-0.7793	2.9192
0.900	-0.7870	3.6470
0.917	-0.8032	4.4941
0.933	-0.8322	5.4571
0.950	-0.8693	6.5072
0.967	-0.9087	7.5944
0.983	-0.9463	8.6613
1.000	-0.9797	9.6539
1.017	-1.0059	10.5200
1.033	-1.0225	11.2056
1.050	-1.0296	11.6586
1.067	-1.0304	11.8426
1.083	-1.0292	11.7513
1.100	-1.0277	11.4120
1.117	-1.0233	10.8736
1.133	-1.0116	10.1862
1.150	-0.9909	9.3833
1.167	-0.9638	8.4801
1.183	-0.9358	7.4885
1.200	-0.9104	6.4368
1.217	-0.8851	5.3765
1.233	-0.8493	4.3703
1.250	-0.7879	3.4709
1.267	-0.6855	2.7080
1.283	-0.5329	2.0894

Table H.1 Filtered Ankle Position Data for Subject 2 (Continued)

	Ankle Position Data (Corrected Direction)	
Time Sec.	Flock 1 (z) cm	Flock 2 (z) cm
1.300	-0.3308	1.6091
1.317	-0.0913	1.2547
1.333	0.1648	1.0113
1.350	0.4158	0.8619
1.367	0.6494	0.7860
1.383	0.8680	0.7577
1.400	1.0842	0.7439
1.417	1.3109	0.7068
1.433	1.5544	0.6115
1.450	1.8157	0.4335
1.467	2.0958	0.1661
1.483	2.3995	-0.1747
1.500	2.7376	-0.5510
1.517	3.1295	-0.9122
1.533	3.6030	-1.2125
1.550	4.1863	-1.4287
1.567	4.8944	-1.5674
1.583	5.7204	-1.6556
1.600	6.6381	-1.7226
1.617	7.6147	-1.7857
1.633	8.6200	-1.8465
1.650	9.6228	-1.8979
1.667	10.5812	-1.9335
1.683	11.4384	-1.9532
1.700	12.1296	-1.9622
1.717	12.5941	-1.9664
1.733	12.7844	-1.9679
1.750	12.6727	-1.9637
1.767	12.2574	-1.9479
1.783	11.5685	-1.9143
1.800	10.6644	-1.8603
1.817	9.6153	-1.7878
1.833	8.4802	-1.7029
1.850	7.2969	-1.6128
1.867	6.0932	-1.5229
1.883	4.9072	-1.4347
1.900	3.7916	-1.3455
1.917	2.7952	-1.2495
1.933	1.9372	-1.1391

Table H.1 Filtered Ankle Position Data for Subject 2 (Continued)

	Ankle Position Data (Corrected Direction)	
Time Sec.	Flock 1 (z) cm	Flock 2 (z) cm
1.950	1.1987	-1.0088
1.967	0.5398	-0.8592
1.983	-0.0665	-0.6984
2.000	-0.6054	-0.5380
2.017	-1.0169	-0.3865
2.033	-1.2267	-0.2446
2.050	-1.1967	-0.1048
2.067	-0.9644	0.0428
2.083	-0.6446	0.2058
2.100	-0.3863	0.3860
2.117	-0.3054	0.5821
2.133	-0.4348	0.7942
2.150	-0.7210	1.0301
2.167	-1.0668	1.3087
2.183	-1.3875	1.6591
2.200	-1.6468	2.1126
2.217	-1.8568	2.6889
2.233	-2.0511	3.3841
2.250	-2.2553	4.1687
2.267	-2.4736	4.9991
2.283	-2.6914	5.8382
2.300	-2.8861	6.6710
2.317	-3.0353	7.5008
2.333	-3.1236	8.3224
2.350	-3.1480	9.0917
2.367	-3.1211	9.7198
2.383	-3.0692	10.1012
2.400	-3.0238	10.1616
2.417	-3.0086	9.8896
2.433	-3.0315	9.3360

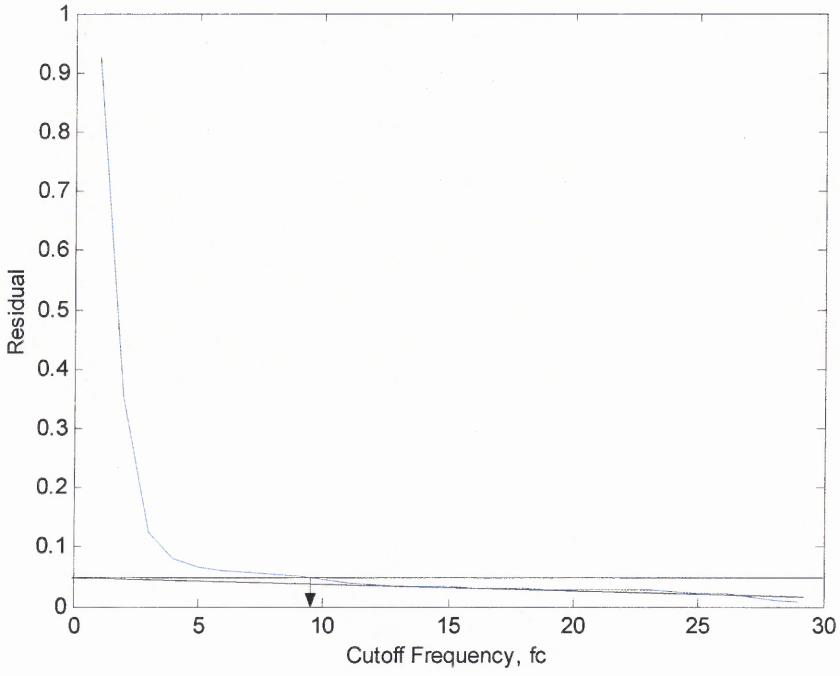

Figure H.1 Left ankle Z-position data residual plot for Table H.1.

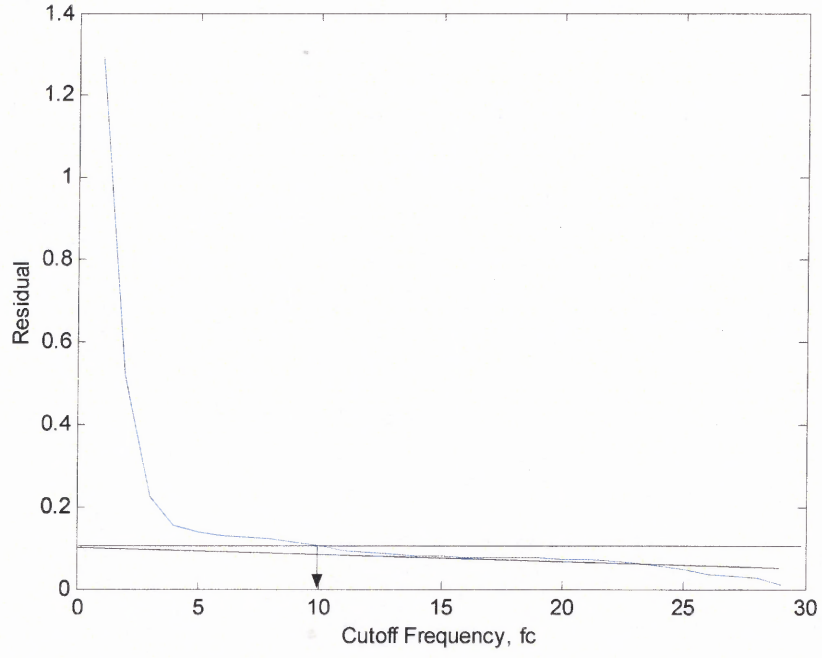

Figure H.2 Right ankle Z-position data residual plot for Table H.1.

APPENDIX I

FILTERED DATA AND RESIDUAL ANALYSIS FOR SLOWER PACED FINGER POSITION

The finger position data shown in Table I.1 was collected at 60 Hz on COM2 using the LabView program CyberFlock. The data was filtered using the cutoff frequencies found in the residual plots shown in Figures I.1 and I.2.

Table I.1 Filtered Index and Middle Finger Position Data, Slower Pace

	Index Finger (Corrected Direction)	Middle Finger (Corrected Direction)
Time Sec.	Flock 1 (z) cm	Flock 2 (z) cm
0.000	-2.5786	-2.9665
0.017	-2.9286	-2.6543
0.033	-2.9353	-2.6230
0.050	-2.9757	-2.6101
0.067	-3.0118	-2.5866
0.083	-3.0196	-2.5474
0.100	-3.0089	-2.5092
0.117	-3.0062	-2.4858
0.133	-3.0251	-2.4719
0.150	-3.0520	-2.4526
0.167	-3.0624	-2.4217
0.183	-3.0493	-2.3866
0.200	-3.0325	-2.3584
0.217	-3.0348	-2.3421
0.233	-3.0558	-2.3360
0.250	-3.0771	-2.3368
0.267	-3.0851	-2.3416
0.283	-3.0833	-2.3481
0.300	-3.0844	-2.3558
0.317	-3.0960	-2.3678
0.333	-3.1136	-2.3885
0.350	-3.1272	-2.4181
0.367	-3.1346	-2.4507
0.383	-3.1432	-2.4779
0.400	-3.1558	-2.4950
0.417	-3.1633	-2.5032
0.433	-3.1563	-2.5075
0.450	-3.1408	-2.5120
0.467	-3.1345	-2.5150
0.483	-3.1454	-2.5118
0.500	-3.1605	-2.5035
0.517	-3.1618	-2.5015
0.533	-3.1487	-2.5183
0.550	-3.1380	-2.5524
0.567	-3.1412	-2.5899
0.583	-3.1517	-2.6235
0.600	-3.1582	-2.6662
0.617	-3.1606	-2.7374
0.633	-3.1655	-2.8389

Table I.1 Filtered Index and Middle Finger Position Data, Slower Pace (Continued)

	Index Finger (Corrected Direction)	Middle Finger (Corrected Direction)
Time	Flock 1 (z)	Flock 2 (z)
Sec.	cm	cm
0.650	-3.1664	-2.9466
0.667	-3.1385	-3.0282
0.683	-3.0645	-3.0679
0.700	-2.9628	-3.0745
0.717	-2.8717	-3.0687
0.733	-2.8009	-3.0627
0.750	-2.7210	-3.0554
0.767	-2.6100	-3.0445
0.783	-2.4897	-3.0362
0.800	-2.4027	-3.0379
0.817	-2.3681	-3.0470
0.833	-2.3703	-3.0528
0.850	-2.3776	-3.0495
0.867	-2.3597	-3.0434
0.883	-2.2995	-3.0444
0.900	-2.2044	-3.0530
0.917	-2.1062	-3.0597
0.933	-2.0380	-3.0556
0.950	-2.0054	-3.0431
0.967	-1.9891	-3.0331
0.983	-1.9737	-3.0325
1.000	-1.9627	-3.0371
1.017	-1.9632	-3.0377
1.033	-1.9735	-3.0322
1.050	-1.9916	-3.0286
1.067	-2.0221	-3.0356
1.083	-2.0665	-3.0518
1.100	-2.1148	-3.0672
1.117	-2.1535	-3.0739
1.133	-2.1791	-3.0741
1.150	-2.1999	-3.0751
1.167	-2.2297	-3.0809
1.183	-2.2771	-3.0886
1.200	-2.3402	-3.0933
1.217	-2.4079	-3.0947
1.233	-2.4659	-3.0959
1.250	-2.5049	-3.0993
1.267	-2.5308	-3.1040
1.283	-2.5640	-3.1071

Table I.1 Filtered Index and Middle Finger Position Data, Slower Pace (Continued)

	Index Finger (Corrected Direction)	Middle Finger (Corrected Direction)
Time	Flock 1 (z)	Flock 2 (z)
Sec.	cm	cm
1.300	-2.6156	-3.1059
1.317	-2.6698	-3.1002
1.333	-2.7035	-3.0940
1.350	-2.7231	-3.0912
1.367	-2.7656	-3.0881
1.383	-2.8556	-3.0725
1.400	-2.9719	-3.0347
1.417	-3.0659	-2.9753
1.433	-3.1066	-2.8989
1.450	-3.1044	-2.8055
1.467	-3.0922	-2.6969
1.483	-3.0913	-2.5870
1.500	-3.0991	-2.4925
1.517	-3.1038	-2.4133
1.533	-3.1035	-2.3330
1.550	-3.1059	-2.2442
1.567	-3.1146	-2.1638
1.583	-3.1237	-2.1160
1.600	-3.1271	-2.1066
1.617	-3.1258	-2.1195
1.633	-3.1249	-2.1352
1.650	-3.1274	-2.1470
1.667	-3.1313	-2.1604
1.683	-3.1331	-2.1831
1.700	-3.1309	-2.2148
1.717	-3.1267	-2.2468
1.733	-3.1252	-2.2696
1.750	-3.1288	-2.2806
1.767	-3.1341	-2.2843
1.783	-3.1360	-2.2847
1.800	-3.1352	-2.2802
1.817	-3.1391	-2.2680
1.833	-3.1513	-2.2526
1.850	-3.1651	-2.2452
1.867	-3.1706	-2.2512
1.883	-3.1677	-2.2627
1.900	-3.1654	-2.2695
1.917	-3.1672	-2.2739
1.933	-3.1654	-2.2900

Table I.1 Filtered Index and Middle Finger Position Data, Slower Pace (Continued)

	Index Finger (Corrected Direction)	Middle Finger (Corrected Direction)
Time	Flock 1 (z)	Flock 2 (z)
Sec.	cm	cm
1.950	-3.1538	-2.3244
1.967	-3.1417	-2.3658
1.983	-3.1426	-2.3964
2.000	-3.1504	-2.4144
2.017	-3.1436	-2.4421
2.033	-3.1161	-2.5100
2.050	-3.0904	-2.6276
2.067	-3.0887	-2.7696
2.083	-3.1008	-2.8938
2.100	-3.0890	-2.9729
2.117	-3.0218	-3.0093
2.133	-2.9002	-3.0219
2.150	-2.7555	-3.0267
2.167	-2.6270	-3.0281
2.183	-2.5346	-3.0245
2.200	-2.4672	-3.0167
2.217	-2.3982	-3.0097
2.233	-2.3165	-3.0076
2.250	-2.2379	-3.0094
2.267	-2.1807	-3.0110
2.283	-2.1394	-3.0113
2.300	-2.0966	-3.0119
2.317	-2.0520	-3.0134
2.333	-2.0251	-3.0132
2.350	-2.0311	-3.0098
2.367	-2.0664	-3.0067
2.383	-2.1127	-3.0094
2.400	-2.1487	-3.0169
2.417	-2.1648	-3.0226
2.433	-2.1753	-3.0224
2.450	-2.2029	-3.0204
2.467	-2.2446	-3.0229
2.483	-2.2712	-3.0306
2.500	-2.2664	-3.0383
2.517	-2.2502	-3.0412
2.533	-2.2507	-3.0401
2.550	-2.2677	-3.0407
2.567	-2.2767	-3.0463
2.583	-2.2594	-3.0526

Table I.1 Filtered Index and Middle Finger Position Data, Slower Pace (Continued)

	Index Finger (Corrected Direction)	Middle Finger (Corrected Direction)
Time Sec.	Flock 1 (z) cm	Flock 2 (z) cm
2.600	-2.2218	-3.0525
2.617	-2.1849	-3.0450
2.633	-2.1642	-3.0374
2.650	-2.1629	-3.0362
2.667	-2.1849	-3.0387
2.683	-2.2374	-3.0359
2.700	-2.3092	-3.0231
2.717	-2.3643	-3.0066
2.733	-2.3873	-2.9984
2.750	-2.4252	-3.0017
2.767	-2.5440	-3.0006
2.783	-2.7359	-2.9709
2.800	-2.9106	-2.9036
2.817	-2.9928	-2.8162
2.833	-2.9954	-2.7352
2.850	-2.9787	-2.6696
2.867	-2.9771	-2.6059
2.883	-2.9893	-2.5269
2.900	-3.0114	-2.4304
2.917	-3.0451	-2.3275
2.933	-3.0805	-2.2314
2.950	-3.0990	-2.1518
2.967	-3.0960	-2.0966
2.983	-3.0874	-2.0714
3.000	-3.0889	-2.0741

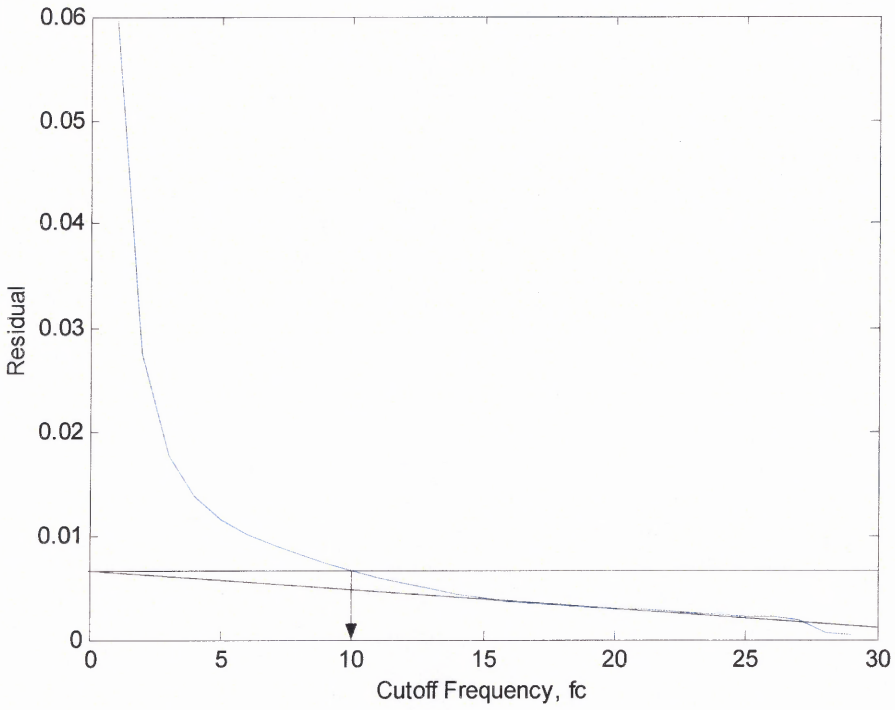

Figure I.1 Index finger Z-position data residual plot for Table I.1.

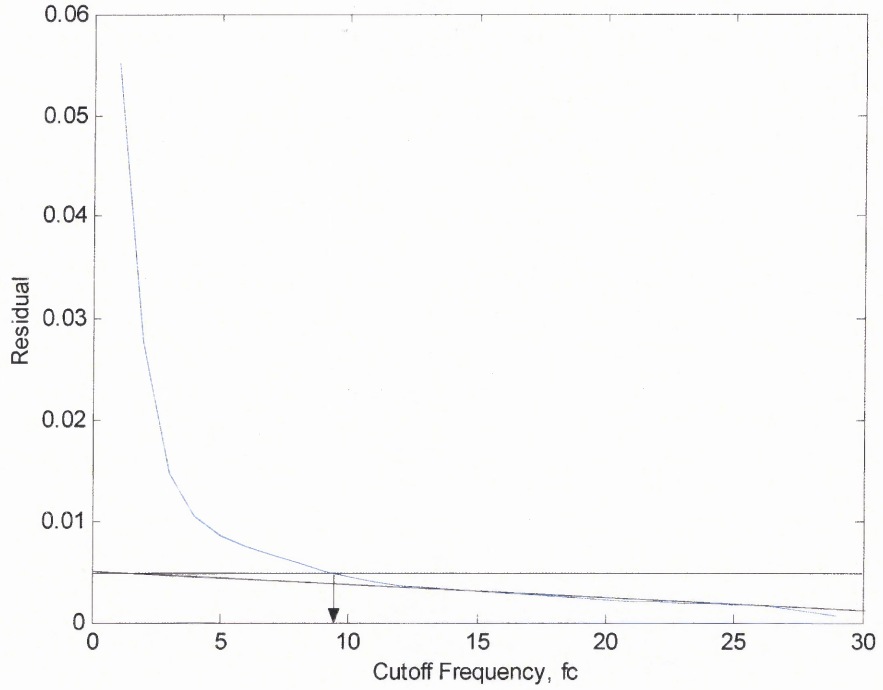

Figure I.2 Middle finger Z-position data residual plot for Table I.1.

APPENDIX J

FILTERED DATA AND RESIDUAL ANALYSIS FOR SIMULTANEOUS FINGER TIP POSITION AND GROUND REACTION FORCE

The finger tip position data shown in Table J.1 was collected at 60 Hz on COM2 using the LabView program CyberFlock. The finger tip ground reaction force data shown in Table H1 was collected on COM1 using the ATI-IA Standalone software. The data was filtered using the cutoff frequencies found in the residual plots shown in Figures J.1 and J.2.

Table J.1 Simultaneous "Finger Walking" Position and Ground Reaction Force Data

Flock 2 (z) Filtered Position Data (Corrected Direction)		Flock 2 (z) Ground Reaction Force Data (Corrected Direction)	
Time Sec.	Z Position cm	Time Sec.	Z Force Counts
0.000	5.8156	0.000	0
0.017	5.8150	0.014	0
0.035	5.8151	0.027	0
0.052	5.8166	0.041	0
0.069	5.8190	0.054	0
0.086	5.8218	0.068	0
0.104	5.8236	0.081	0
0.121	5.8235	0.095	0
0.138	5.8203	0.108	0
0.155	5.8138	0.122	0
0.173	5.8049	0.135	0
0.190	5.7955	0.149	0
0.207	5.7872	0.163	0
0.225	5.7800	0.176	0
0.242	5.7721	0.190	0
0.259	5.7626	0.203	0
0.276	5.7529	0.217	0
0.294	5.7472	0.230	0
0.311	5.7491	0.244	0
0.328	5.7584	0.257	0
0.346	5.7713	0.271	0
0.363	5.7832	0.284	0
0.380	5.7910	0.298	0
0.397	5.7940	0.311	0
0.415	5.7928	0.325	0
0.432	5.7893	0.339	0
0.449	5.7876	0.352	0
0.466	5.7965	0.366	0
0.484	5.8291	0.379	0
0.501	5.8994	0.393	0
0.518	6.0153	0.406	0
0.536	6.1740	0.420	0
0.553	6.3621	0.433	0
0.570	6.5597	0.447	0
0.587	6.7444	0.460	0
0.605	6.8964	0.474	0
0.622	7.0031	0.488	0

Table J.1 Simultaneous "Finger Walking" Position and Ground Reaction Force Data (Continued)

Flock 2 (z) Filtered Position Data (Corrected Direction)		Flock 2 (z) Partially Filtered GRF Data (Corrected Direction)	
Time Sec.	Z Position cm	Time Sec.	Z Force Counts
0.639	7.0632	0.501	0
0.657	7.0845	0.515	0
0.674	7.0778	0.528	0
0.691	7.0514	0.542	0
0.708	7.0127	0.555	0
0.726	6.9710	0.569	0
0.743	6.9364	0.582	0
0.760	6.9135	0.596	0
0.777	6.8944	0.609	0
0.795	6.8613	0.623	0
0.812	6.7952	0.636	0
0.829	6.6869	0.650	0
0.847	6.5421	0.664	0
0.864	6.3783	0.677	0
0.881	6.2180	0.691	0
0.898	6.0817	0.704	0
0.916	5.9814	0.718	0
0.933	5.9177	0.731	0
0.950	5.8820	0.745	0
0.967	5.8612	0.758	0
0.985	5.8441	0.772	0
1.002	5.8247	0.785	0
1.019	5.8017	0.799	0
1.037	5.7771	0.813	0
1.054	5.7535	0.826	0
1.071	5.7337	0.840	0
1.088	5.7200	0.853	0
1.106	5.7133	0.867	0
1.123	5.7132	0.880	2.0004
1.140	5.7168	0.894	12.9303
1.158	5.7211	0.907	30.9820
1.175	5.7239	0.921	55.5012
1.192	5.7249	0.934	79.4372
1.209	5.7251	0.948	97.1714
1.227	5.7247	0.962	109.0587
1.244	5.7223	0.975	118.4893
1.261	5.7161	0.989	126.4701

Table J.1 Simultaneous "Finger Walking" Position and Ground Reaction Force Data (Continued)

Flock 2 (z) Filtered Position Data (Corrected Direction)		Flock 2 (z) Partially Filtered GRF Data (Corrected Direction)	
Time Sec.	Z Position cm	Time Sec.	Z Force Counts
1.278	5.7059	1.002	130.6208
1.296	5.6944	1.016	129.1065
1.313	5.6861	1.029	123.6517
1.330	5.6846	1.043	117.6118
1.348	5.6916	1.056	112.3677
1.365	5.7070	1.070	107.2615
1.382	5.7311	1.083	102.3613
1.399	5.7660	1.097	99.2283
1.417	5.8149	1.110	98.5970
1.434	5.8801	1.124	98.8859
1.451	5.9611	1.138	97.9753
1.469	6.0532	1.151	95.6344
1.486	6.1488	1.165	93.3152
1.503	6.2402	1.178	92.0713
1.520	6.3227	1.192	91.5111
1.538	6.3968	1.205	90.6062
1.555	6.4648	1.219	88.9313
1.572	6.5275	1.232	87.0947
1.589	6.5811	1.246	86.1931
1.607	6.6182	1.259	86.8100
1.624	6.6331	1.273	88.4938
1.641	6.6267	1.287	90.2696
1.659	6.6075	1.300	91.4940
1.676	6.5877	1.314	91.9117
1.693	6.5760	1.327	90.9948
1.710	6.5716	1.341	87.7108
1.728	6.5644	1.354	81.1473
1.745	6.5392	1.368	71.2040
1.762	6.4838	1.381	58.7201
1.779	6.3962	1.395	45.2197
1.797	6.2876	1.408	32.4988
1.814	6.1782	1.422	22.0830
1.831	6.0881	1.435	14.7629
1.849	6.0278	1.449	10.4003
1.866	5.9945	1.463	8.0567
1.883	5.9765	1.476	6.5155
1.900	5.9618	1.490	5.0010

Table J.1 Simultaneous "Finger Walking" Position and Ground Reaction Force Data (Continued)

Flock 2 (z) Filtered Position Data (Corrected Direction)		Flock 2 (z) Partially Filtered GRF Data (Corrected Direction)	
Time Sec.	Z Position cm	Time Sec.	Z Force Counts
1.918	5.9443	1.503	3.4430
1.935	5.9250	1.517	2.0173
1.952	5.9083	1.530	0
1.970	5.8973	1.544	0
1.987	5.8916	1.557	0
2.004	5.8883	1.571	0
2.021	5.8848	1.584	0
2.039	5.8806	1.598	0
2.056	5.8766	1.612	0
2.073	5.8741	1.625	0
2.090	5.8739	1.639	0
2.108	5.8758	1.652	0
2.125	5.8791	1.666	0
2.142	5.8827	1.679	0
2.160	5.8859	1.693	0
2.177	5.8893	1.706	0
2.194	5.8944	1.720	0
2.211	5.9026	1.733	0
2.229	5.9136	1.747	0
2.246	5.9246	1.761	0
2.263	5.9323	1.774	0
2.281	5.9348	1.788	0
2.298	5.9332	1.801	0
2.315	5.9304	1.815	0
2.332	5.9284	1.828	0
2.350	5.9271	1.842	0
2.367	5.9251	1.855	0
2.384	5.9214	1.869	0
2.401	5.9175	1.882	0
2.419	5.9171	1.896	0
2.436	5.9232	1.909	0
2.453	5.9358	1.923	0
2.471	5.9516	1.937	0
2.488	5.9652	1.950	0
2.505	5.9731	1.964	0
2.522	5.9757	1.977	0
2.540	5.9784	1.991	0

Table J.1 Simultaneous "Finger Walking" Position and Ground Reaction Force Data (Continued)

Flock 2 (z) Filtered Position Data (Corrected Direction)		Flock 2 (z) Partially Filtered GRF Data (Corrected Direction)	
Time Sec.	Z Position cm	Time Sec.	Z Force Counts
2.557	5.9891	2.004	0
2.574	6.0146	2.018	0
2.591	6.0566	2.031	0
2.609	6.1094	2.045	0
2.626	6.1639	2.058	0
2.643	6.2129	2.072	0
2.661	6.2563	2.086	0
2.678	6.2990	2.099	0
2.695	6.3445	2.113	0
2.712	6.3908	2.126	0
2.730	6.4311	2.140	0
2.747	6.4589	2.153	0
2.764	6.4700	2.167	0
2.782	6.4623	2.180	0
2.799	6.4347	2.194	0
2.816	6.3891	2.207	0
2.833	6.3318	2.221	0
2.851	6.2727	2.234	0
2.868	6.2218	2.248	0
2.885	6.1850	2.262	0
2.902	6.1613	2.275	0
2.920	6.1454	2.289	0
2.937	6.1307	2.302	0
2.954	6.1134	2.316	0
2.972	6.0937	2.329	0
		2.343	0
		2.356	0
		2.370	0
		2.383	0
		2.397	0
		2.411	0
		2.424	0
		2.438	0
		2.451	0
		2.465	0
		2.478	0
		2.492	0

Table J.1 Simultaneous "Finger Walking" Position and Ground Reaction Force Data (Continued)

Flock 2 (z) Partially Filtered GRF Data (Corrected Direction)	
Time Sec.	Z Force Counts
2.505	0
2.519	0
2.532	0
2.546	0
2.560	0
2.573	0
2.587	0
2.600	0
2.614	0
2.627	0
2.641	0
2.654	0
2.668	0
2.681	0
2.695	0
2.708	0
2.722	0
2.736	0
2.749	0
2.763	0
2.776	0
2.790	0
2.803	0
2.817	0
2.830	0
2.844	0
2.857	0
2.871	0
2.885	0
2.898	0
2.912	0
2.925	0
2.939	0
2.952	0
2.966	0
2.979	0
2.993	0

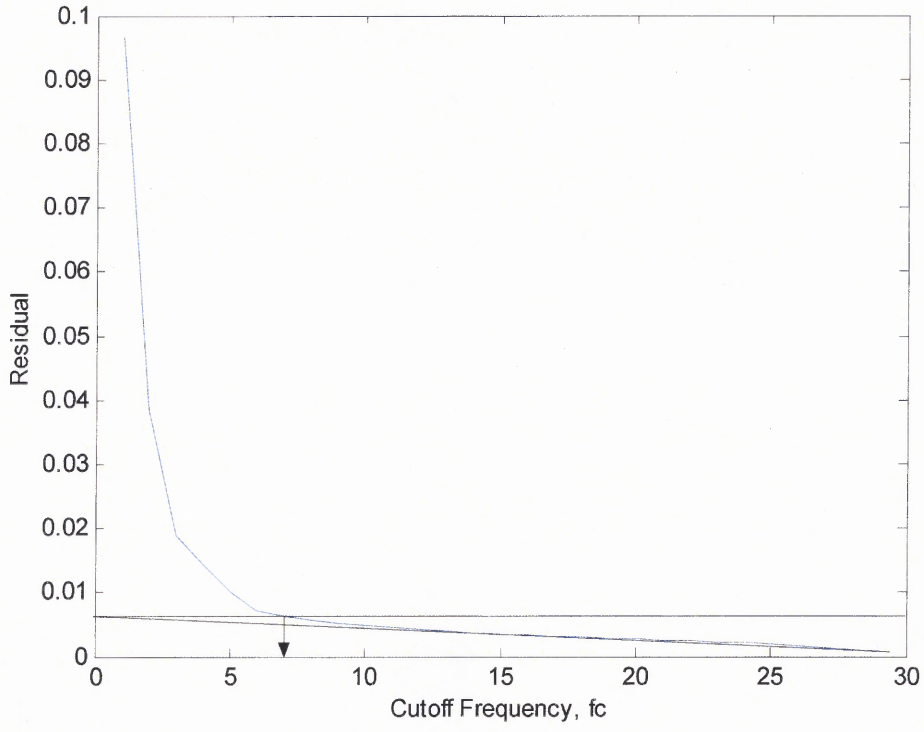

Figure J.1 Middle finger Z-position data residual plot for Table J.1.

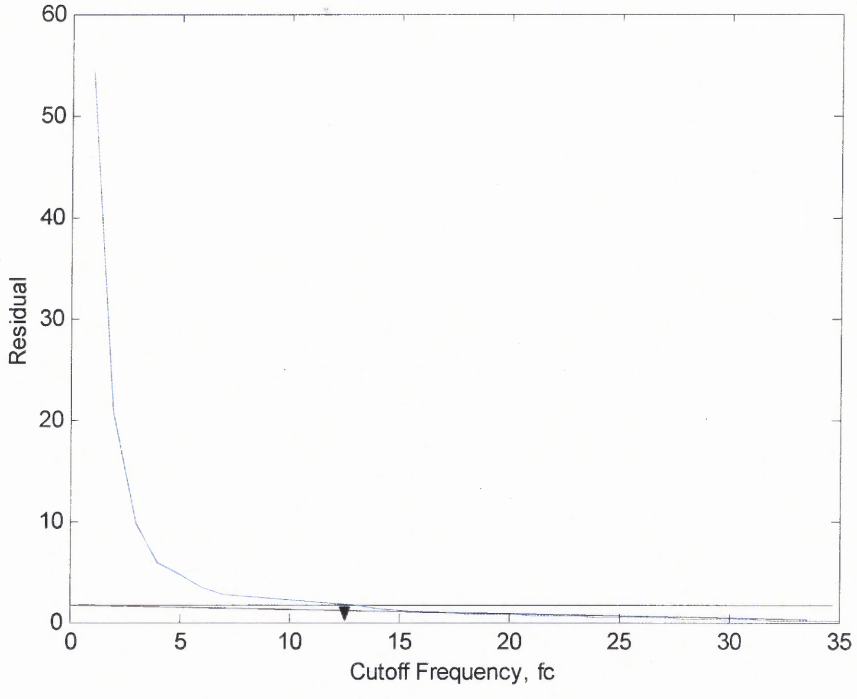

Figure J.2 Middle finger Z-force data residual plot for Table J.1.

APPENDIX K

NORMALIZED AVERAGE AND STANDARD DEVIATION FINGER TIP FORCE VALUES FOR SUBJECT 1

Ten ground reaction force data samples were collected on COM1 using the ATI-IA Standalone software. The average and standard deviations were calculated for the normalized curves at each data point. These calculated values are shown in Table K.1.

Table K.1 Finger Tip Normalized Ground Reaction Force Data for Subject 1

	Finger Tip Normalized GRF			
Time	X-Force Average	X-Force Standard Dev.	Z-Force Average	Z-Force Standard Dev.
0.000	-0.0375	0.0135	0.0279	0.0056
0.028	-0.0144	0.0396	0.1103	0.0462
0.056	-0.0274	0.0754	0.2259	0.0569
0.083	-0.0799	0.1038	0.3470	0.0728
0.111	-0.1421	0.1404	0.4859	0.1122
0.139	-0.1698	0.1568	0.6370	0.1021
0.167	-0.1615	0.1718	0.7628	0.0954
0.194	-0.1203	0.1783	0.8655	0.0850
0.222	-0.0516	0.1684	0.9188	0.0600
0.250	0.0515	0.1601	0.9597	0.0350
0.278	0.1605	0.1652	0.9779	0.0349
0.306	0.2933	0.1544	0.9470	0.0501
0.333	0.4401	0.1345	0.8903	0.0532
0.361	0.5371	0.1394	0.8415	0.0537
0.389	0.5986	0.1597	0.7965	0.0611
0.417	0.6356	0.1650	0.7516	0.0628
0.444	0.6471	0.1602	0.7145	0.0606
0.472	0.6343	0.1540	0.6885	0.0566
0.500	0.6148	0.1537	0.6713	0.0460
0.528	0.6007	0.1448	0.6581	0.0359
0.556	0.5961	0.1454	0.6468	0.0251
0.583	0.6165	0.1471	0.6368	0.0228
0.611	0.6416	0.1515	0.6310	0.0258
0.639	0.6568	0.1512	0.6246	0.0313
0.667	0.6712	0.1501	0.6190	0.0348
0.694	0.6879	0.1451	0.6126	0.0339
0.722	0.7128	0.1402	0.6032	0.0334
0.750	0.7407	0.1321	0.5897	0.0364
0.778	0.7529	0.1135	0.5694	0.0456
0.806	0.7450	0.1162	0.5218	0.0605
0.833	0.6736	0.1501	0.4478	0.0939
0.861	0.5145	0.2216	0.3515	0.1202
0.889	0.3267	0.2511	0.2498	0.0933
0.917	0.1838	0.1967	0.1490	0.0651
0.944	0.0895	0.1154	0.0802	0.0345
0.972	0.0546	0.0471	0.0457	0.0112
1.000	0.0581	0.0219	0.0291	0.0038

APPENDIX L

NORMALIZED AVERAGE AND STANDARD DEVIATION FINGER TIP FORCE VALUES FOR SUBJECT 2

Ten ground reaction force data samples were collected on COM1 using the ATI-IA Standalone software. The average and standard deviations were calculated for the normalized curves at each data point. These calculated values are shown in Table L.1.

Table L.1 Finger Tip Normalized Ground Reaction Force Data for Subject 2

	Finger Tip Normalized GRF			
Time	X-Force Average	X-Force Standard Dev.	Z-Force Average	Z-Force Standard Dev.
0.000	-0.0082	0.0906	0.0033	0.0344
0.029	-0.2099	0.1998	0.2337	0.0831
0.059	-0.3633	0.2808	0.4511	0.1201
0.088	-0.4329	0.3127	0.6325	0.1203
0.118	-0.4440	0.3333	0.7538	0.1053
0.147	-0.3855	0.3740	0.8498	0.0891
0.176	-0.3057	0.3888	0.9140	0.0662
0.206	-0.2313	0.3865	0.9413	0.0442
0.235	-0.1676	0.3797	0.9513	0.0283
0.265	-0.1245	0.3811	0.9488	0.0363
0.294	-0.0889	0.3876	0.9400	0.0437
0.324	-0.0511	0.3896	0.9342	0.0437
0.353	-0.0091	0.3857	0.9278	0.0451
0.382	0.0307	0.3792	0.9200	0.0542
0.412	0.0678	0.3706	0.9036	0.0636
0.441	0.0980	0.3551	0.8767	0.0691
0.471	0.1286	0.3388	0.8540	0.0739
0.500	0.1585	0.3395	0.8376	0.0783
0.529	0.1737	0.3473	0.8319	0.0785
0.559	0.1813	0.3469	0.8398	0.0822
0.588	0.1911	0.3335	0.8450	0.0869
0.618	0.2182	0.3194	0.8412	0.0952
0.647	0.2512	0.3148	0.8307	0.1079
0.676	0.2822	0.3126	0.8135	0.1189
0.706	0.3145	0.2918	0.7877	0.1235
0.735	0.3418	0.2582	0.7562	0.1254
0.765	0.3689	0.2226	0.7187	0.1299
0.794	0.4055	0.2041	0.6745	0.1453
0.824	0.4382	0.2016	0.6329	0.1645
0.853	0.4345	0.2029	0.5768	0.1562
0.882	0.3874	0.1934	0.4737	0.1375
0.912	0.2765	0.1719	0.3395	0.1102
0.941	0.1440	0.1498	0.2081	0.0747
0.971	0.0469	0.1387	0.1036	0.0492
1.000	-0.0037	0.1478	0.0250	0.0376

APPENDIX M

FILTERED PUBLISHED HUMAN ANKLE POSITION DATA

Raw ankle position data [20] was filtered and can be found in Table M.1. The data was filtered using the cutoff frequencies found in the residual plots shown in Figures M.1 and M.2.

Table M.1 Filtered Position Data for the Right Ankle [20]

	Filtered Coordinate Data	
Time	X	Y
Sec.	cm	cm
0.000	9.23	21.45
0.014	12.93	22.58
0.029	16.75	23.55
0.043	20.73	24.21
0.057	24.90	24.49
0.072	29.26	24.39
0.086	33.78	23.94
0.100	38.44	23.22
0.114	43.23	22.26
0.129	48.14	21.11
0.143	53.19	19.82
0.157	58.38	18.43
0.172	63.72	17.02
0.186	69.19	15.66
0.200	74.74	14.44
0.215	80.33	13.41
0.229	85.89	12.61
0.243	91.36	12.04
0.257	96.68	11.71
0.272	101.78	11.60
0.286	106.57	11.67
0.300	110.95	11.86
0.315	114.81	12.10
0.329	118.07	12.25
0.343	120.69	12.22
0.357	122.70	11.93
0.372	124.19	11.41
0.386	125.31	10.77
0.400	126.21	10.16
0.415	126.99	9.71
0.429	127.70	9.47
0.443	128.34	9.40
0.458	128.88	9.44
0.472	129.31	9.48
0.486	129.62	9.49
0.500	129.84	9.45
0.515	130.01	9.41
0.529	130.13	9.37
0.543	130.22	9.35
0.558	130.27	9.35
0.572	130.28	9.35

Table M.1 Filtered Position Data for the Right Ankle [20] (Continued)

	Filtered Coordinate Data	
Time	X	Y
Sec.	cm	cm
0.586	130.25	9.39
0.601	130.19	9.47
0.615	130.14	9.60
0.629	130.12	9.75
0.643	130.13	9.90
0.658	130.20	10.01
0.672	130.30	10.07
0.686	130.44	10.10
0.701	130.60	10.12
0.715	130.76	10.14
0.729	130.92	10.19
0.744	131.08	10.26
0.758	131.22	10.38
0.772	131.37	10.56
0.786	131.52	10.83
0.801	131.67	11.18
0.815	131.83	11.60
0.829	132.02	12.08
0.844	132.29	12.60
0.858	132.70	13.17
0.872	133.32	13.81
0.887	134.21	14.55
0.901	135.40	15.41
0.915	136.93	16.37
0.929	138.78	17.41
0.944	140.95	18.49
0.958	143.43	19.57
0.972	146.21	20.65
0.987	149.29	21.70
1.001	152.62	22.68
1.015	156.21	23.52
1.030	160.01	24.11
1.044	164.03	24.37
1.058	168.25	24.25
1.072	172.67	23.79
1.087	177.29	23.02
1.101	182.09	22.03
1.115	187.07	20.86
1.130	192.20	19.57
1.144	197.45	18.18
1.158	202.80	16.73

Table M.1 Filtered Position Data for the Right Ankle [20] (Continued)

	Filtered Coordinate Data	
Time	X	Y
Sec.	cm	cm
1.173	208.24	15.29
1.187	213.77	13.93
1.201	219.38	12.73
1.215	225.06	11.77
1.230	230.78	11.09
1.244	236.45	10.70
1.258	241.95	10.60
1.273	247.14	10.73
1.287	251.82	10.99
1.301	255.88	11.27
1.316	259.22	11.40
1.330	261.84	11.31
1.344	263.83	10.97
1.358	265.34	10.47
1.373	266.54	9.95
1.387	267.59	9.54
1.401	268.56	9.31
1.416	269.46	9.22
1.430	270.25	9.22
1.444	270.85	9.23
1.459	271.20	9.19
1.473	271.28	9.09
1.487	271.12	8.97
1.501	270.82	8.83

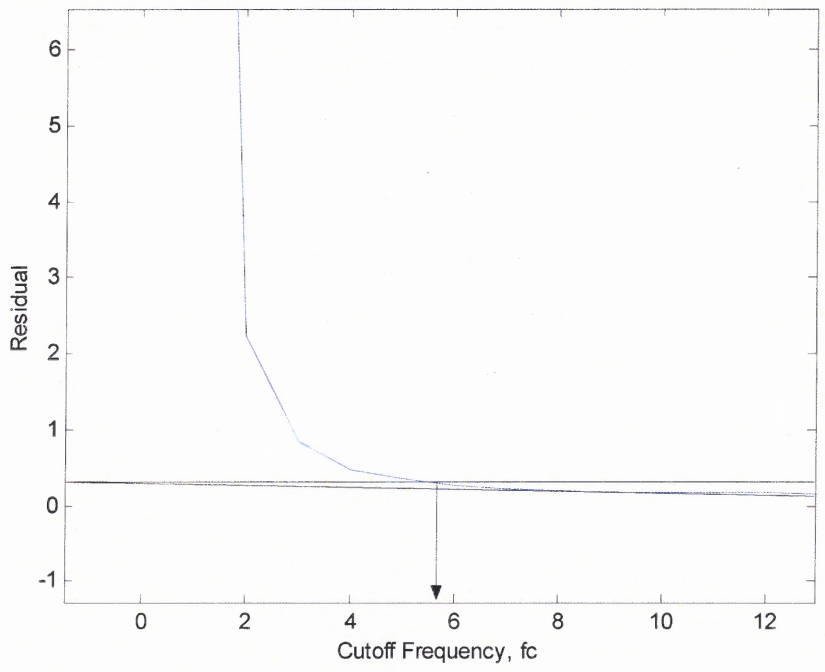

Figure M.1 Published ankle X-position data residual plot.

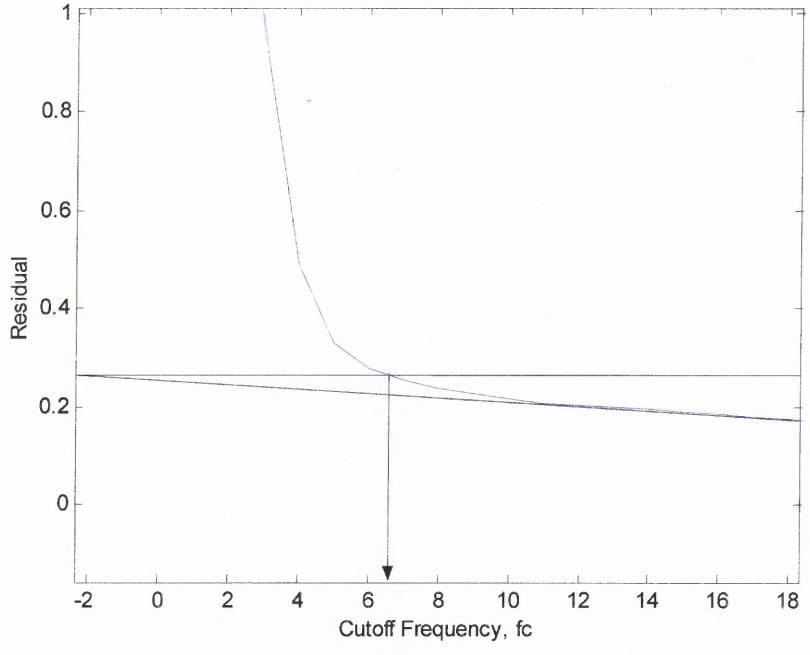

Figure M.2 Published ankle Y-position data residual plot.

APPENDIX N

NORMALIZED PUBLISHED HUMAN GROUND REACTION FORCE DATA

Normalized ground reaction force data [20] can be found in Table N.1.

Table N.1 Normalized Ground Reaction Forces for Normal Human Walking [20]

Time	X-Force	Z-Force
0.000	0.1623	0.1423
0.024	-0.0183	0.3147
0.049	-0.1902	0.4968
0.073	-0.3220	0.6603
0.098	-0.3999	0.7786
0.122	-0.4469	0.8523
0.146	-0.4809	0.9033
0.171	-0.4970	0.9472
0.195	-0.4809	0.9796
0.220	-0.4269	0.9876
0.244	-0.3473	0.9637
0.268	-0.2698	0.9118
0.293	-0.2119	0.8441
0.317	-0.1732	0.7734
0.341	-0.1436	0.7081
0.366	-0.1175	0.6540
0.390	-0.0949	0.6161
0.415	-0.0788	0.5963
0.439	-0.0722	0.5919
0.463	-0.0731	0.5988
0.488	-0.0731	0.6126
0.512	-0.0631	0.6308
0.537	-0.0418	0.6540
0.561	-0.0165	0.6842
0.585	0.0096	0.7205
0.610	0.0379	0.7610
0.634	0.0718	0.8066
0.659	0.1166	0.8559
0.683	0.1745	0.9028
0.707	0.2385	0.9423
0.732	0.2963	0.9734
0.756	0.3464	0.9943
0.780	0.3951	1.0000
0.805	0.4417	0.9840
0.829	0.4804	0.9412
0.854	0.5030	0.8664
0.878	0.4983	0.7564
0.902	0.4578	0.6164
0.927	0.3838	0.4609
0.951	0.2859	0.3106
0.976	0.1802	0.1810
1.000	0.0801	0.0725

REFERENCES

[1] National Spinal Cord Injury Statistical Center, "Spinal Cord Injury: Facts and Figures at a Glance - December 2003" [online], Birmingham, AL: Spinal Cord Injury Information Network, 2003 [cited March 30, 2004], available from World Wide Web: <http://www.spinalcord.uab.edu/show.asp?durki=21446>.

[2] Rehab Team Site, "Overview: Functional Outcomes: Thoracic, Lumbar, and Sacral Injuries – Paraplegia" [online], Miami, FL: Louis Calder Memorial Library of the University of Miami/Jackson Memorial Medical Center, 1998 [cited March 30, 2004], available from World Wide Web: <http://calder.med.miami.edu/providers/MEDICINE/parap.html>.

[3] Linda Lindsey and Phil Klebine, "Understanding Spinal Cord Injury & Functional Goal" [online], Birmingham, AL: Spinal Cord Injury Information Network, June 2000 [cited March 30, 2004], available from World Wide Web: <http://www.spinalcord.uab.edu/show.asp?durki=22408>.

[4] Lauralee Sherwood, *Human Physiology: From Cells to Systems*, 4th ed., Pacific Grove, CA: Brooks/Cole, 2001.

[5] MedAssist Group, "MedAssist/OrthAbility - Knee Ankle Foot Orthoses, Product Descriptions, Pictures, Patient Profiles" [online], Tampa, FL: MedAssist Group, 2001 [cited March 30, 2004], available from World Wide Web: <http://www.medassistgp.com/medprod3.html>.

[6] Fillauer, Inc., "Reciprocating Gait Orthosis: A Pictorial Description and Application Manual" [online], Chatt., TN: Fillauer, Inc., [cited March 30, 2004], available from World Wide Web: <http://www.fillauer.com/customfab/pdfs/M009-RGO.pdf>.

[7] Center for Orthotics Design, "Center for Orthotics Design > ISOCENTRIC RGO" [online], Campbell, CA: Center for Orthotics Design, [cited March 30, 2004], available from World Wide Web: <http://www.centerfororthoticsdesign.com/isocentric_rgo/index.html>.

[8] M. R. Popovic, T. Keller, I. P. I. Pappas, D. Volker, and M. Morari, "Surface-Stimulation Technology for Grasping and Walking Neuroprostheses," *IEEE Engineering in Medicine and Biology,* Jan./Feb. 2001, pp. 82-93.

[9] Carl Billian and Jeanne O. Teeter, "Functional Electrical Stimulation and Paralysis: A MEDICAL FACT SHEET from the FES Information Center" [online], Cleveland, OH: Cleveland FES Information Center, Mar. 1992 [cited Apr. 2, 2004], available from World Wide Web: <http://feswww.fes.cwru.edu/info/fes&para.php>.

[10] E. Ayyappa, "Normal Human Locomotion, Part 1: Basic Concepts and Terminology," *Journal of Prosthetics & Orthotics,* vol. 9, no. 1, 1997, pp. 10-17.

[11] Roger M. Enoka, *Neuromechanics of Human Movement*, 3rd ed., Champaign, IL: Human Kinetics, 2002.

[12] Nigel Palastanga, Derek Field, and Roger Soames, *Anatomy and Human Movement*, 4th ed., Boston, MA: Butterworth-Heinemann, 2002.

[13] Frederic H. Martini, *Fundamentals of Anatomy & Physiology*, 5th ed., Upper Saddle River, NJ: Prentice-Hall, 2001.

[14] Ascension Technology Corporation, "Ascension Products – Flock of Birds" [online], Burlington, VT: Ascension Technology Corporation, 2004 [cited April 7, 2004], available from World Wide Web: <http://www.ascension-tech.com/products/flockofbirds.php>

[15] Ascension Technology Corporation, *Flock of Birds: Six Degree-of-Freedom Measurement Device: Technical Description of DC Magnetic Trackers,* Burlington, VT: Ascension Technologies Corporation, 2000.

[16] R. M. De Marco, *Data Recording and Analysis of American Sign Language*, M.S. thesis, Dept. of Biomedical Engineering. New Jersey Institute of Technology, Newark, NJ, May 2003.

[17] Assurance Technologies, Inc., *Product Catalog: Multi-Axis Force/Torque Sensor F/T,* Apex, NC: Assurance Technologies, 2003.

[18] National Physical Laboratory: The UK's National Measurement Laboratory, "Types of Force Transducers" [online], Middlesex, UK: National Physical Laboratory, 2004 [cited April 6, 2004], available from World Wide Web: <http://www.npl.co.uk/force/faqs/transtypes.html>.

[19] National Physical Laboratory: The UK's National Measurement Laboratory, "Force Transducer Characteristics" [online], Middlesex, UK: National Physical Laboratory, 2004 [cited April 6, 2004], available from World Wide Web: <http://www.npl.co.uk/force/faqs/transcharacter.html>.

[20] David A. Winter, *Biomechanics and Motor Control of Human Movement*, 2nd ed., New York, NY: John Wiley & Sons, 1990.